



Transient response of a 2-tank flash evaporator
by Thomas William Holzberger

A thesis submitted to the Graduate Faculty in partial fulfillment of the requirements for the degree of DOCTOR OF PHILOSOPHY in Chemical Engineering
Montana State University
© Copyright by Thomas William Holzberger (1969)

Abstract:

To provide information for the design of flash desalination plants, the dynamics of a 2-tank flash evaporator were studied. Using the 2-tank evaporator available in the Montana State University Chemical Engineering Laboratory, transient data were obtained for step increases and decreases in the temperature of the hot feed water to the first flash tank in the system. A digital computer model was written for the 2-tank evaporator that describes the dynamic response of the system. The computer model was rewritten to describe a 4-tank evaporator, and tested for stability to upsets in temperature of the inlet flow streams.

The digital computer model proved to be very versatile in predicting both steady-state operating conditions and responses to various upsets in the inlet streams. Stability of a multi-tank flash evaporator follows from the stability of the end tanks of the system. Stable operation exists only over a narrow range of temperature and flow rates near specified design values. Upsets in the entering stream temperatures of greater than 5—10 degrees Centigrade cause the water levels in the evaporator tanks to rise or fall beyond the range of stable operations. Increasing the evaporator tank size slows the rate of response to upsets but does not change the equilibrium operating conditions. Changing the tube bundle heat transfer rate changes the equilibrium operating conditions but does not affect stability. Proportional-Integral control of the inlet temperature and flow rate to the first flash tank is necessary for stable operation. If the feed brine temperature is variable, it must also be controlled. Temperature upsets entering the system are quickly corrected by Proportional-Integral control, and do not upset the system more than 1/2 degree Centigrade past the second tank.

TRANSIENT RESPONSE OF A 2-TANK FLASH EVAPORATOR

by

THOMAS WILLIAM HOLZBERGER

A thesis submitted to the Graduate Faculty in partial
fulfillment of the requirements for the degree

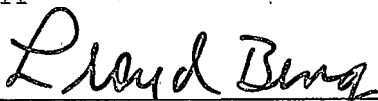
of

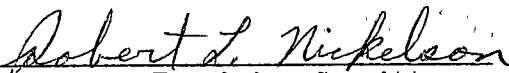
DOCTOR OF PHILOSOPHY

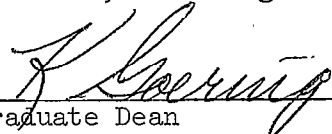
in

Chemical Engineering

Approved:


Head, Major Department


Chairman, Examining Committee


Graduate Dean

MONTANA STATE UNIVERSITY
Bozeman, Montana

December, 1969

TABLE OF CONTENTS

	Page
Vita	ii
Table of Contents	iii
List of Figures	iv
Abstract	vii
Introduction	1
Background	3
Description of Equipment	8
Experimental Data	13
Theoretical Development	25
Analog Computer Model	29
Digital Computer Model	34
1. 2-Tank Simulation	34
2. 4-Tank Simulation	49
3. Stability of a Flash Evaporator	63
4. Rate of Response to Upsets	65
Control of a Flash Evaporator	69
Conclusion	84
Suggestions for Further Work	86
Appendix	88
Literature Cited	119

LIST OF FIGURES

Figure	Page
1. N-Stage Flash Evaporator	4
2. Existing Instrumentation	9
3. Modified Equipment Diagram	11
4. Data Acquisition System	12
5. Experimental Data, 2-Tank Evaporator, Step Rise in T_o , T_1 Response Curve	15
6. Experimental Data, 2-Tank Evaporator, Step Rise in T_o , ΔT Response Curve	16
7. Experimental Data, 2-Tank Evaporator, Step Rise in T_o , ΔP Response Curve	17
8. Experimental Data, 2-Tank Evaporator, Step Rise in T_o , Height Response Curves	18
9. Experimental Data, 2-Tank Evaporator, Step Drop in T_o , T_1 Response Curve	19
10. Experimental Data, 2-Tank Evaporator, Step Drop in T_o , ΔT Response Curve	20
11. Experimental Data, 2-Tank Evaporator, Step Drop in T_o , ΔP Response Curve	21
12. Experimental Data, 2-Tank Evaporator, Step Drop in T_o , Height Response Curves	22
13. Analog Simulation - Step Response Data	32
14. Analog Simulation - H_2 as a Function of F_o	33
15. Comparison Between Experimental Data and 2-Tank Simulation, Step Drop in T_o , T_1 Response Curve	40
16. Comparison Between Experimental Data and 2-Tank Simulation, Step Drop in T_o , ΔT Response Curve	41

LIST OF FIGURES. (Cont.)

Figure	Page
17. Comparison Between Experimental Data and 2-Tank Simulation, Step Drop in T_o , ΔP Response Curve	42
18. Comparison Between Experimental Data and 2-Tank Simulation, Step Drop in T_o , Height Response Curves	43
19. Comparison Between Experimental Data and 2-Tank Simulation, Step Rise in T_o , T_1 Response Curve	44
20. Comparison Between Experimental Data and 2-Tank Simulation, Step Rise in T_o , ΔT Response Curve	45
21. Comparison Between Experimental Data and 2-Tank Simulation, Step Rise in T_o , ΔP Response Curve	46
22. Comparison Between Experimental Data and 2-Tank Simulation, Step Rise in T_o , Height Response Curves	47
23. 4-Tank Simulation, Step Drop in T_o from 104 - 101 °C, Temperature Response Curves	52
24. 4-Tank Simulation, Step Drop in T_o from 104 - 101 °C, ΔT Response Curves	53
25. 4-Tank Simulation, Step Drop in T_o from 104 - 101 °C, ΔP Response Curves	54
26. 4-Tank Simulation, Step Drop in T_o from 104 - 101 °C, Height Response Curves	55
27. 4-Tank Simulation, Step Drop in T_c from 73 - 68 °C, Temperature Response Curves	57
28. 4-Tank Simulation, Step Drop in T_c from 73 - 68 °C, Height Response Curves	58
29. 4-Tank Simulation, Step Rise in T from 103 - 106 °C, Response of T_1 for Evaporators with Tank Areas of 8 ft ² , 20 ft ² , and 50 ft ²	60

LIST OF FIGURES (Cont.)

Figure	Page
30. 4-Tank Simulation, Step Rise in T_o from 103 - 106 °C, Response of T_1 for Evaporators with Tube Bundle Heat-Removal Rates of 2000 BTU/hr °F, 4000 BTU/hr °F, and 8000 BTU/hr °F .	62
31. Frequency Response Study	66
32. Existing Control	70
33. 4-Tank Simulation, P-I Control of T_o and F_o , 5 °C Step Rise in Inlet Stream to T_o Heat Exchanger, Temperature Response Curves	73
34. 4-Tank Simulation, P-I Control of T_o and F_o , 5 °C Step Rise in Inlet Stream to T_o Heat Exchanger, Height Response Curves	74
35. 4-Tank Simulation, P-I Control of T_o and F_o , Step Drop in T_c from 73 - 68 °C, Temperature Response Curves	75
36. 4-Tank Simulation, P-I Control of T_o and F_o , Step Drop in T_c from 73 - 68 °C, Height Response Curves	76
37. 4-Tank Simulation, P-I Control of T_c and F_o , 5 °C Step Rise in Inlet Stream to T_c Heat Exchanger, Temperature Response Curves	77
38. 4-Tank Simulation, P-I Control of T_c and F_o , 5 °C Step Rise in Inlet Stream to T_c Heat Exchanger, Height Response Curves	78
39. 4-Tank Simulation, P-I Control of T_o and F_o , Change of T_o Set Point from 104 ° - 101 °C, Temperature Response Curves .	80
40. 4-Tank Simulation, P-I Control of T_o and F_o , Change of T_o Set Point from 104 ° - 101 °C, Height Response Curves	81
41. 4-Tank Simulation, P-I Control of T_c and F_o , Change of T_c Set Point from 73 ° - 76 °C, Temperature Response Curves . .	82
42. 4-Tank Simulation, P-I Control of T_c and F_o , Change of T_c Set Point from 73 ° - 76 °C, Height Response Curves	83

ABSTRACT

To provide information for the design of flash desalination plants, the dynamics of a 2-tank flash evaporator were studied. Using the 2-tank evaporator available in the Montana State University Chemical Engineering Laboratory, transient data were obtained for step increases and decreases in the temperature of the hot feed water to the first flash tank in the system. A digital computer model was written for the 2-tank evaporator that describes the dynamic response of the system. The computer model was rewritten to describe a 4-tank evaporator, and tested for stability to upsets in temperature of the inlet flow streams.

The digital computer model proved to be very versatile in predicting both steady-state operating conditions and responses to various upsets in the inlet streams. Stability of a multi-tank flash evaporator follows from the stability of the end tanks of the system. Stable operation exists only over a narrow range of temperature and flow rates near specified design values. Upsets in the entering stream temperatures of greater than 5-10 degrees Centigrade cause the water levels in the evaporator tanks to rise or fall beyond the range of stable operations. Increasing the evaporator tank size slows the rate of response to upsets but does not change the equilibrium operating conditions. Changing the tube bundle heat transfer rate changes the equilibrium operating conditions but does not affect stability. Proportional-Integral control of the inlet temperature and flow rate to the first flash tank is necessary for stable operation. If the feed brine temperature is variable, it must also be controlled. Temperature upsets entering the system are quickly corrected by Proportional-Integral control, and do not upset the system more than 1/2 degree Centigrade past the second tank.

INTRODUCTION

The steady growth of urban population centers in arid areas and the fixed quantities of ground water in non-arid areas have forced man to look to the sea to meet the ever-increasing demand for fresh water. Presently, the cheapest way to purify seawater or brackish water for human consumption is by flash desalination. In this evaporative process, seawater is heated to about 250 °C and cascaded through a series of tanks, each at a succeeding lower temperature and pressure. Vapor flashes off from the brine and is condensed, yielding pure fresh water. Two flash desalination plants, one in Florida and one in Cuba, are currently producing fresh water from seawater where other supplies of fresh water are not available. The Office of Saline water, an agency of the Department of the Interior, is working to develop the technology of flash desalination to the point that fresh water from the sea will be economically attractive.

The proper design and instrumentation of a large flash desalination plant demands a knowledge of both steady-state and transient response data. No transient data for a flash evaporator has been published in the literature, and no digital computer model is available that describes unsteady-state behavior. This study was undertaken to obtain transient data from the 2-stage flash evaporator available in the Montana State University chemical engineering laboratory and to describe the transient behavior of the system in a digital

computer simulation. It is hoped that the results of this study may be useful in the design of future flash evaporators.

BACKGROUND

A schematic drawing of an N-stage flash evaporator is given in Figure 1. Fresh seawater feed is circulated through a tube bundle starting with stage N. As the feed moves toward stage 1, it is warmed from its entering temperature. The warmed seawater exits from the evaporator and enters the steam heat exchanger, where its temperature reaches the inlet temperature. Seawater enters tank 1 and flashes to an equilibrium temperature less than the inlet temperature and reaches a corresponding vapor pressure. The water that flashes is condensed into drip trays and removed as product. The heat of condensation warms the incoming feed in the tube bundle. Tank 2 contains water at a lower temperature and vapor pressure; hence water flashes across the orifice between the two tanks. This process continues through tank N, where roughly 50% of the water has been flashed off. The waste brine is discarded. A more detailed flowsheet is available (19).

The first practical multi-stage flash evaporation plant constructed in the United States was completed at San Diego in 1962 and moved to the Guantanamo Naval Base in Cuba in 1964 (12,6), where it was combined with a steam power generation plant. Subsequently, the Bolga Island project was proposed in Southern California as a combined power-desalting project, but was discontinued when cost estimates rose dramatically. The Office of Saline Water (OSW) has proposed other large projects, ranging from 50 to 250 million gallons product water per day. Designs with comprehensive

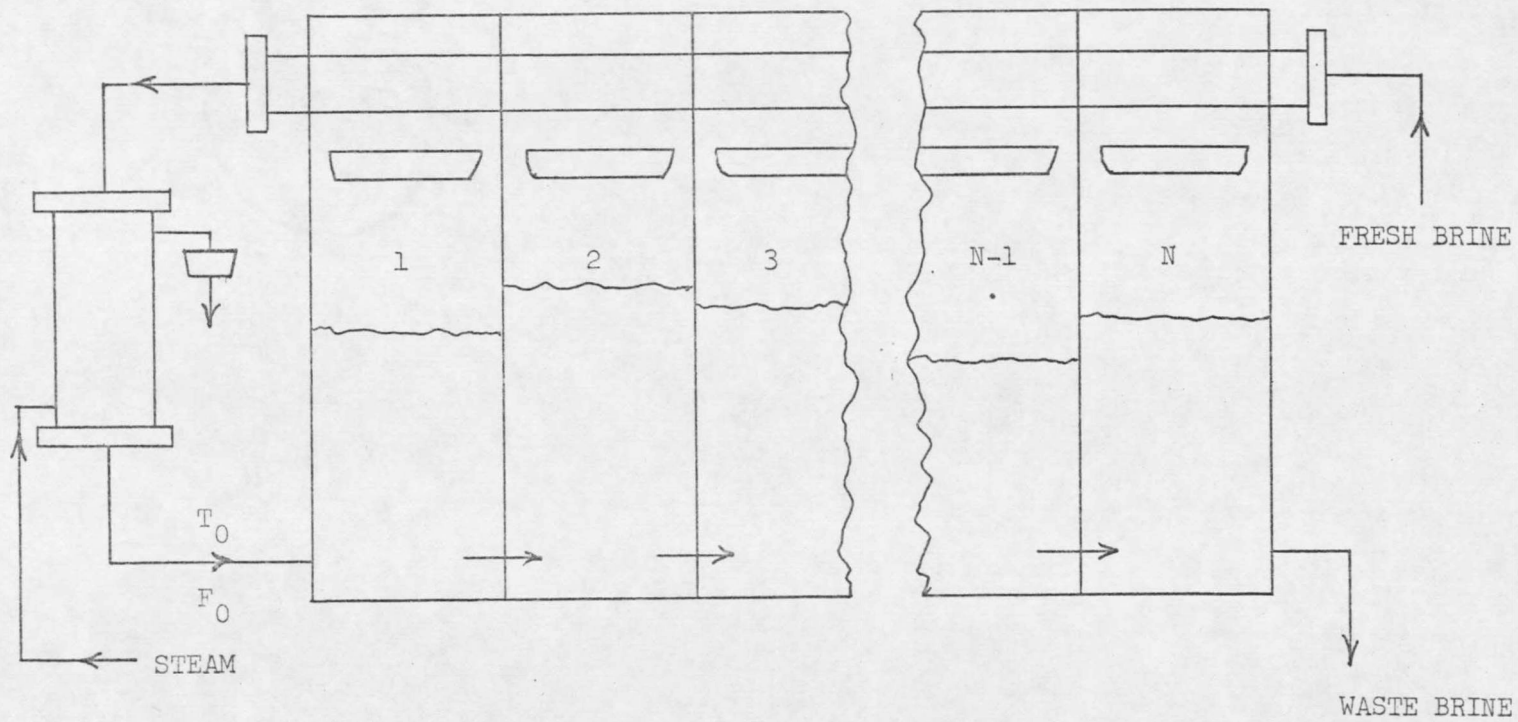


Figure 1. N-Stage Flash Evaporator

cost estimates and complete scale drawings of equipment and instrumentation were done (18,19,20), but no flash desalination plants were constructed. A comprehensive hybrid computer simulation (21) was written by Electronic Associates, Inc., to test the design submitted by Fluor (19) to the Office of Saline Water. Using 12 differential equations and 44 supporting equations to describe the conditions in each flash tank, EAI developed a mathematical model for a 39-tank flash evaporator. Because no experimental data were available describing the operation of a flash evaporator, Electronics Associates, Inc., could not test the model for transient response to upsets. By estimating data where needed, EAI did develop a startup procedure and predict that for steady-state operation the specified product water rates could be met. To supply practical experimental data for large flash desalination plants, the OSW is presently building a flash test module with a capacity of 17 million gallons product water per day (22).

Kogan (14) derived equations that describe the flash evaporator with respect to greatest steam economy and maximum thermodynamic efficiency. Arad (4) has done a system analysis of a large flash desalination plant in which he studied plant cost versus plant life, performance, efficiency, and effectiveness. Narsimhan (17) derived the differential equations describing a multiple-effect concentrating evaporator, simplified these equations, applied boundary conditions, and solved the differential equations mathematically. Andre and Ritter (3)

took experimental data on a double-effect concentrating evaporator and wrote a digital computer model describing their system. Andersen, Glasson, and Lees (2) compared experimental data from a single-effect concentrating evaporator with the results of an analog computer simulation of the system, and suggested possible control schemes. Itahara (11) used dynamic programming to optimize the design and operation of both a multiple-effect concentrating evaporator and a multi-stage multi-effect flash evaporator in the steady state.

Dynamic studies have been done concerning the behavior of reactors (7,15), packed liquid-liquid extraction columns (5), and distillation columns (24). Several other papers, perhaps more closely related, have been written concerning heat exchanger dynamics (1,8,13). In each paper, a mathematical model was analyzed using an analog computer, a digital computer, or a tabulated solution to a differential equation.

When this project was begun in October 1966, no experimental data could be found in the literature describing either the transient or steady-state operation of a flash evaporator. No computer simulation of a flash evaporator was available at that time. The EAI hybrid computer simulation was completed in October 1967, and the results were published in condensed form in January 1969. A complete copy of the EAI simulation was not obtained until September 1969.

Transient experimental data were taken on the flash evaporator in the Montana State University chemical engineering laboratory from September 1968 through February 1969. To explain the data, a simulation of the 2-tank flash evaporator was needed. First an analog computer simulation was used, and when this proved inadequate a digital computer simulation was written. The subsequent examination of the complete EAI report showed that the approach of each of the two projects was considerably different. A detailed comparison will be made later.

DESCRIPTION OF EQUIPMENT

The 2-stage flash evaporator available in the Montana State University chemical engineering laboratory had been used previously to correlate 2-phase flow through an orifice (10). Original instrumentation consisted of 10 thermocouples used to measure various temperatures, 2 temperature recorder-controllers, a temperature recorder, a thermopile, and 2 U-tube manometers. (See Figure 2.)

To better monitor the evaporator and produce controlled upsets, several changes in instrumentation were made. A Masoneilan Little Scotty 1/2" pneumatic control valve was placed in the inlet flow line and connected to a Foxboro proportional flow controller to regulate the inlet flow rate. Two Magnetrol level transducers were purchased, one for each tank, to indicate the liquid levels. A pressure transducer was obtained to monitor the pressure in tank 1, and a differential pressure transducer was ordered to monitor the pressure drop between tanks. Thermocouple wells 2, 3, and AA' (Figure 2) were used to monitor respectively the inlet temperature, the temperature in tank 1, and the temperature drop between tanks.

Modifications to the equipment included:

1. Closing the valve to the product-water pump so that no air could leak back into the system through the pump packing. Product water condensed as before, maintaining the heat balance, and dripped back into the tank in small quantities that did not alter the material balance.

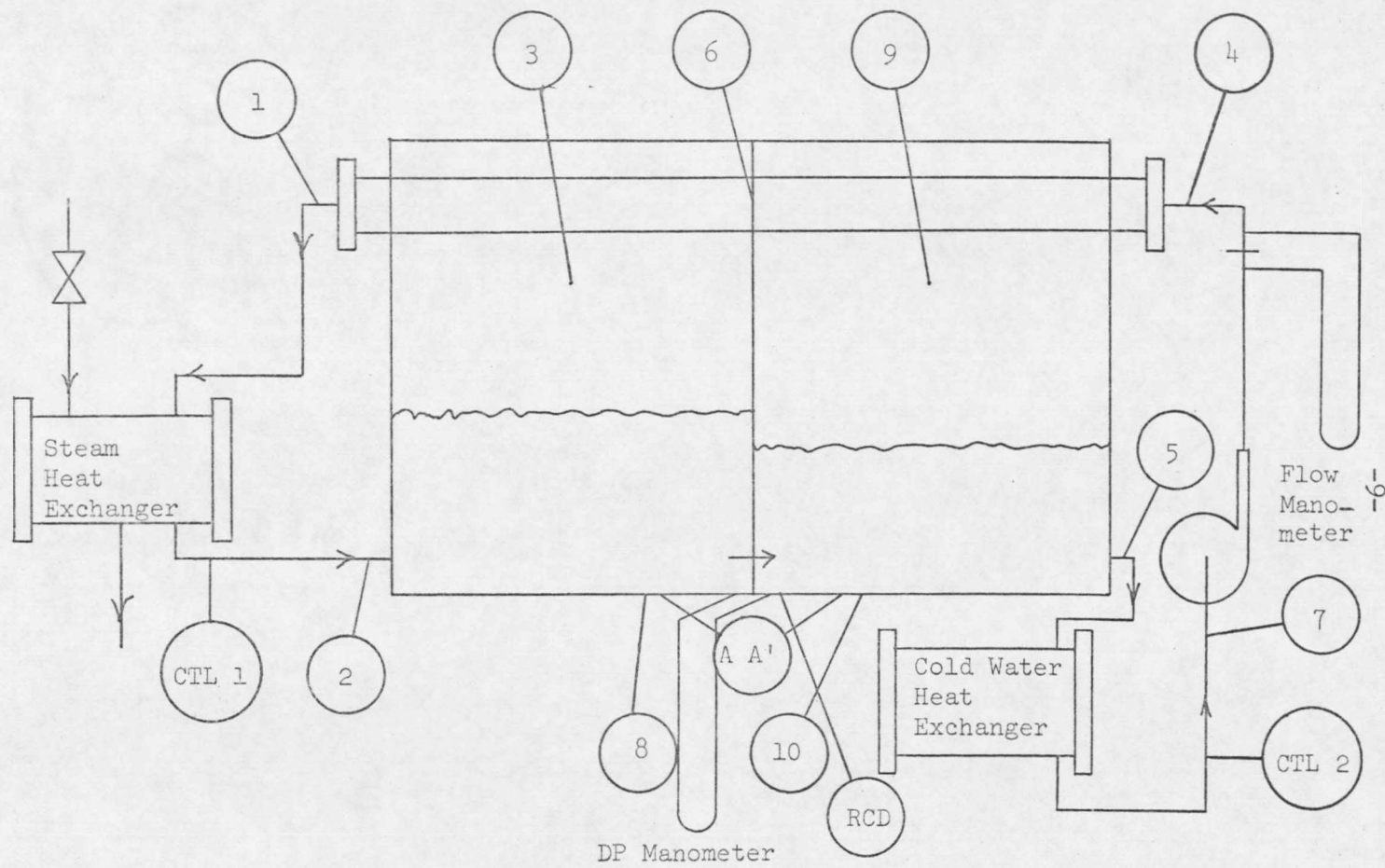


Figure 2. Existing Instrumentation

2. Placing vapor bleed lines to a vacuum pump so that any air leaking into the system was removed.
3. Inserting a bypass around the pneumatic steam-supply valve to the steam heat exchanger so that better step changes in the inlet temperature could be made.
4. Permanently placing a 0.875" diameter orifice in place between tanks 1 and 2. (See Figure 3.)
5. Using pure water (no salt added).
6. Recycling all water in a closed system so that a constant mass balance was maintained.

A data acquisition system, developed by the Electronics Research Laboratory (ERL) at MSU (Figure 4), was used to collect the raw data. Ten input channels were monitored each 20 seconds by the digital voltmeter. Output by the teletype was both a data listing and a punched paper tape. The punched paper tapes from each run were converted to data card decks to enable analysis on MSU's SDS Sigma-7 computer. The reduced data were listed and plotted using the computer lineprinter.

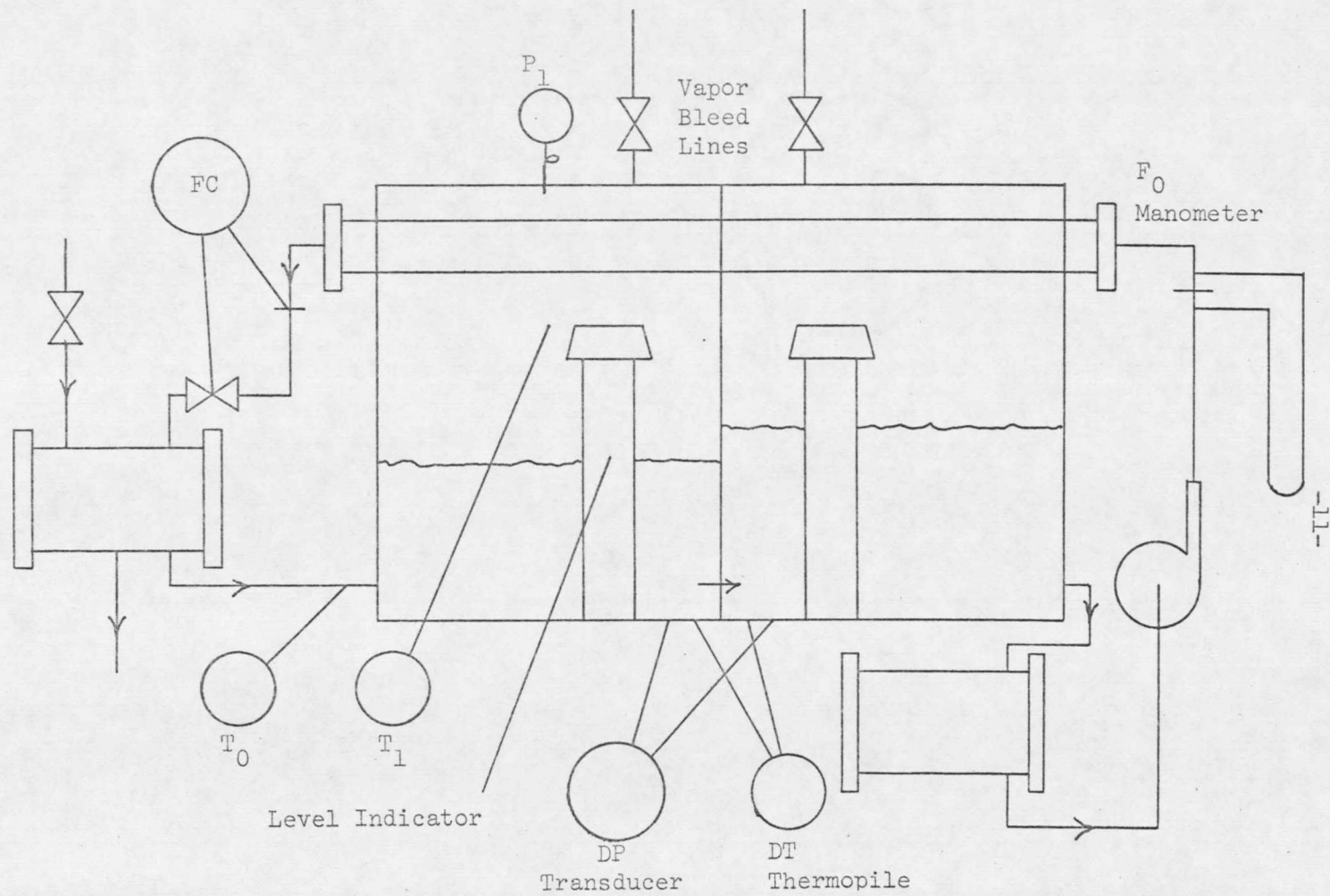


Figure 3. Modified Equipment Diagram

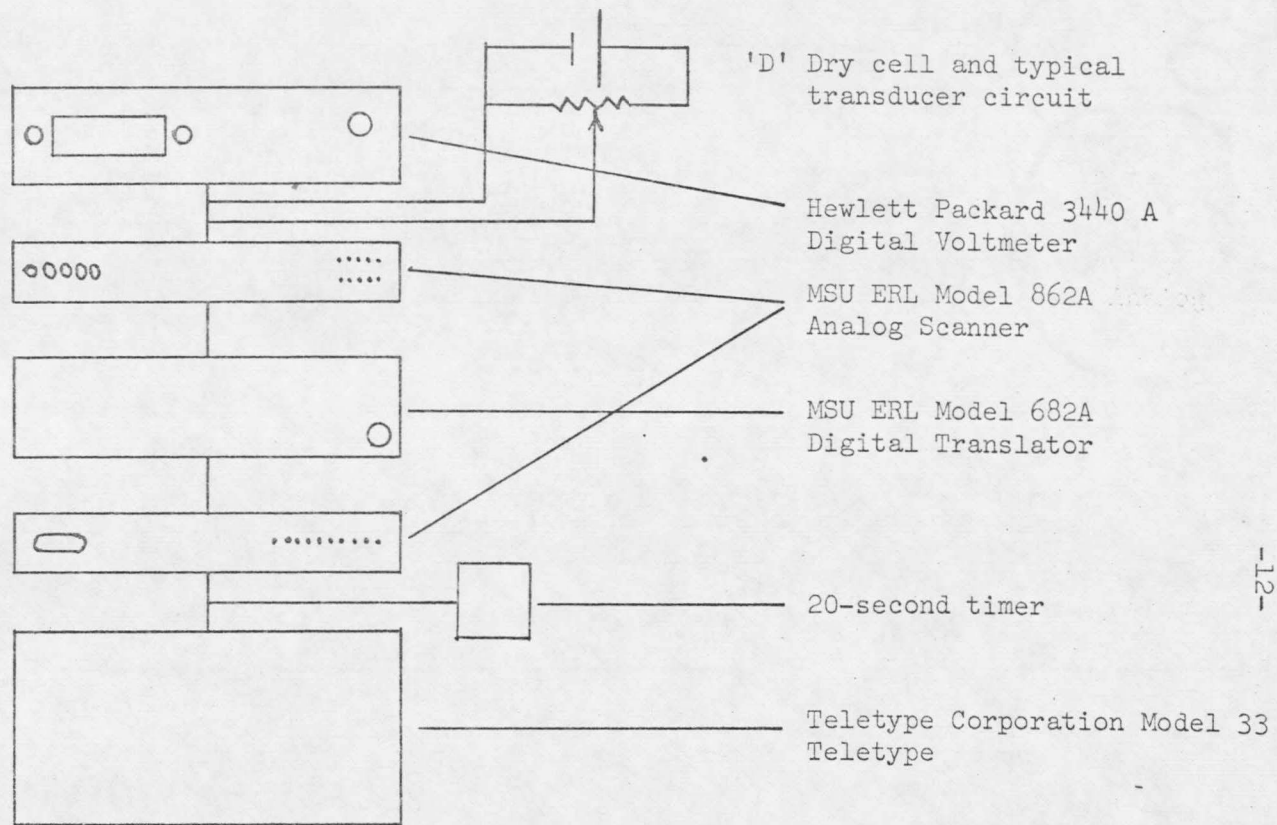


Figure 4. Data Acquisition System

EXPERIMENTAL DATA

The data inputs read by the data acquisition system are listed below:

1. T_0 temperature of feed brine entering tank 1
2. T_1 temperature in tank 1
3. ΔT temperature drop from tank 1 to tank 2
4. P_1 vapor pressure in tank 1
5. ΔP pressure drop from tank 1 to tank 2
6. H_1 height of water in tank 1
7. H_2 height of water in tank 2

(See Appendix 1 for a complete definition of variable names.) The 3 additional channels of the data acquisition system were used to monitor the source voltage of the 'D' dry cell.

The scan rate of 1 scan every 20 seconds gave 3 data points for each variable each minute. The digital voltmeter read to a maximum value of 99.99 millivolts, with an accuracy of $\pm .01$ mv. For T_0 and T_1 , with typical readings of 5.00 mv, measurement error was $\pm .01$ mv. per 5.00 mv. or 0.4% of calibration. For ΔT , with a typical reading of 1.00 mv., measurement error was $\pm .01$ mv. per 1.00 mv. or 2% of calibration. P_1 , ΔP , H_1 , and H_2 were measured above 10.00 mv., and hence were accurate to the accuracy of the calibration.

T_0 and T_1 were calibrated between an ice bath and a boiling-water

bath. Since all runs were near the boiling point, the calibrations were felt to be good within $1/2^{\circ}\text{C}$. ΔT was calibrated between 2 boiling water baths and an ice water-boiling water bath, a difference of 95°C . The total mv. output at a difference of 95°C matched that given in the thermocouple tables for an iron-constantan thermocouple. However, since a small temperature difference was measured ($3-4^{\circ}\text{C}$) compared to the calibration, the calibration accuracy was unknown. P_1 was calibrated during every run because of drift. H_1 and H_2 were stable to drift but were dependent upon the water density, which was temperature dependent. Since temperature increase runs and temperature decrease runs covered different temperature ranges, one calibration of H_1 and H_2 was run for temperature increase runs, and one calibration was run for temperature decrease runs. The source 'D' cell was replaced periodically to insure source stability.

Startup and lineout of the evaporator took from 2-3 hours, while each run lasted from 35-40 minutes. Step increases and decreases in T_0 were run because they were the easiest to produce and, therefore, the most reproducible and accurate. Eight temperature increase runs and 4 temperature decrease runs were chosen out of many of each type as reproducible runs at one set of operating conditions. The runs of each type were averaged arithmetically for initial steady-state value, maximum value from the step upset, and final line-out value to give a composite run for a step rise in T_0 and a step drop in T_0 . (Figures 5-12.)

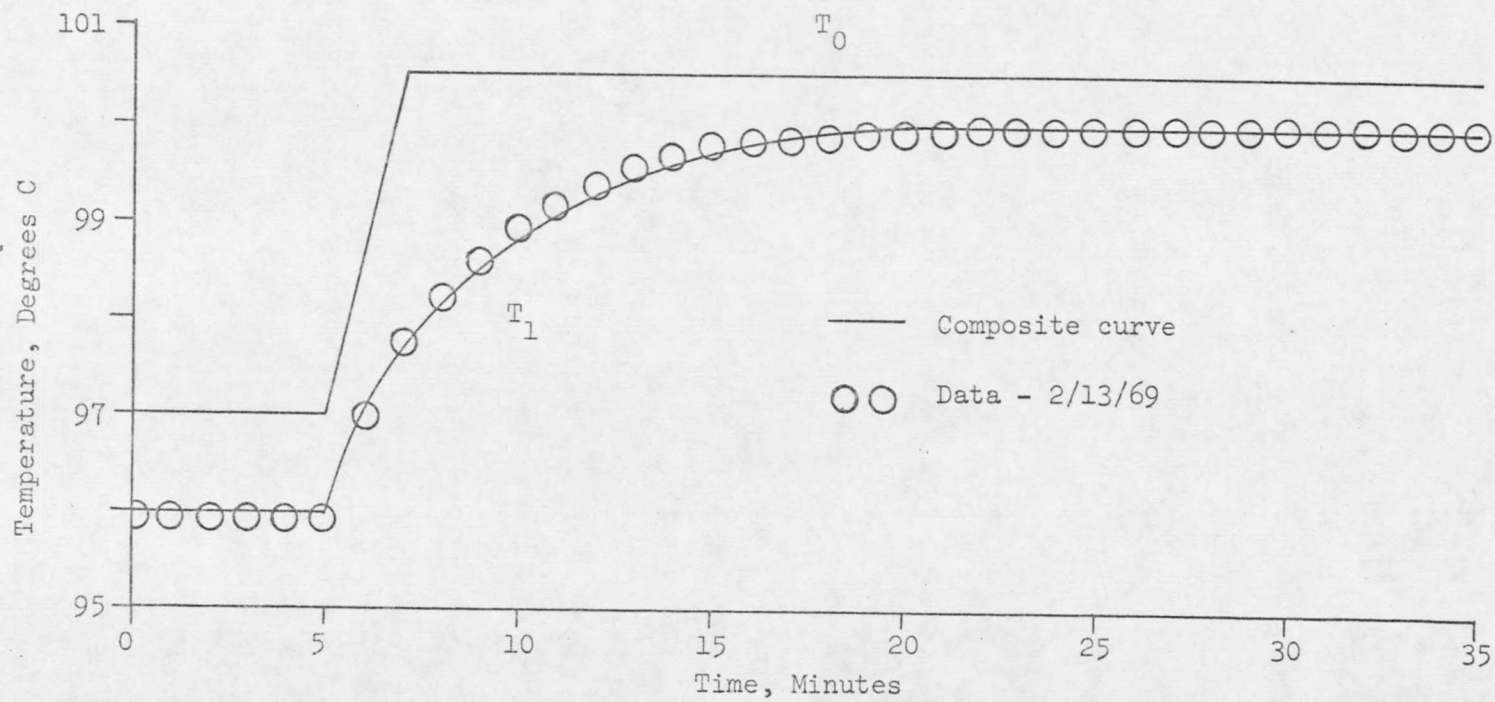


Figure 5. Experimental Data, 2-Tank Evaporator, Step Rise in T_0
 T_1 Response Curve

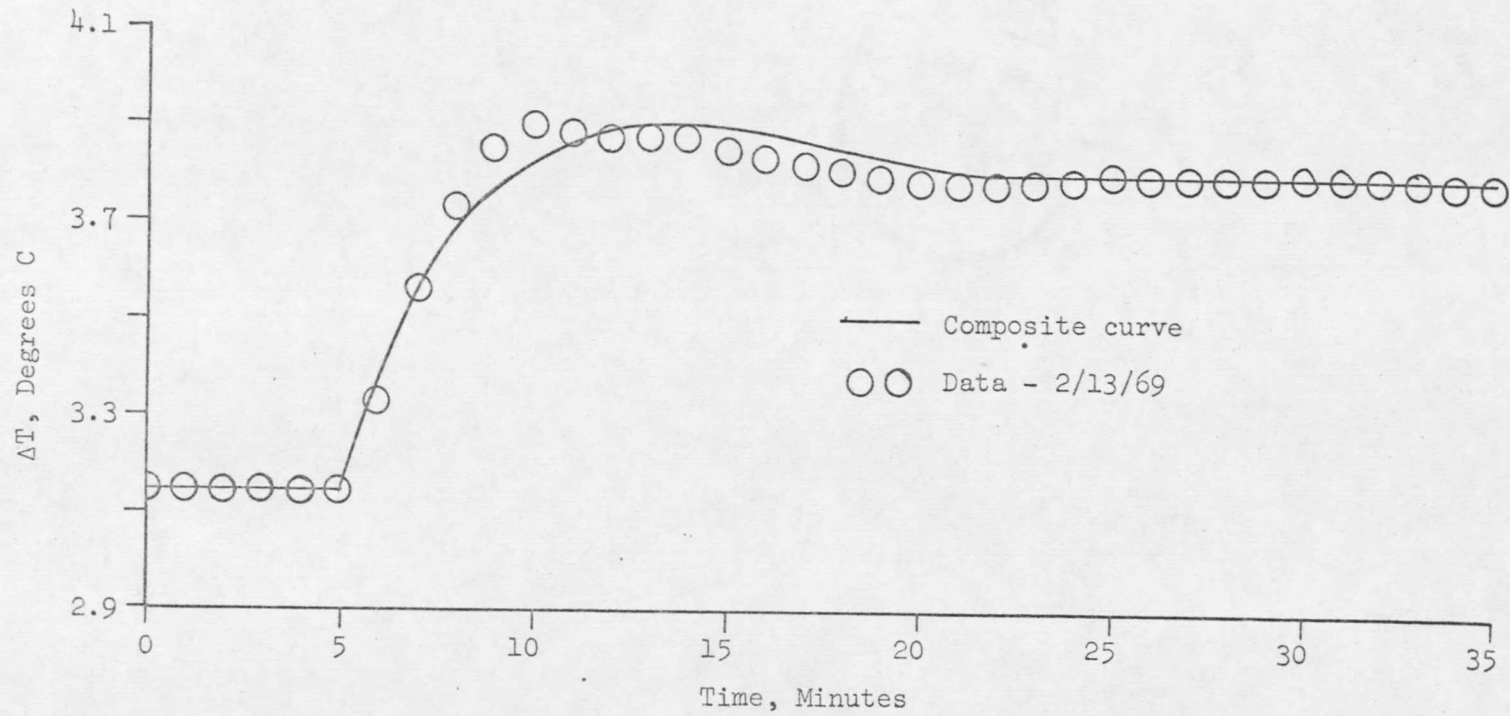


Figure 6. Experimental Data, 2-Tank Evaporator, Step Rise in T_0
 ΔT Response Curve

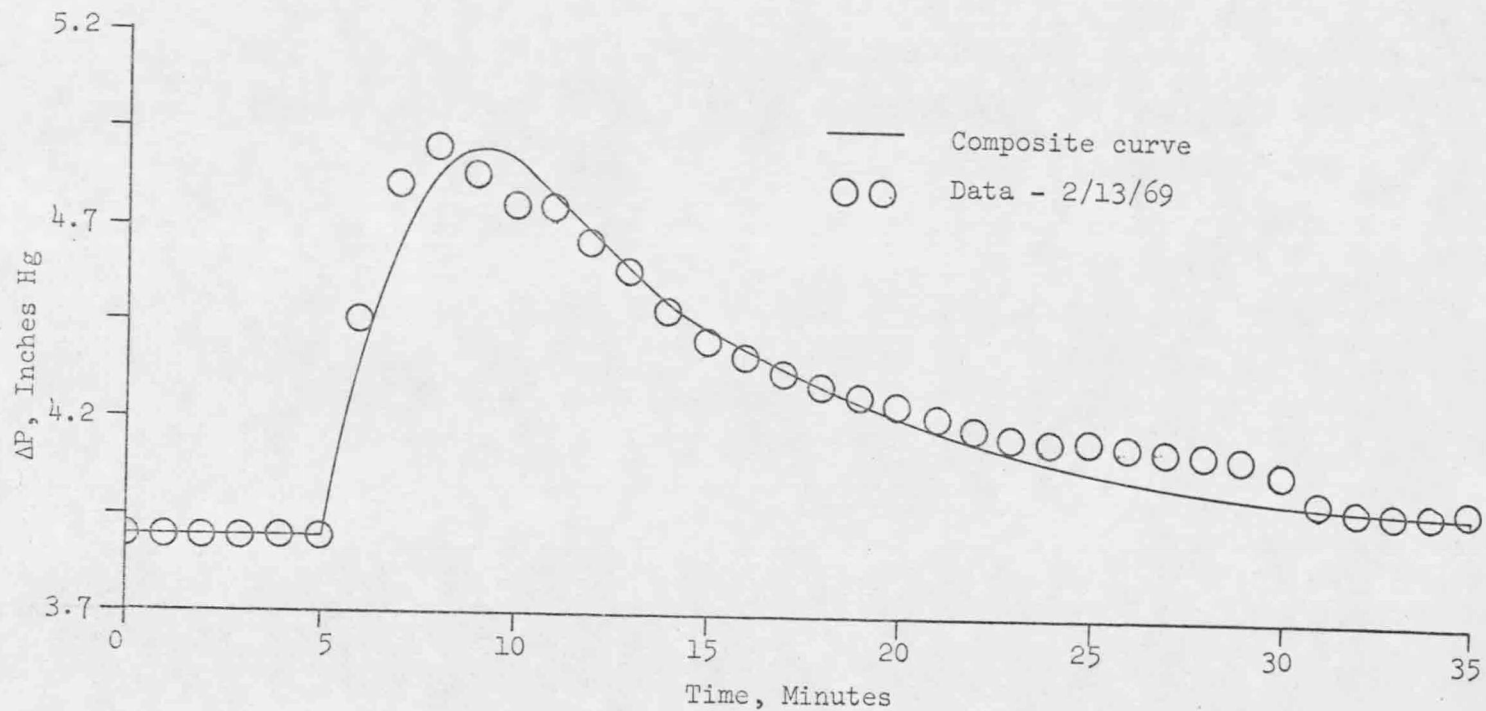


Figure 7. Experimental Data, 2-Tank Evaporator, Step Rise in T_0
 ΔP Response Curve

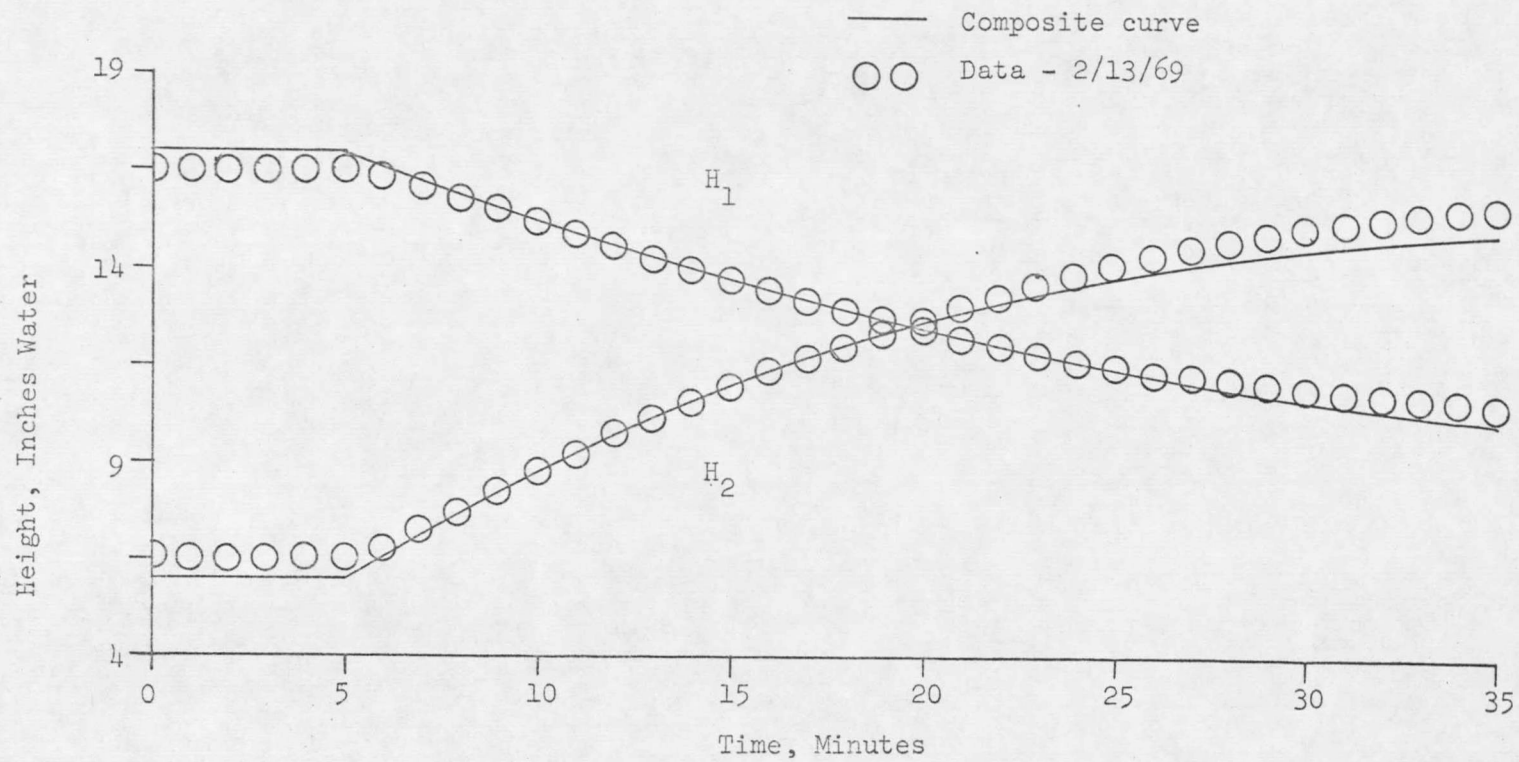


Figure 8. Experimental Data, 2-Tank Evaporator, Step Rise in T_0
Height Response Curves

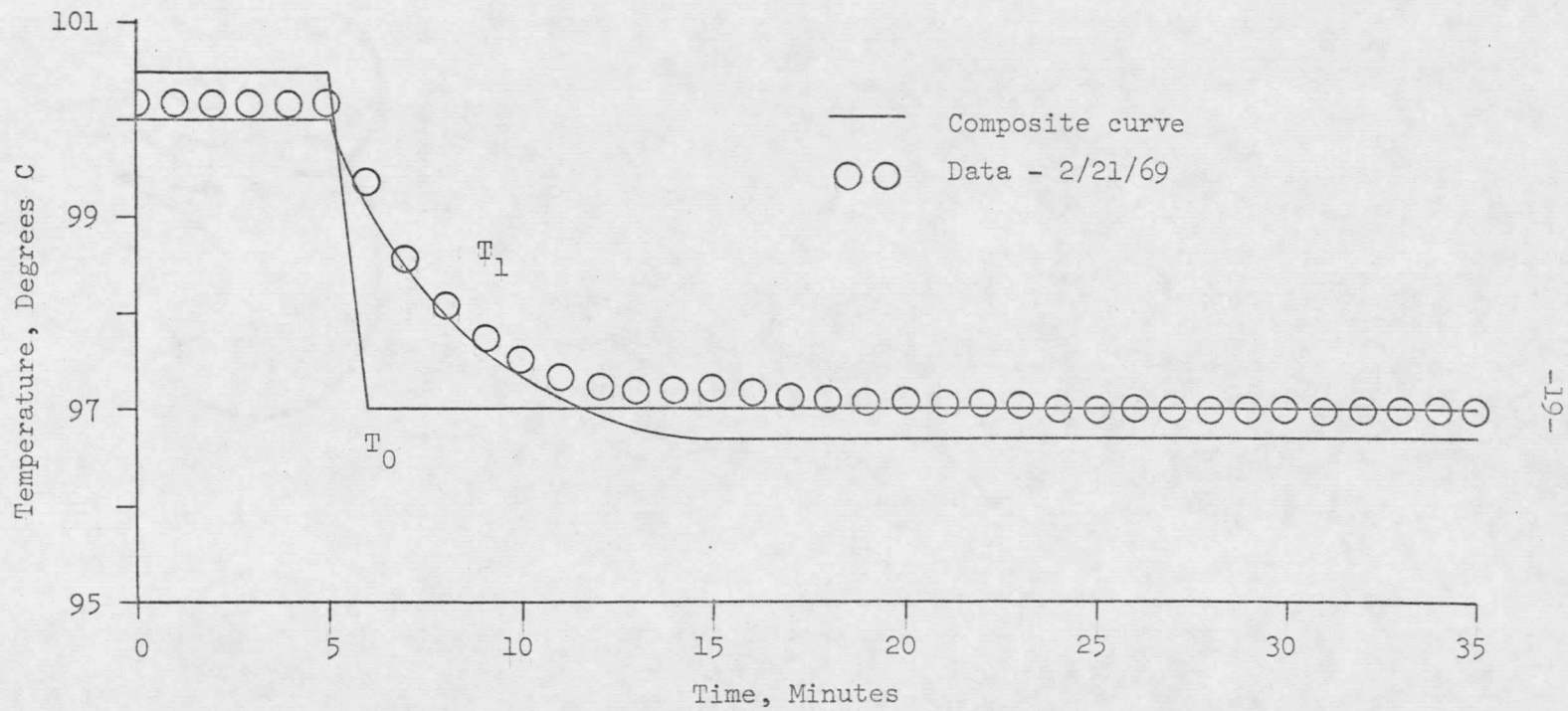
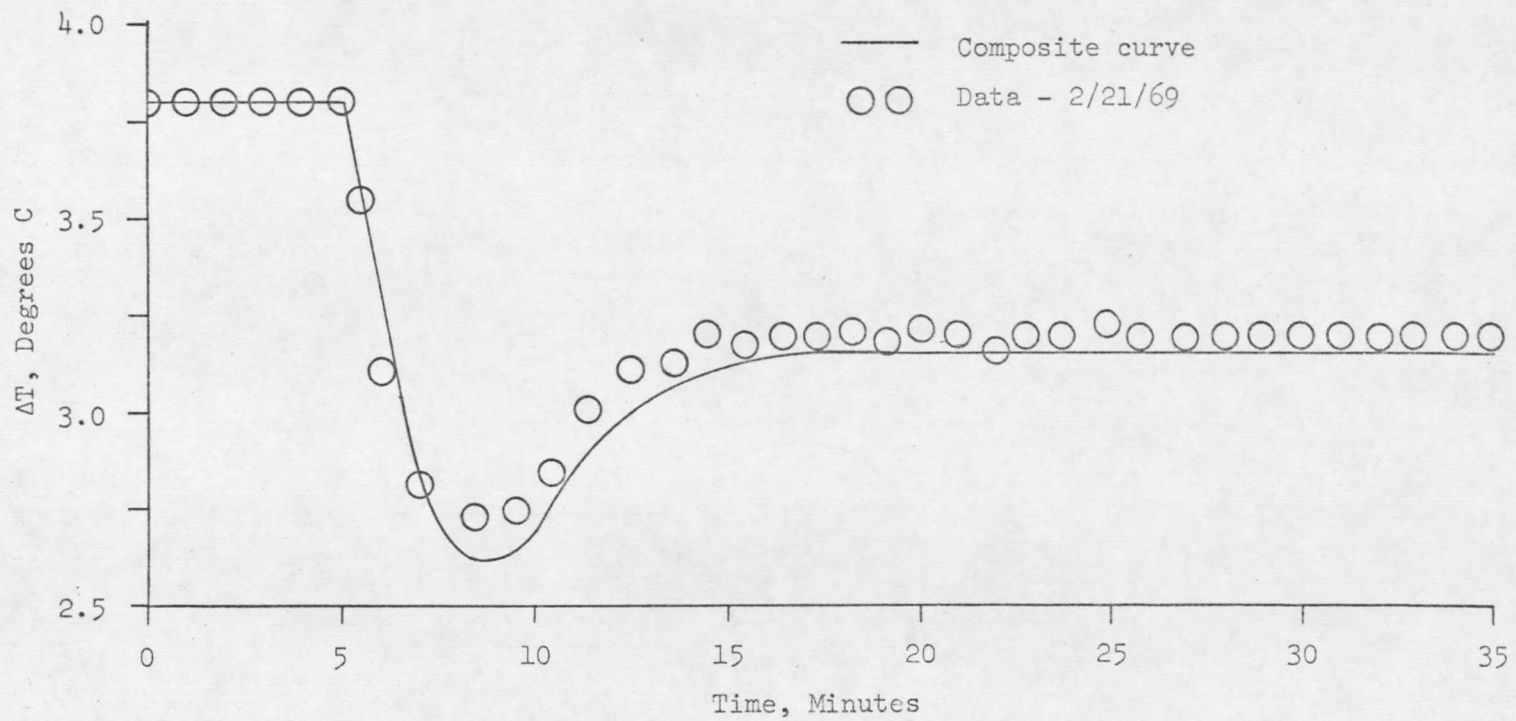


Figure 9. Experimental Data, 2-Tank Evaporator, Step Drop in T_0
 T_1 Response Curve



-20-

Figure 10. Experimental Data, 2-Tank Evaporator, Step Drop in T_0
 ΔT Response Curve

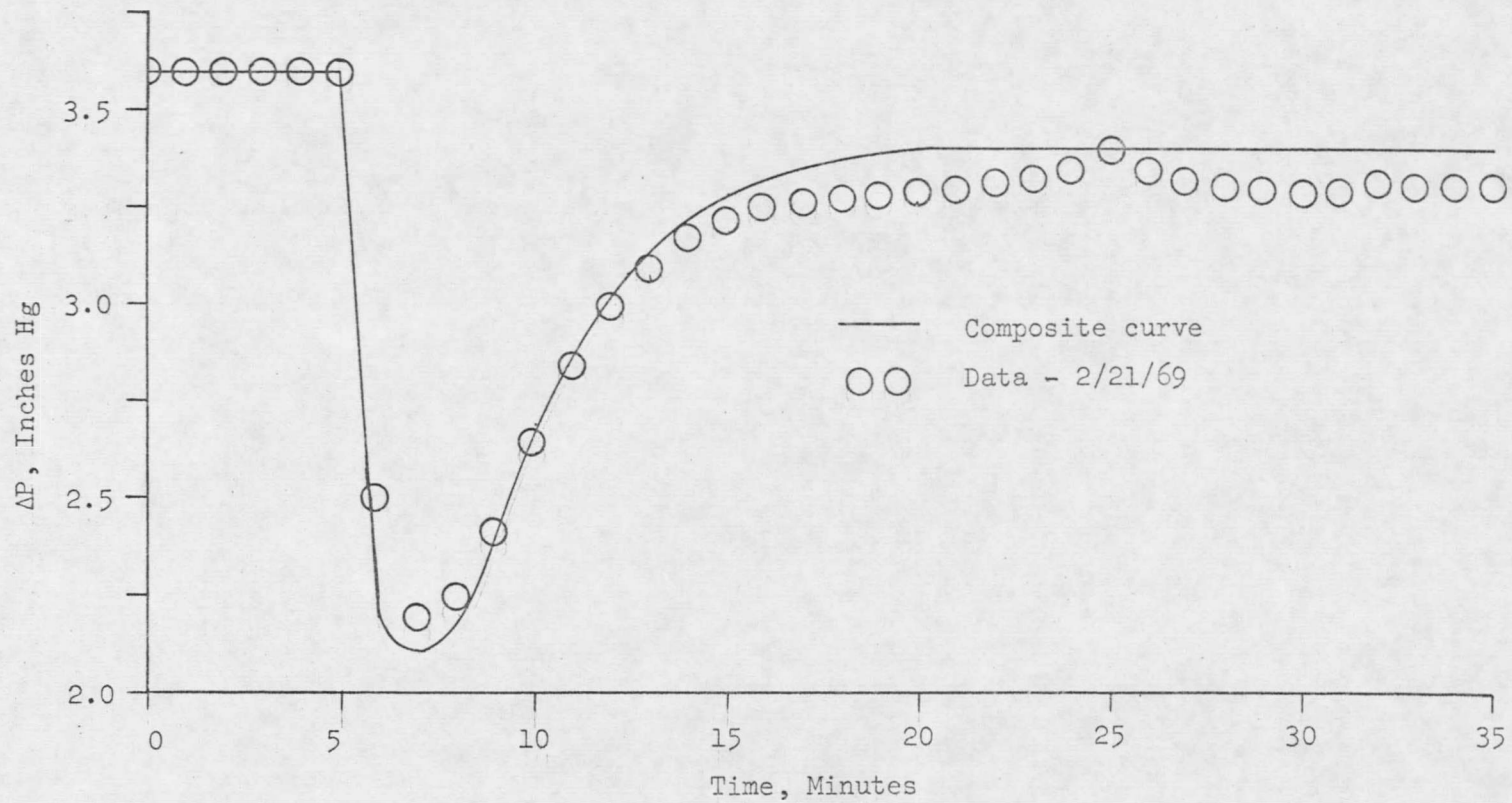


Figure 11. Experimental Data, 2-Tank Evaporator, Step Drop in T_0
 ΔP Response Curve

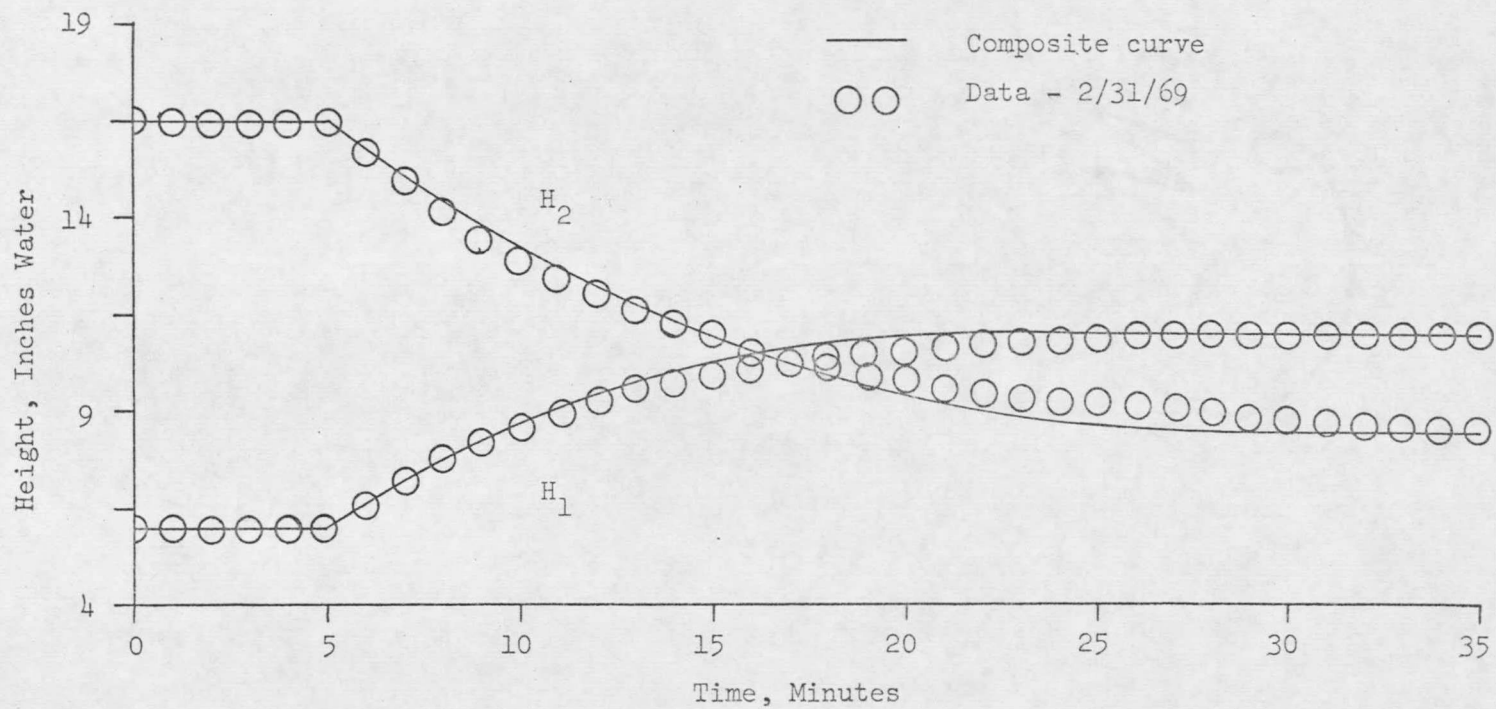


Figure 12. Experimental Data, 2-Tank Evaporator, Step Drop in T_0
Height Response Curves

The solid lines are composite runs; the points are actual points from one run. A rise in T_0 produces a corresponding rise in T_1 and upsets in ΔT and ΔP . A rise in T_1 increases the vapor pressure in tank 1, forcing more water out of tank 1 into tank 2, thus raising the level in tank 2. ΔT and ΔP rise sharply as hotter water enters tank 1, and then fall to new equilibrium values as the hotter water enters tank 2. A drop in T_0 produces a corresponding drop in T_1 and upsets in ΔT and ΔP . A drop in T_1 decreases the pressure in tank 1, forcing less water out of tank 1 into tank 2, thus dropping the level in tank 2. ΔT and ΔP drop sharply as cooler water enters tank 1, and then rise to new equilibrium values as the cooler water enters tank 2. For a temperature rise, the flow rate is 9450 #/hr. For a temperature drop, the flow rate is 9300 #/hr.

Upon examination of the composite curves, several peculiarities of the system were noticed. Response of the system to a step increase in inlet temperature is slower than the response of the system to a step decrease in inlet temperature. Furthermore, although the ΔP curves return nearly to the initial values, the ΔT curves do not. Nor do the ΔT curves follow similar but inverted paths as do the ΔP and T_1 curves. And, the displacement of the T_1 curve from the T_0 curve is not constant, but varies from run to run and within any one run itself.

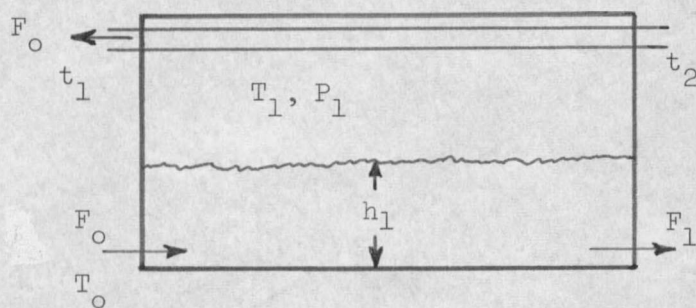
In spite of the seemingly inconsistent features of these runs, the

curves resulting from step input temperature changes were reproducible.

The composite runs agree very well with at least one run for each temperature upset.

THEORETICAL DEVELOPMENT

In order to explain the transient behavior of the 2-tank flash evaporator, the theoretical relationships between the variables were developed. Differential equations were written describing the process. About stage 1 (see Appendix 1 for a complete definition of terms used):



Heat balance:

$$\text{Input } [F_0 C_p (T_0 - t_{\text{ref}}) + F_0 C_p (t_2 - t_{\text{ref}})] \Delta\theta$$

$$\text{Output } [F_1 C_p (T_1 - t_{\text{ref}}) + F_0 C_p (t_1 - t_{\text{ref}})] \Delta\theta$$

$$\text{Accumulation } \rho_L V_1 C_p (T_1 - t_{\text{ref}}) + \rho_{V_1} v_1 H_1 + W_1 C_p \left(\frac{t_1 + t_2}{2} - t_{\text{ref}} \right) |_{\theta} + \Delta\theta$$

$$- \left\{ \rho_L V_1 C_p (T_1 - t_{\text{ref}}) + \rho_{V_1} v_1 H_1 + W_1 C_p \left(\frac{t_1 + t_2}{2} - t_{\text{ref}} \right) \right\} |_{\theta}$$

$$\text{Or, } F_0 C_p (T_0 - t_{\text{ref}}) + F_0 C_p (t_2 - t_{\text{ref}}) - F_1 C_p (T_1 - t_{\text{ref}})$$

$$- F_0 C_p (t_1 - t_{\text{ref}}) = \rho_L C_p V_1 \frac{dT_1}{d\theta} + \rho_L C_p T_1 \frac{dV_1}{d\theta} - \rho_L C_p t_{\text{ref}} \frac{dV_1}{d\theta} \quad (1)$$

$$+ H_1 \rho_{V_1} \frac{dv_1}{d\theta} + H_1 v_1 \frac{d\rho_{V_1}}{d\theta} + \frac{W_1}{2} C_p \left(\frac{dt_1}{d\theta} + \frac{dt_2}{d\theta} \right)$$

Mass Balance:

$$\text{Input } F_o \Delta\theta$$

$$\text{Output } F_1 \Delta\theta$$

$$\text{Accumulation } (V_1 \rho_L + v_1 \rho_{v_1})|_{\theta + \Delta\theta} - (V_1 \rho_L + v_1 \rho_{v_1})|_{\theta}$$

$$\text{Or, } F_o - F_1 = \frac{d}{d\theta} (V_1 \rho_L + v_1 \rho_{v_1}) \quad (2)$$

Energy balance on vapor space:

$$\text{Input } F_o C_p (T_o - T_1) \Delta\theta$$

$$\text{Output } (UA)_1 (T_1 - \frac{t_1 + t_2}{2}) \Delta\theta$$

$$\text{Accumulation } \lambda_{T_1} \rho_{v_1} v_1 |_{\theta + \Delta\theta} - \lambda_{T_1} \rho_{v_1} v_1 |_{\theta}$$

$$\text{Or, } F_o C_p (T_o - T_1) - (UA)_1 (T_1 - \frac{t_1 + t_2}{2}) =$$

$$\lambda_{T_1} \rho_{v_1} \frac{dv_1}{d\theta} + \lambda_{T_1} v_1 \frac{d\rho_{v_1}}{d\theta} \quad (3)$$

Volume in stage 1:

$$V_1 + v_1 = \text{Constant}$$

$$\frac{dV_1}{d\theta} = -\frac{dv_1}{d\theta} \quad (4)$$

The flow of water between flash tanks of a flash evaporator through a sharp-edged orifice was correlated by R. C. Huntsinger (10) as:

$$\frac{Q(-\Delta P)^2 g_c^{1/2}}{\mu \lambda^{3/2}} = 37.83 \left(\frac{D(-\Delta P) g_c^{1/2}}{\mu^{1/2}} \right)^{1.826} \left(\frac{-\Delta P}{\rho \lambda} \right)^{.7434}$$

Or, with D = .875 in.

$$Q = 0.19207 \frac{\mu^{.174} \rho^{.2566}}{\lambda^{.1564}} (-\Delta P)^{.5694} \quad \text{\#/min.} \quad (5)$$

Where, μ = #/ft.-hr.

ρ = #/ft³

λ = ft - lb/lb_m

ΔP = lbf/ft²

Q = flow, #/min.

Vapor pressure equation:

$$\text{Log}_{10} P = 7.9668 - \frac{1668.21}{228 + t} \quad \begin{array}{l} t = ^\circ\text{C} \\ P = \text{mmHg} \end{array} \quad (6)$$

For stage 2, the following equations were developed as those for stage 1:

Heat balance, stage 2:

$$\begin{aligned} & F_1 C_p (T_1 - t_{\text{ref}}) + F_3 C_p (t_3 - t_{\text{ref}}) - F_2 (T_2 - t_{\text{ref}}) - F_0 C_p (t_2 - t_{\text{ref}}) = \\ & \rho_L C_p V_2 \frac{dT_2}{d\theta} + \rho_L C_p T_2 \frac{dV_2}{d\theta} - \rho_L C_p t_{\text{ref}} \frac{dV_2}{d\theta} + \rho_{v_2} \frac{H_{v_2}}{v_2} \frac{dv_{v_2}}{d\theta} \\ & + H_{v_2} v_2 \frac{d\rho_{v_2}}{d\theta} + \frac{W_2}{2} C_p \left(\frac{dt_2}{d\theta} + \frac{dt_3}{d\theta} \right) \end{aligned} \quad (7)$$

Mass balance, stage 2:

$$F_1 - F_o = \frac{d}{d\theta} (V_2 \rho_L + v_2 \rho_v) \quad (8)$$

Energy balance, vapor space, stage 2:

$$F_1 C_p (T_1 - T_2) - (UA)_2 (T_2 - \frac{t_3 + t_2}{2}) = \lambda_{T_2} v_2 \frac{d\rho_v}{d\theta} + \lambda_{T_2} \rho_v v_2 \frac{dv_2}{d\theta} \quad (9)$$

Volume, stage 2:

$$\frac{dV_2}{d\theta} = -\frac{dv_2}{d\theta} \quad (10)$$

These equations define the 2-tank flash evaporator.

ANALOG COMPUTER MODEL

The first attempt to solve the system of differential equations and auxiliary equations describing the 2-stage flash evaporator was made using the TR-48 analog computer. The following simplifications were made:

1. Temperature drops t_1-t_2 and t_2-t_3 in the tube bundle were given fixed values because of the limiting calculation capabilities of the analog computer.
2. The vapor pressure of water as $f(T^{\circ}\text{F})$ was linearized as
$$P = 1.36*T - 212.6 \text{ cm Hg.}$$
3. The vapor density of water as $f(T^{\circ}\text{F})$ was linearized as
$$\rho_v = .0006*T - .0902 \text{ \#/ft}^3\text{-}^{\circ}\text{F.}$$
4. For average values, $\rho_L = 60.0 \text{ \#/ft}^3$ and $\rho_v = 0.032 \text{ \#/ft}^3$.
5. A heat capacity for water of 1 BTU/ $\text{\#-}^{\circ}\text{F}$ was used.

The area of tank 1 was measured at 8.88 ft^2 , and the area of tank 2 was measured at 6.57 ft^2 . The total rectangular volume of each tank was measured, and the tube bundle volume was subtracted from each, giving volumes 1 and 2 equal to 24.9 ft^3 and 18.9 ft^3 , respectively.

Neglecting tube bundle holdup w_1 and vapor density and volume terms, changing the volume terms to height times area terms and expressing the heights in inches, and letting $t_{\text{ref}} = 0^{\circ}\text{F}$ in Equation 1 gives:

$$\frac{dT_1}{d\theta} = \frac{12}{\rho_L A_1 h_1} \{F_0 (T_0 - t_1 + t_2) - F_1 T_1 - \frac{\rho_L T_1 A_1}{12} \frac{dh_1}{d\theta}\} \quad (11)$$

The total differential of Equation 2 is:

$$F_0 - F_1 = \rho_L \frac{dV_1}{d\theta} + V_1 \frac{d\rho_L}{d\theta} + v_1 \frac{d\rho_{v_1}}{d\theta} + \rho_{v_1} \frac{dv_1}{d\theta}$$

The sum of the last three terms is less than 1, while $\rho_L \frac{dV_1}{d\theta}$ is greater than 100, allowing the last three terms to be neglected. Thus, Equation 2 becomes:

$$\frac{dV_1}{d\theta} = \frac{1}{\rho_L} (F_0 - F_1) \quad (12)$$

Or,

$$\frac{dh_1}{d\theta} = \frac{12}{A_1 \rho_L} (F_0 - F_1), \quad h_1 = \text{inches} \quad (13)$$

Similarly for stage 2, neglecting the tube bundle holdup w_2 and vapor density and volume terms, and letting $t_{ref} = 0.0$ in Equation 7 gives:

$$\frac{dT_2}{d\theta} = \frac{12}{\rho_L A_2 h_2} \{F_1 T_1 - F_0 (T_2 - t_3 + t_2) - \frac{\rho_L T_2 A_2}{12} \frac{dh_2}{d\theta}\} \quad (14)$$

And, for Equation 8, by expanding to the total differential and neglecting the last 3 terms, the resulting mass balance on stage 2 is:

$$\frac{dh_2}{d\theta} = \frac{12}{\rho_L A_2} (F_1 - F_0), \quad h_2 = \text{inches} \quad (15)$$

Auxiliary Equation 5 reduces to:

$$F_1 = 2433.859 (-\Delta P)^{.5694}, \quad \#/\text{hr.} \quad (16)$$

The pressure drop between tanks, using a linearized vapor pressure for water, is:

$$(-\Delta P) = .1867 (h_1 - h_2) + 1.36(T_1 - T_2) \quad (17)$$

This system of equations was amplitude scaled and time scaled and wired onto the TR-48 analog computer. Using this simple system, 46 of the 48 available amplifiers were used, as well as all multiplier units and one VDFG unit to generate $F_1 = f(\Delta P)$. This simplified system simulation behaved only qualitatively like the experimental data for H_1 and H_2 corresponding to a step change in T_0 (Figure 13). The simulation showed such great stability that values of H_1 and H_2 returned to original levels. Values of H_2 as a function of F_0 (Figure 14) lined out to steady-state levels from a picked starting value of 12 inches of water qualitatively the same as real evaporator data would. However, time response of the simulation was 2 to 3 times slower than the experimental data. Because the TR-48 analog computer was used to capacity for this simplified model, no changes were made in the model and analog computer work was dropped in favor of a digital simulation.

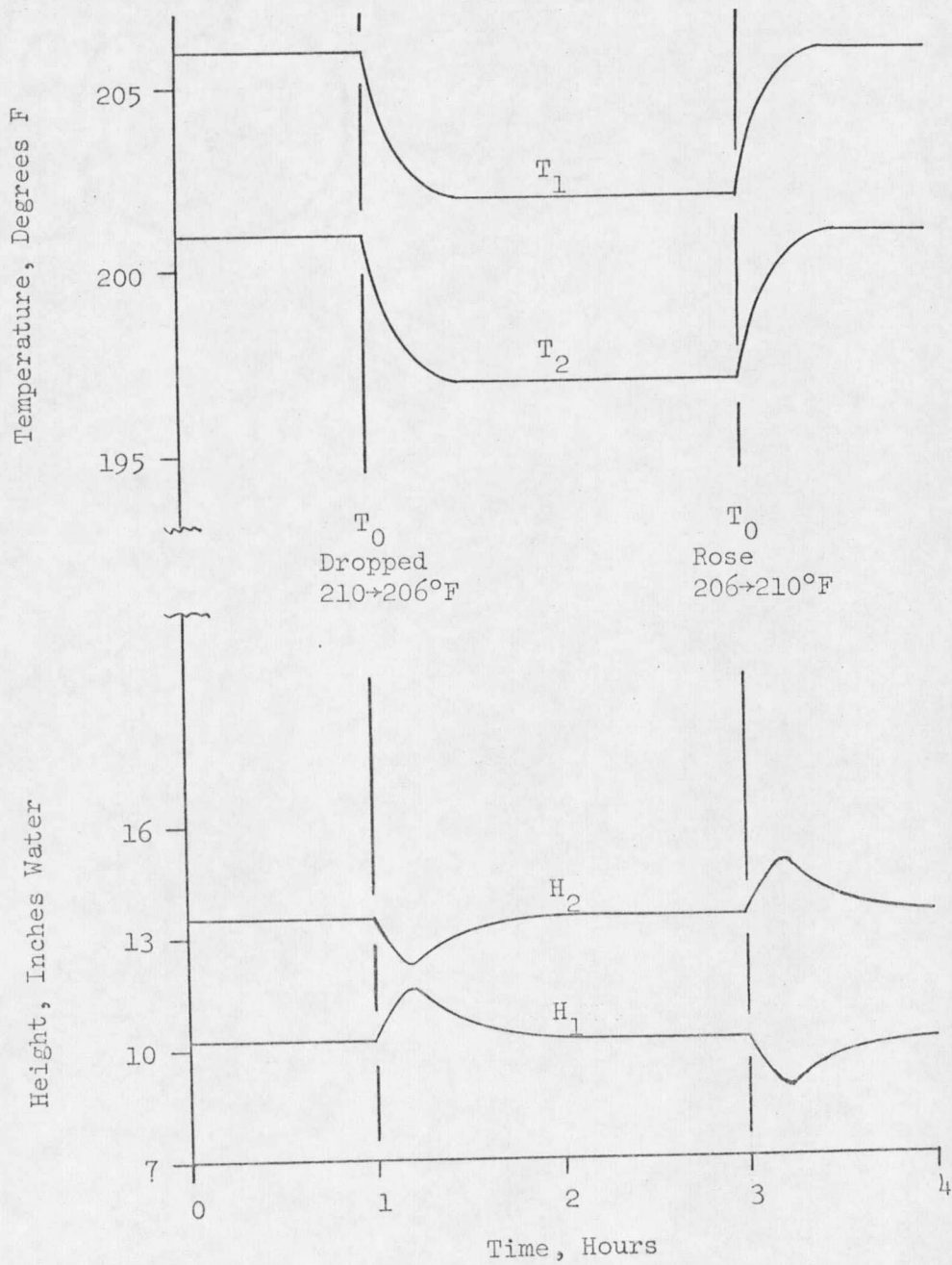


Figure 13. Analog Simulation - Step Response Data

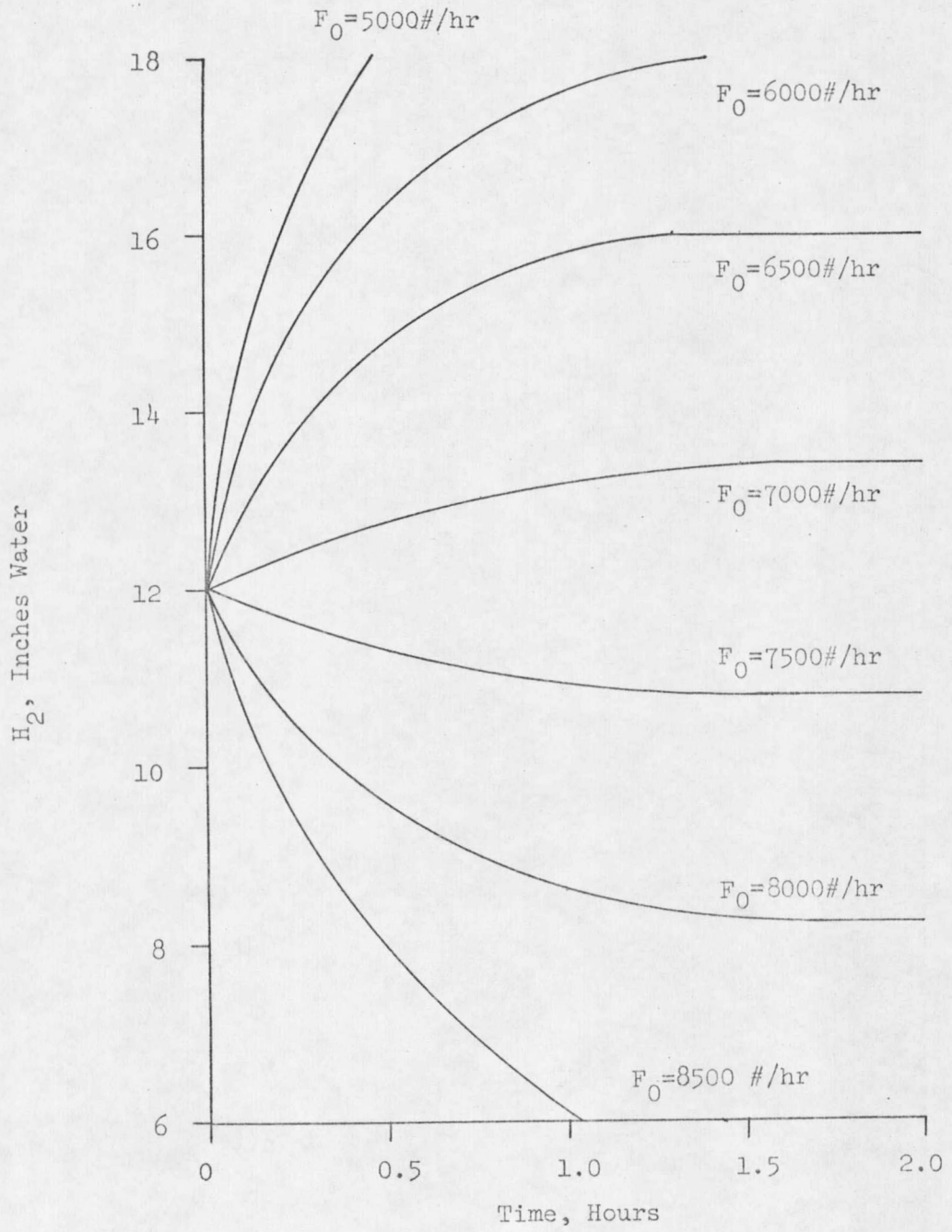


Figure 14. Analog Simulation - H_2 As A Function of F_0

DIGITAL COMPUTER MODEL

2-Tank Simulation

A search for a general-purpose computer program that would solve a system of non-linear differential equations using MSU's SDS Sigma-7 digital computer showed that no such program was available. Therefore, a simulation computer program was written to solve the specific set of equations describing the 2-tank flash evaporator. The integration technique chosen was the Runge-Kutta method as described by Kreyszig(16). To enable the simulation to be run on a computer other than the SDS Sigma-7, the simulation was written in Fortran IV-H. Results of the simulation were listed and printed using the computer lineprinter. The 2-tank simulation is given in Appendix B-1; the plot program is listed in Appendix B-2.

Use of the digital computer provided a simulation that described the 2-tank flash evaporator much better than the analog computer simulation did. The greatest advantage of the digital computer was that it gave greater accuracy and flexibility in the selection of auxiliary equations. For flow from tank 1 to tank 2, Equation 5 was used in its complete form having μ , ρ , and λ as functions of temperature. Equation 6, the vapor pressure of water as a function of temperature, was written into the simulation exactly, without linearization.

Work with the system of differential equations using MSU's SDS

Sigma-7 digital computer showed that a further simplification in the system of differential equations could be made. Using Equation 13 to eliminate $\frac{dh_1}{d\theta}$ in Equation 11 yields:

$$\frac{dT_1}{d\theta} = \frac{12}{\rho_L A_1 h_1} \{F_o(T_o - T_1) - F_o(t_1 - t_2)\} \quad (18)$$

Using Equation 15 to eliminate $\frac{dh_2}{d\theta}$ in Equation 14 gives:

$$\frac{dT_2}{d\theta} = \frac{12}{\rho_L A_2 h_2} \{F_1(T_1 - T_2) - F_o(t_2 - t_3)\} \quad (19)$$

Equations 18 and 19 were further modified by defining $(t_1 - t_2) = \text{TDROP1}$ and $(t_2 - t_3) = \text{TDROP2}$, where TDROP1 and TDROP2 were functions of the temperature difference between the tube bundle and the temperature of the condensing vapor inside each tank:

$$\frac{dT_1}{d\theta} = \frac{12}{\rho_L A_1 h_1} \{F_o(T_o - T_1) - F_o(\text{TDROP1})\} \quad (20)$$

$$\frac{dT_2}{d\theta} = \frac{12}{\rho_L A_2 h_2} \{F_1(T_1 - T_2) - F_o(\text{TDROP2})\} \quad (21)$$

Equations 20, 21, 13, and 15 comprise the system of differential equations describing the 2-tank flash evaporator.

The performance of the evaporator was found to be highly sensitive to the amount of heat removed by the tube bundle in each tank. The heat removed was expressed as a temperature rise in the cooling water flowing through each tank. The limiting heat transfer mode in the tube bundle in each tank was found to be the heat transfer rate from each tube to

the cooling water flowing through the tube. If Q is the heat removed by the tube bundle, M is the flow rate per unit time through the tube bundle, UA is the overall heat transfer coefficient inside tube area of the tube bundle, ΔT_{lm} is the log mean temperature driving force, and ΔT_{rise} is the increase in the temperature of the cooling water, then the following equation holds:

$$Q = (UA) \Delta T_{lm} = MC_p \Delta T_{rise}$$

Or,

$$\Delta T_{rise} = \frac{(UA) \Delta T_{lm}}{MC_p}$$

If the temperature difference is small, a log mean temperature difference approximately equals an arithmetic temperature difference. For a tube of temperature T_s filled with brine of entering temperature T_c , the temperature rise of the brine is:

$$\Delta T_{rise} = \frac{(UA)}{MC_p} \left\{ \frac{(T_s - T_c) + (T_s - T_c - \Delta T_{rise})}{2} \right\}$$

Or,

$$\Delta T_{rise} = \frac{\frac{(UA)}{MC_p}}{1 + \frac{UA}{2MC_p}} + (T_s - T_c)$$

For $C_p = 1 \text{ BTU/#-}^\circ\text{F}$, the temperature rise is:

$$\Delta T_{rise} = \frac{2(UA)}{2M + (UA)} + (T_s - T_c)$$

The change in the temperature of the cooling water flowing through the tube bundle in each tank is then:

$$\text{TDROP}_2(T_2) = \frac{2(UA)_2}{2M + (UA)_2} * (T_2 - T_c) \quad (22)$$

$$\text{TDROP}_1(T_1, T_2) = \frac{2(UA)_1}{2M + (UA)_1} * (T_1 - T_c - \text{TDROP}_2(T_2)) \quad (23)$$

For the 2-tank evaporator, the tube bundle in tank 1 had an inner-tube heat transfer area of 37.8 ft², and the tank 2 tube bundle had an inside area of 26.9 ft². The best fit of the experimental data by the 2-tank simulation was found for U₁ = 7.5 BTU/hr-ft²-°F and U₂ = 90 BTU/hr-ft²-°F. The flow rate through the tube bundle was slightly over 9000 #/hr, which gave a tube Reynolds number of 4000 to 5000 and a calculated heat transfer coefficient of approximately 200 BTU/hr-ft²-°F. The value of U₂ appears reasonable because the evaporator had been run extensively under corrosive conditions. The value of U₁ is very low, and can only be explained by assuming that either extreme scale existed in tube bundle 1 or that the difference measured between T₀ and T₁ was in error. However, there are no inconsistencies in the data; there is less than 1°C difference between T₀ and T₁ in every run.

The development of the 2-tank digital simulation did show why the laboratory evaporator behaved as it did. The amount of heat removed by the tube bundle in each stage accounted for several important effects. The amount of heat removed governed the temperature drop from stage to stage. The variation in the heat-removal rate caused the varying

displacement between the T_0 and T_1 curves, and explains the differences between the ΔT curves for a temperature rise in T_0 and a temperature drop in T_0 . In a temperature step rise upset, hotter water entering tank 2 increases the temperature driving force for heat transfer in the tank 2 tube bundle. Thus, the water in tube bundle 2 reaches a higher temperature and warmer water enters the tank 1 tube bundle. In tank 1, the temperature driving force between the tube bundle and the flashing vapor is less, enabling T_1 to reach an equilibrium temperature nearer to T_0 than it had reached before the upset. Under this same upset, ΔT increases to a higher value after the upset without dropping back to its initial level because of the increased heat transfer in the second tube bundle. For a temperature drop, ΔT tends to return closer to its initial value because the upset decreases the temperature driving force between the tube bundle and the flashing vapor in tank 2. Less heat is removed by the tube bundle in tank 2, which raises T_2 slightly from what it would have been if the heat transfer rate to the tube bundle had remained constant. T_1 undergoes little change because of its low heat transfer coefficient, so ΔT increases to only about half way between the peak upset value and initial value.

The varying heat-removal rate also gave heights of water in the two tanks that lined out to new levels slowly, without returning to the original height levels as the analog simulation did. The rate of flow of water through the evaporator and the temperature drop from

tank to tank set the pressure differential between tanks. In tank 2, the amount of heat lost to the surroundings was found to be negligible compared to that removed by the tube bundle. In tank 1, the heat lost to the surroundings may have had some effect because U_1 was so small. The inlet temperature of the cooling water was found to be one of the important variables regulating the performance of the entire system.

A comparison between the experimental data and the computer simulation is shown in Figures 15-22. For both temperature rise and temperature drop curves, T_1 curves agree well. The ΔT curves, which were the least reliable experimentally, are off by 0.3 to 0.5 °C, but do agree well in shape. The ΔP curves agree well for initial and final values, but disagree in the total deviation at the height of the upset. Since there was some overshoot (up to 2 °C) in the feed temperature T_0 in each run in an attempt to make a sharp step change, this difference does not seem unreasonable. The height curves agree fairly well in each case. All steps show excellent response rates to those rates observed experimentally. For a temperature drop, the simulation flow rate of 9120 #/hr is 1.9% less than the experimental flow rate of 9300 #/hr. For a temperature rise, the simulation flow rate of 9600 #/hr is 1.6% higher than the experimental flow rate of 9450 #/hr. A cooling water inlet temperature of 77 °C was used for the temperature drop run; one of 78 °C for the temperature rise run.

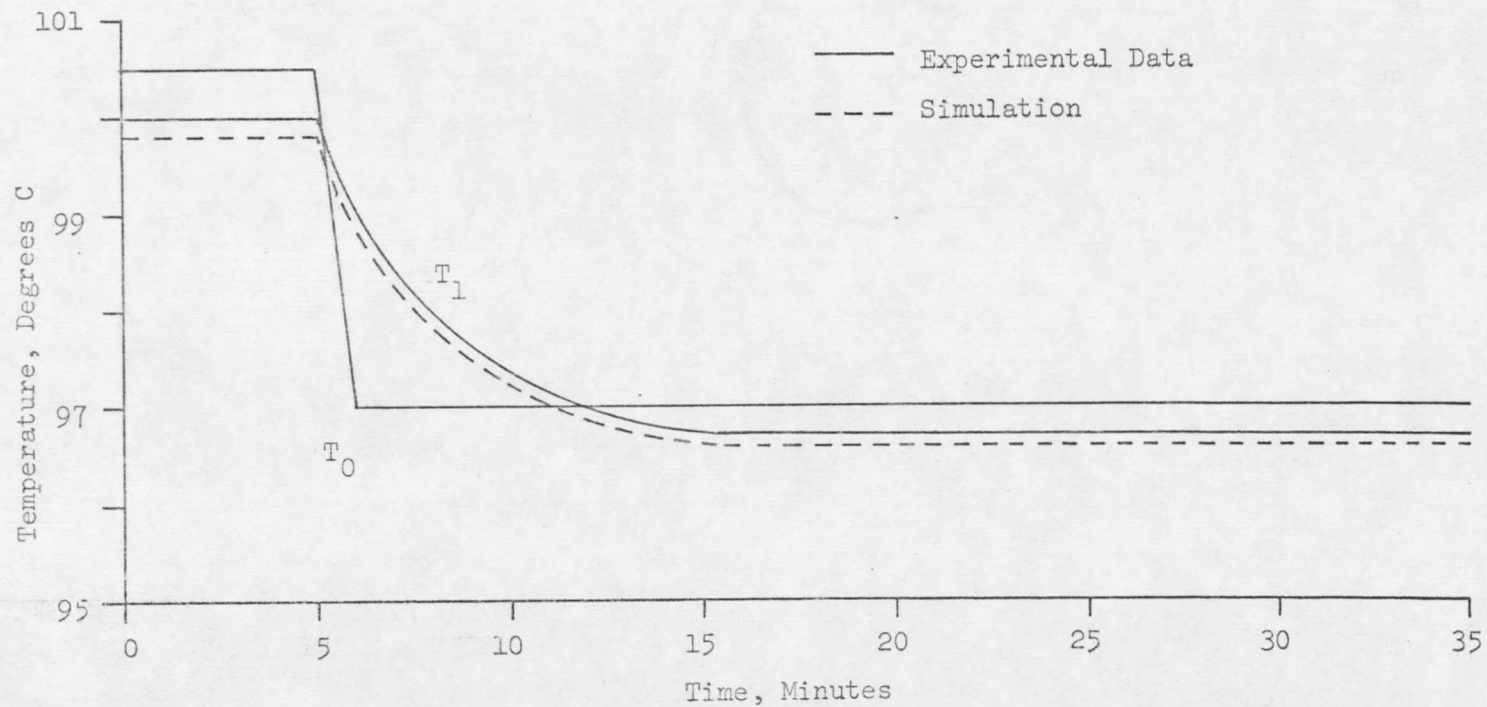


Figure 15. Comparison Between Experimental Data and 2-Tank Simulation, Step Drop in T_0 , T_1 Response Curve

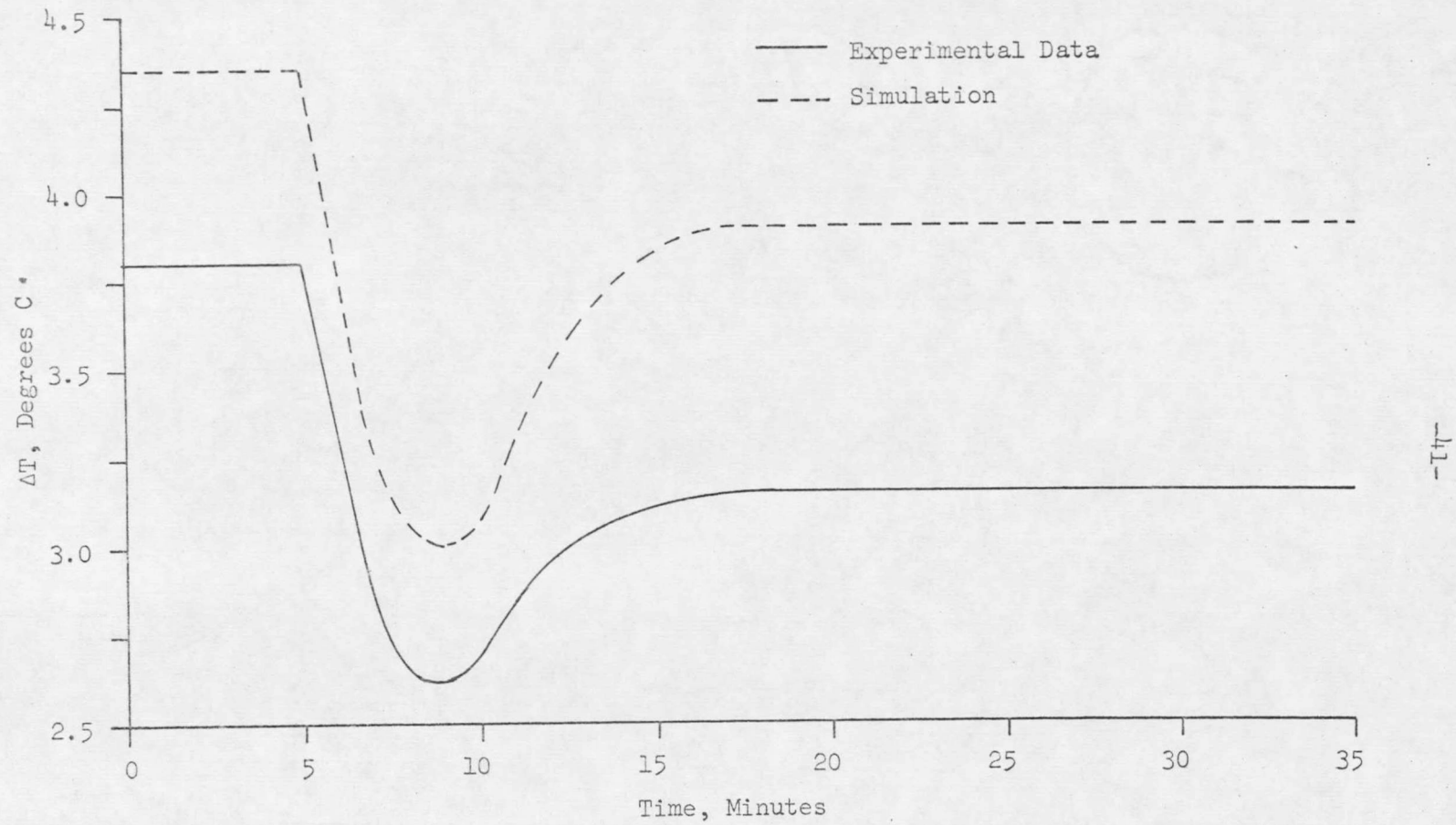


Figure 16. Comparison Between Experimental Data and 2-Tank Simulation, Step Drop in T_0 , ΔT Response Curve

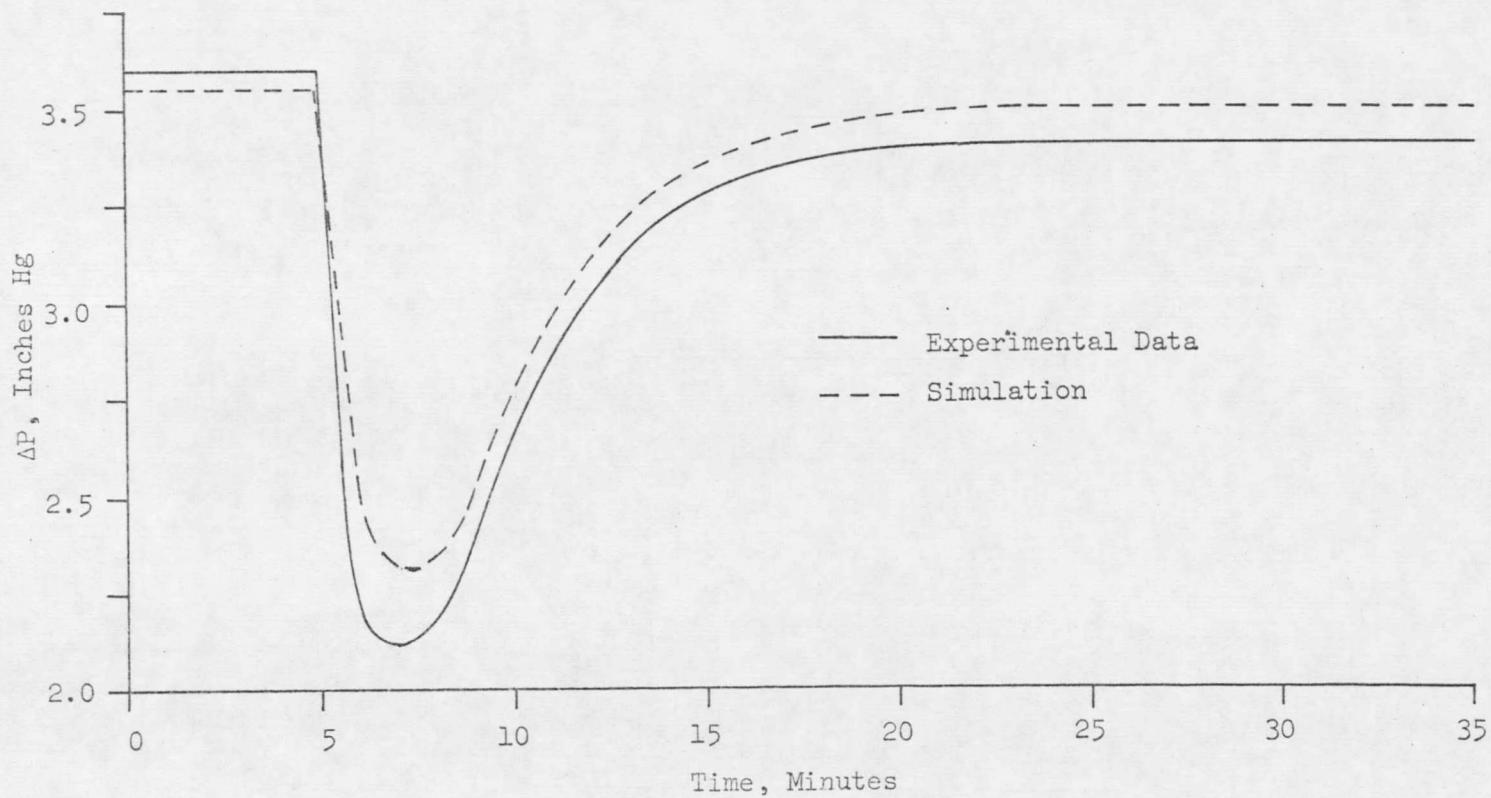


Figure 17. Comparison Between Experimental Data and 2-Tank Simulation
Step Drop in T_0 , ΔP Response Curve

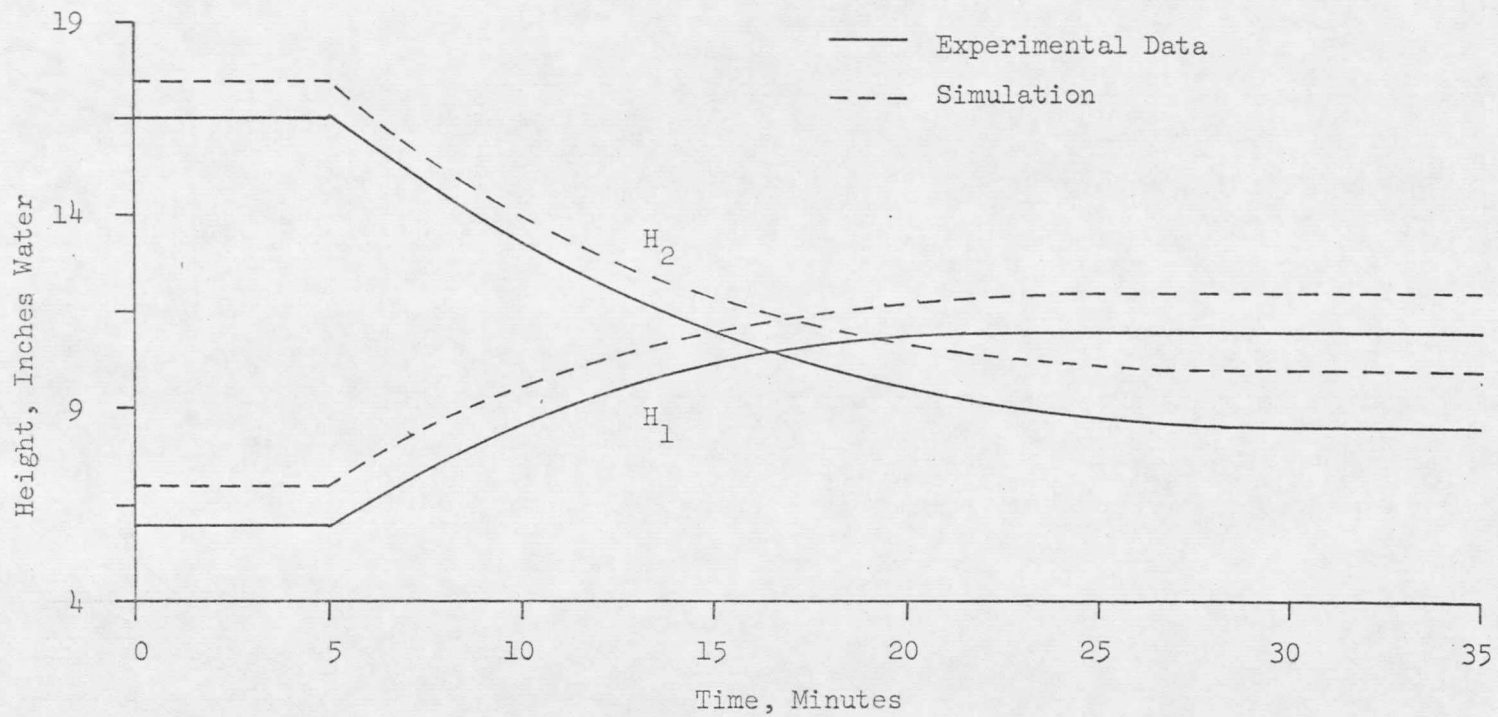


Figure 18. Comparison Between Experimental Data and 2-Tank Simulation, Step Drop in T_0 , Height Response Curves

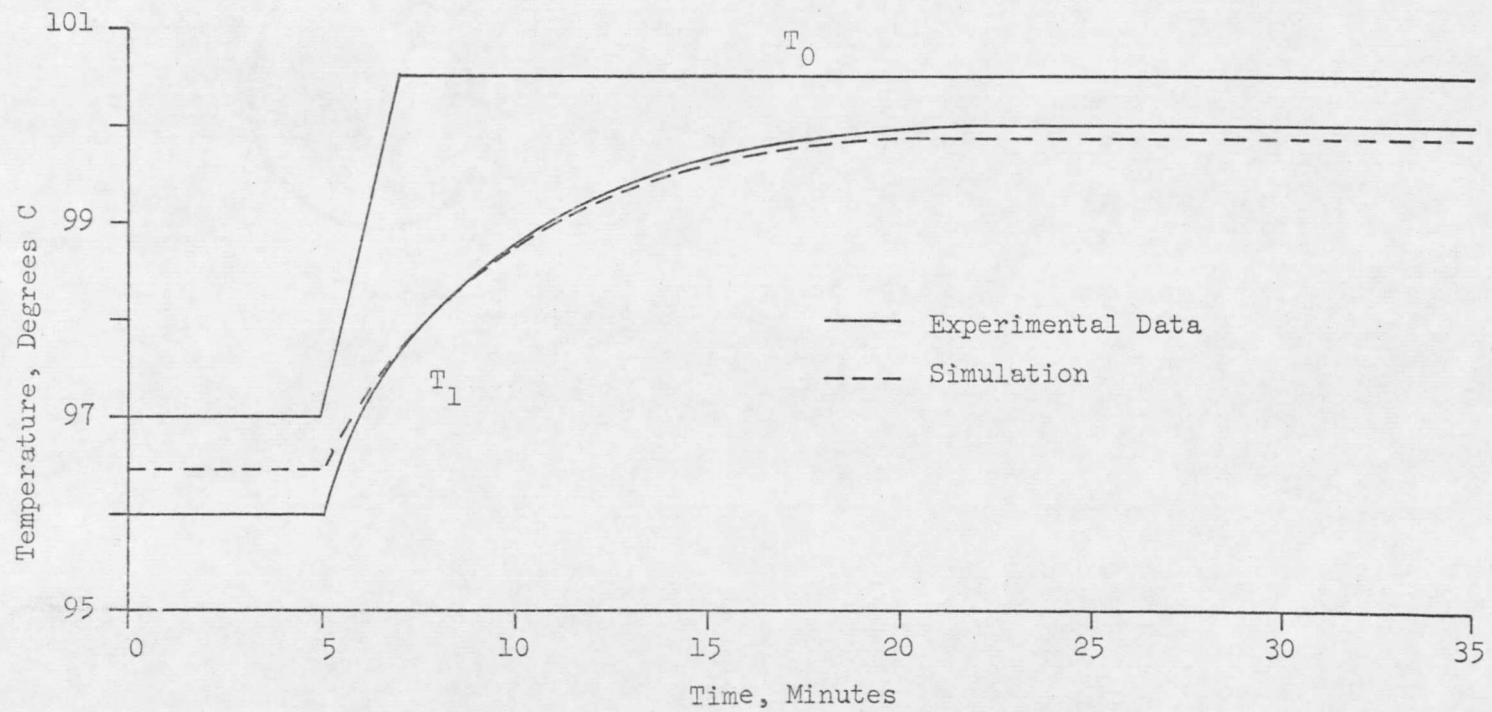


Figure 19. Comparison Between Experimental Data and 2-Tank Simulation, Step Rise in T_0 ; T_1 Response Curve

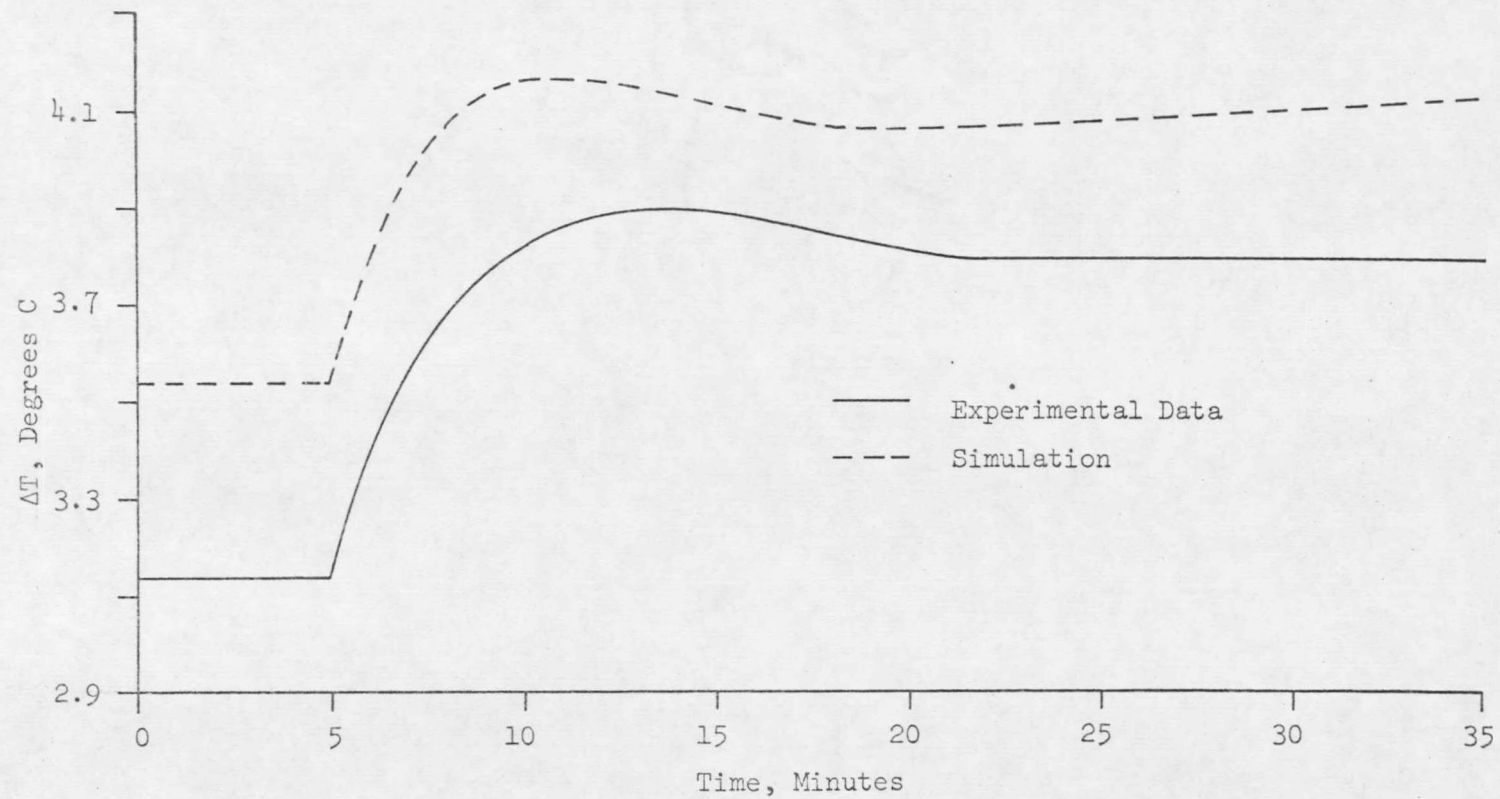


Figure 20. Comparison Between Experimental Data and 2-Tank Simulation, Step Rise in T_0 , ΔT Response Curve

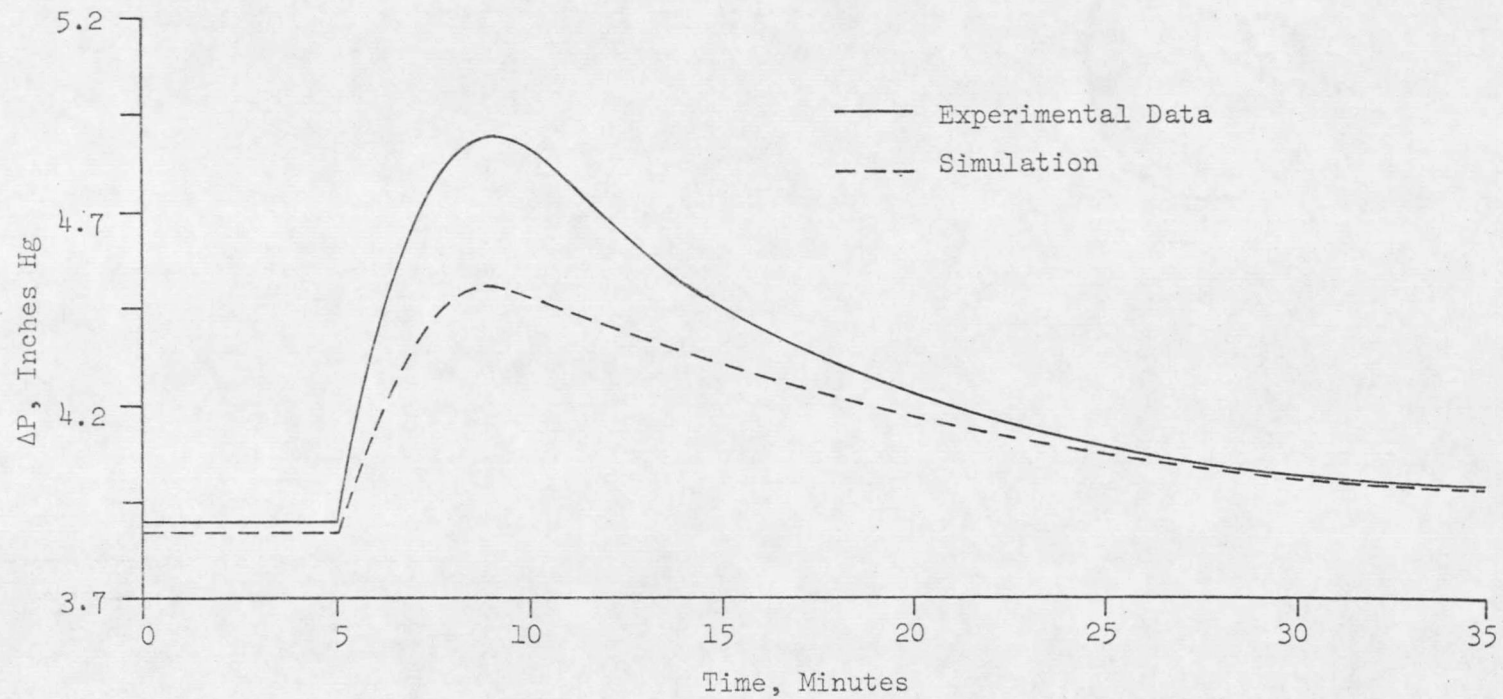


Figure 21. Comparison Between Experimental Data and 2-Tank Simulation, Step Rise in T_0 , ΔP Response Curve

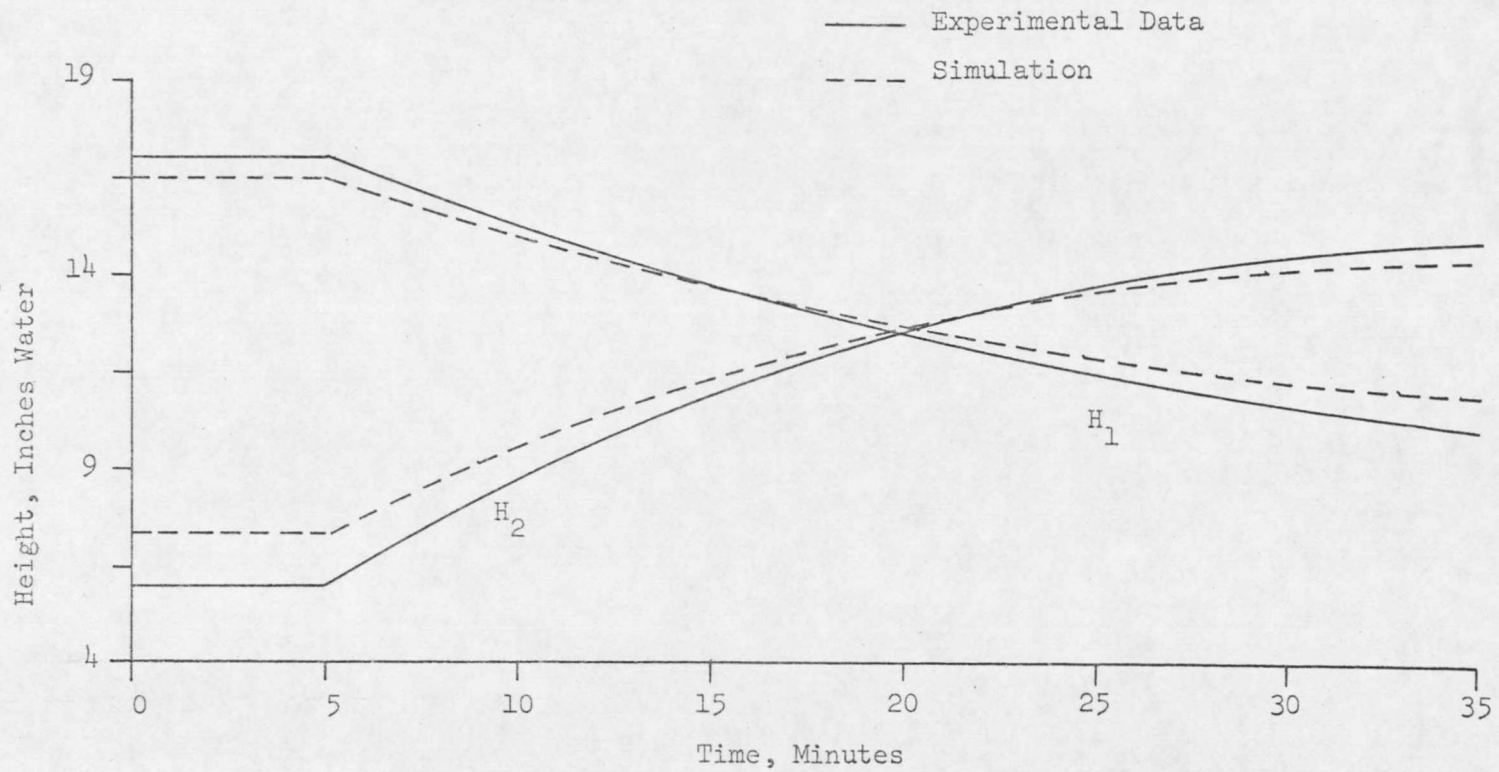


Figure 22. Comparison Between Experimental Data and 2-Tank Simulation, Step Rise in T_0 , Height Response Curves

The 2-tank simulation developed in this paper is quite different from the simulation developed by Electronics Associates, Inc. The EAI simulation uses 12 differential equations and 44 supporting equations that require extensive design and experimental data. Every possible effect upon the operation of the system is represented. Not only are heat and mass balances written for the brine, but a mass balance for the salt concentration, the effect of boiling point rise, and the changes in vapor pressure from the finite rate of air leaking into the system are also included. Even the pressure drop of the vapor as it moves through the demisters to the tube bundle is represented. If the water level in any tank drops below the orifice opening between tanks, the correlation for flow between tanks changes from 2-phase liquid-vapor flow to include vapor flow also. The complexity of the model gives prohibitively long execution times for a digital computer, forcing the solution for the system of equations to be calculated using the hybrid computer.

The 2-tank digital simulation represents the differential mass and energy balance for the brine in relation to the heat removal rate of the tube bundle. The effects of salt concentration and design features other than orifice size, tank size, and tube bundle heat-removal rate are neglected. With these simplifications, the model still represents accurately the response of the laboratory evaporator to upsets in inlet temperature. The less complicated model permits

the solution to the model to be obtained using the digital computer.

Although the digital simulation is much less involved than the hybrid simulation, the hybrid simulation is much faster in execution than the digital simulation. Sixty minutes of simulated time for a 39 tank evaporator takes 20 minutes of execution time using the hybrid computer. Sixty minutes of simulated time for a 2-tank evaporator takes 9.78 minutes of execution time using the digital computer, and extrapolates to 3 hours of execution time for a 39-tank digital simulation run of 60 minutes. However, much pertinent data can be obtained for a large flash evaporator by examining only a few tanks. Thus, the digital model may be used to simulate less than the total number of tanks in the system, and execution times will be less than 3 hours.

4-Tank Simulation

The 2-tank flash evaporator available in the MSU chemical engineering laboratory was unique for several reasons. First, the tube bundles in each tank were different from each other, and hence made each tank behave differently. Second, the laboratory evaporator consisted of only 2 tanks, and could not show experimentally if an evaporator with more than 2 tanks would behave similarly. Third, the water was recirculated in a closed system. If tank 1 rose, then tank 2 fell, giving an artificial stability. To overcome these limitations

and describe more fully the dynamics of the 2-tank flash evaporator, a simulation of a 4-tank flash evaporator was written.

The general differential equations of a 4-tank flash evaporator were derived like those for the 2-tank evaporator and simplified to the following forms:

$$\frac{dT_1}{d\theta} = \frac{12}{\rho_L A_1 h_1} \{F_o(T_o - T_1) - F_o(TDROPI)\} \quad (24)$$

$$\frac{dT_2}{d\theta} = \frac{12}{\rho_L A_2 h_2} \{F_1(T_1 - T_2) - F_o(TDROPI)\} \quad (25)$$

$$\frac{dT_3}{d\theta} = \frac{12}{\rho_L A_3 h_3} \{F_2(T_2 - T_3) - F_o(TDROPI)\} \quad (26)$$

$$\frac{dT_4}{d\theta} = \frac{12}{\rho_L A_4 h_4} \{F_3(T_3 - T_4) - F_o(TDROPI)\} \quad (27)$$

$$\frac{dh_1}{d\theta} = \frac{12}{\rho_L A_1} (F_o - F_1) \quad (28)$$

$$\frac{dh_2}{d\theta} = \frac{12}{\rho_L A_2} (F_1 - F_2) \quad (29)$$

$$\frac{dh_3}{d\theta} = \frac{12}{\rho_L A_3} (F_2 - F_3) \quad (30)$$

$$\frac{dh_4}{d\theta} = \frac{12}{\rho_L A_4} (F_3 - F_4) \quad (31)$$

These equations were programmed using Fortran IV-H, and are given as the complete program in Appendix B-3. A program was also written

(Appendix B-4) to plot the simulation results.

The physical parameters of the 4-tank evaporator were chosen to be similar to those of the 2-tank laboratory evaporator. Tank area was standardized at 8 ft^2 for each of the 4 tanks compared to 8.88 ft^2 and 6.57 ft^2 for the 2-tank evaporator. The maximum allowable height of water in each tank was set at 20 inches, the same as in the 2-tank evaporator. The tube bundle cooling capacity was set at $2000 \text{ BTU/hr-}^\circ\text{F}$ compared to $2440 \text{ BTU/hr-}^\circ\text{F}$ for tank 2 and $285 \text{ BTU/hr-}^\circ\text{F}$ for tank 1 of the 2-tank evaporator. The diameter of the orifice between each of the 4 tanks was set at 0.875 inches.

Using the 4-tank simulation, open loop response studies were run of step changes in T_o and T_c . The results of a 3°C step drop in T_o are shown in Figures 23-26. The temperature curves, ΔT curves, and ΔP curves show that the temperature upset tends to decrease in size as it progresses through the system. The upset moves more rapidly through the tanks than the rate of flow of water from tank to tank would indicate; the upset reaches tank 4 within 3 minutes after being initiated into tank 1, while it would take at least 8 minutes for the water in the first 3 tanks to be totally exchanged by the hotter water now entering tank 1. The height curves tend to line out to new equilibrium values. H_1 follows an exponential-decay-shaped path, while H_2 and H_3 react to prevalent conditions. H_4 declines and finally levels out. The size of the upset

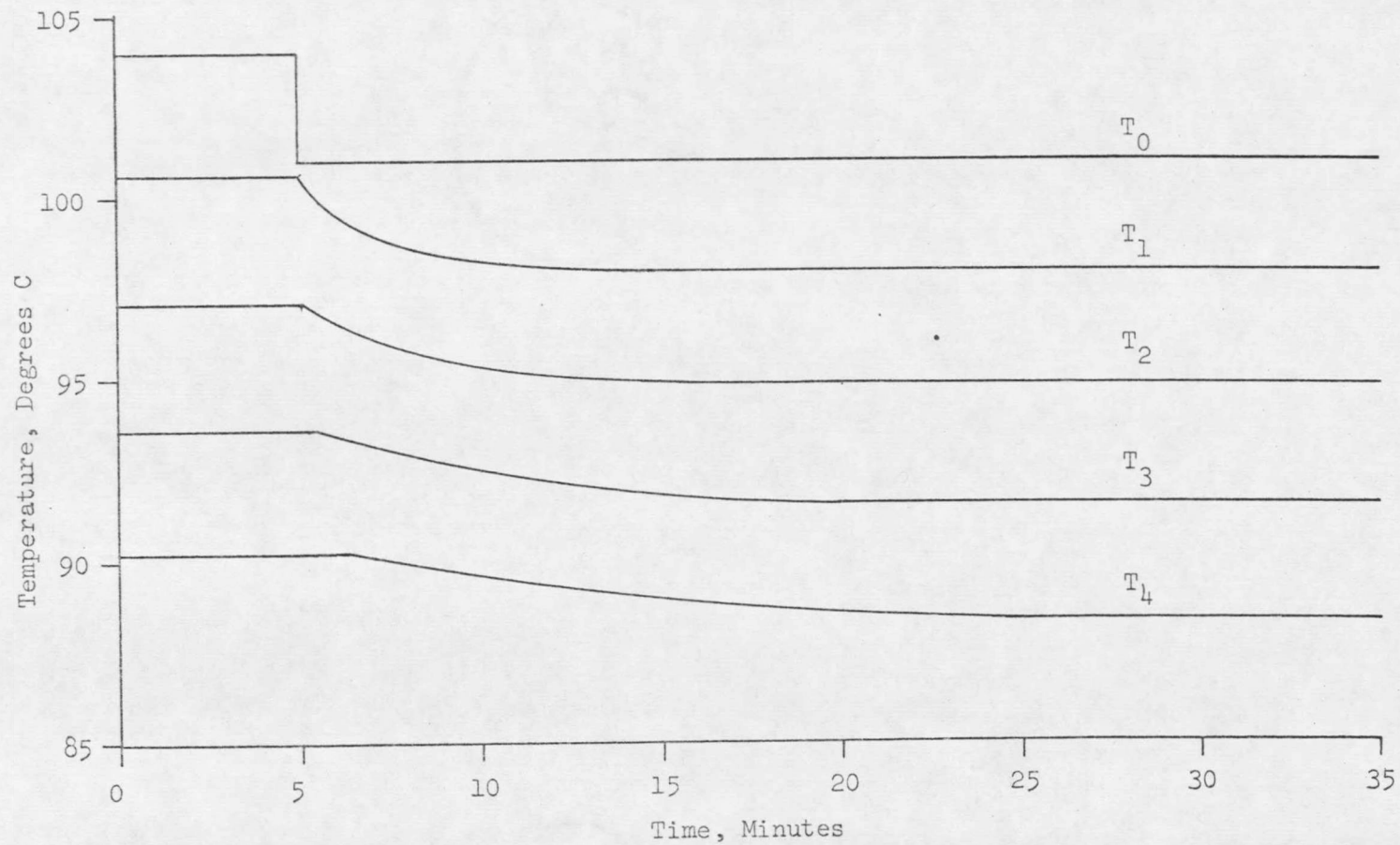


Figure 23. 4-Tank Simulation, Step Drop in T_0 from 104 - 101 °C, Temperature Response Curves

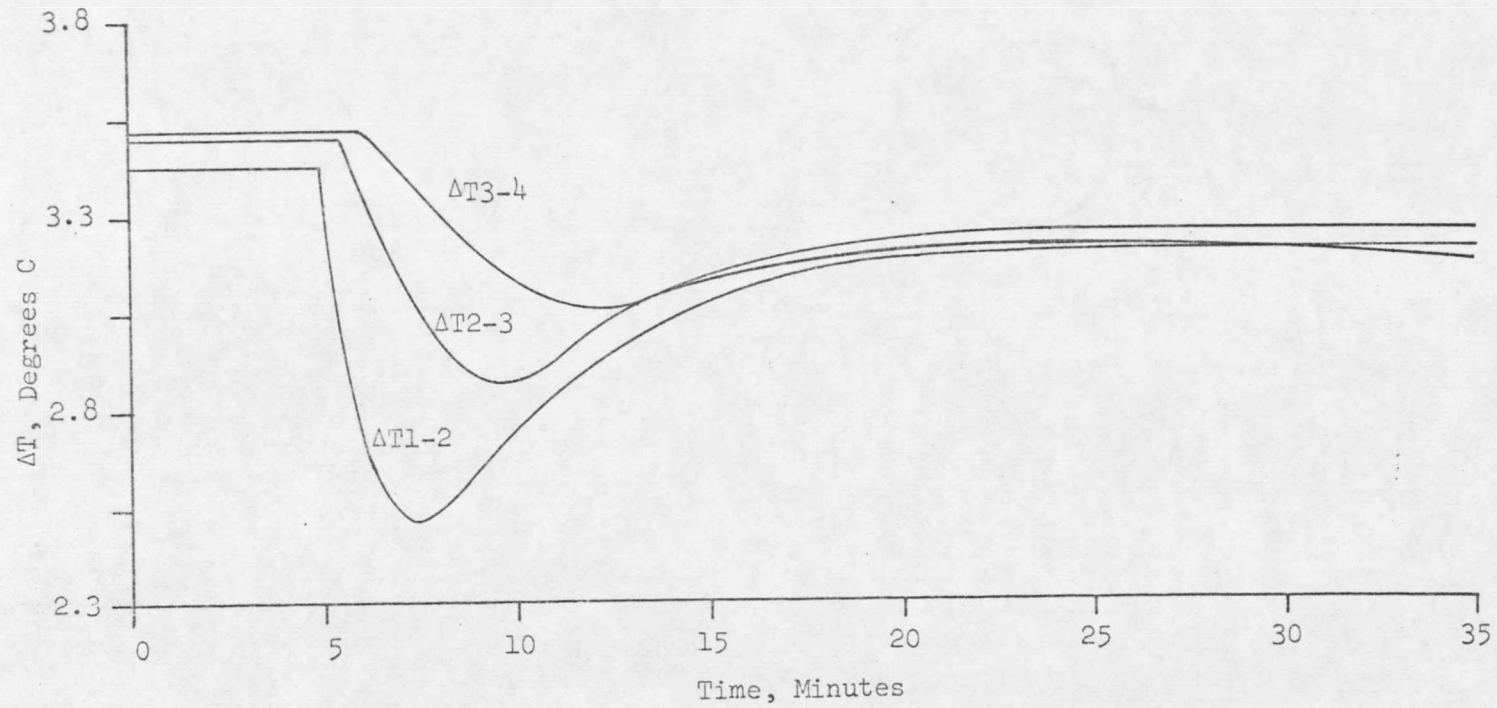


Figure 24. 4-Tank Simulation, Step Drop in T_0 from 104 - 101 °C, ΔT Response Curves

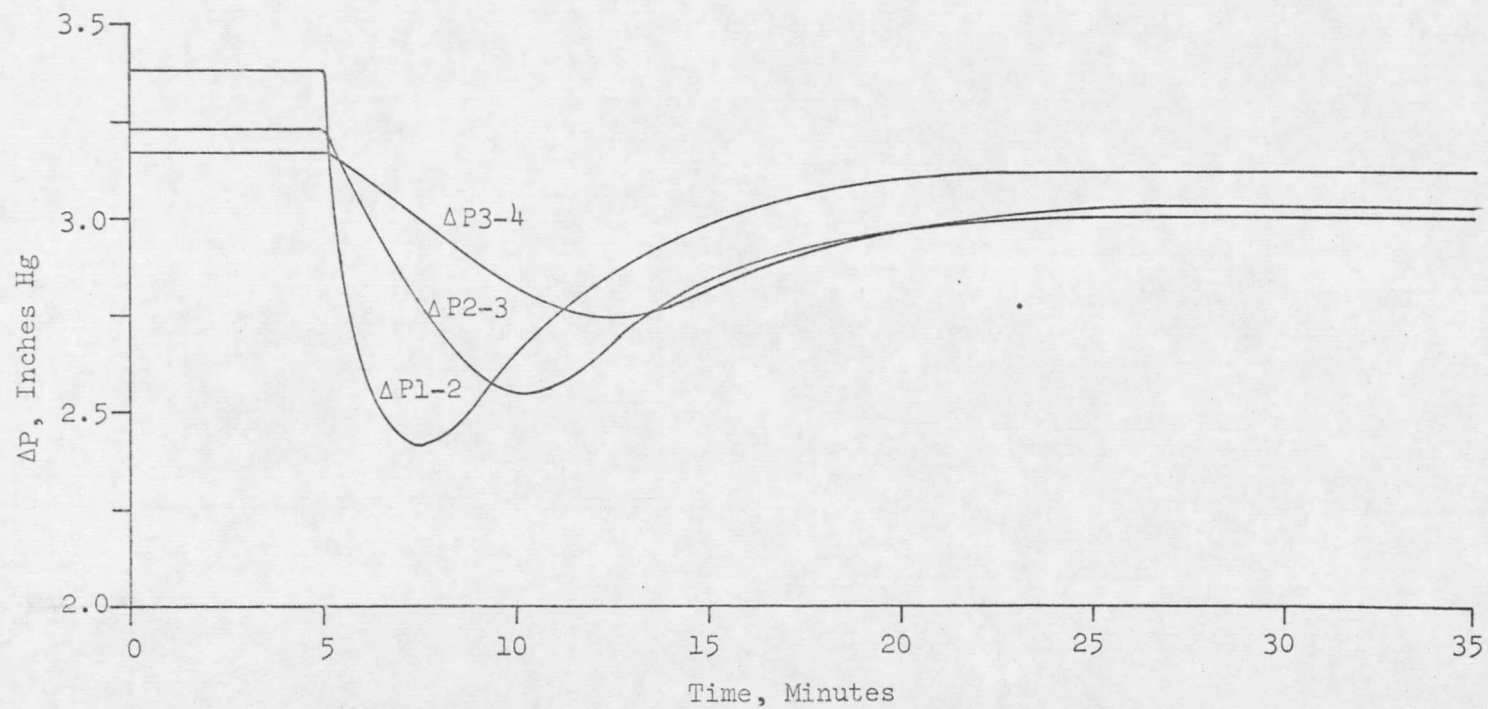
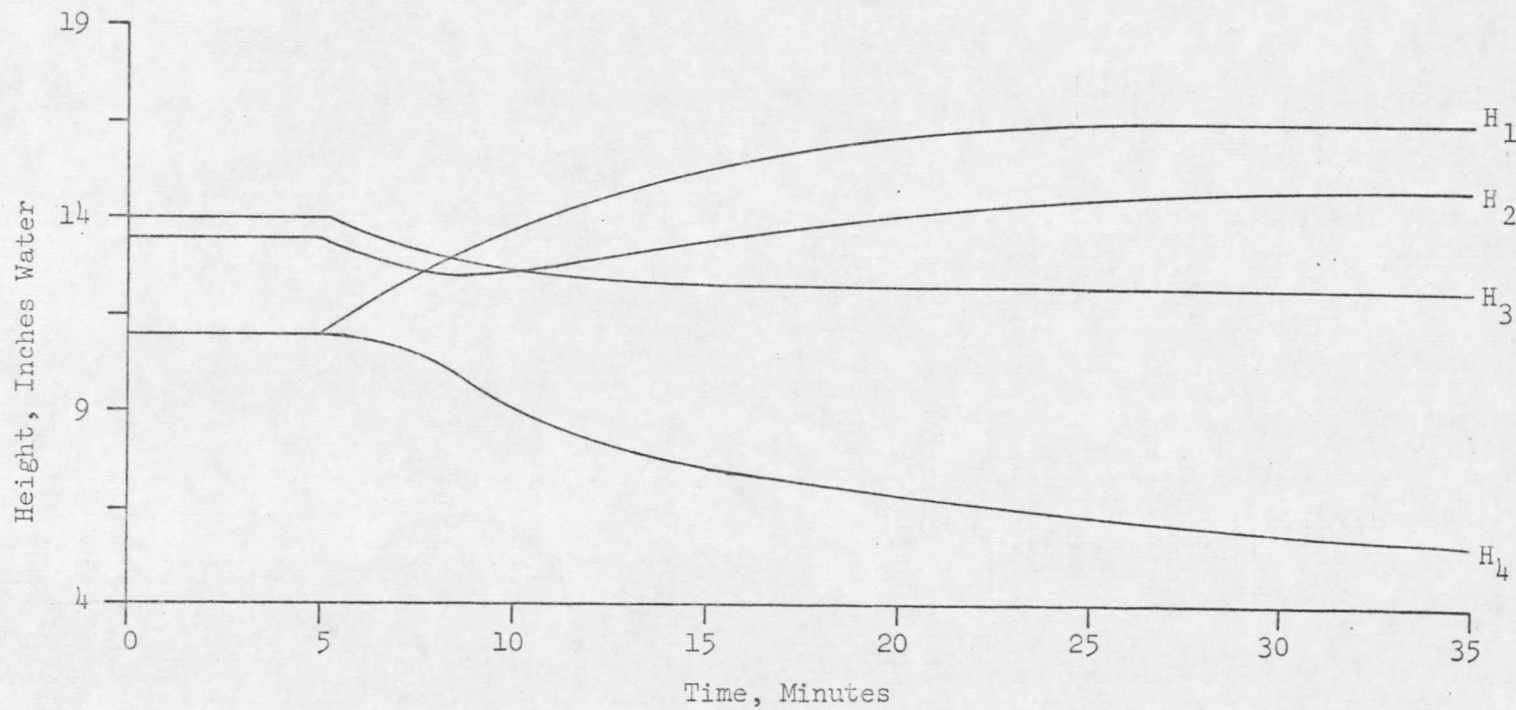


Figure 25. 4-Tank Simulation, Step Drop in T_0 from 104 - 101 °C, in ΔP Response Curves



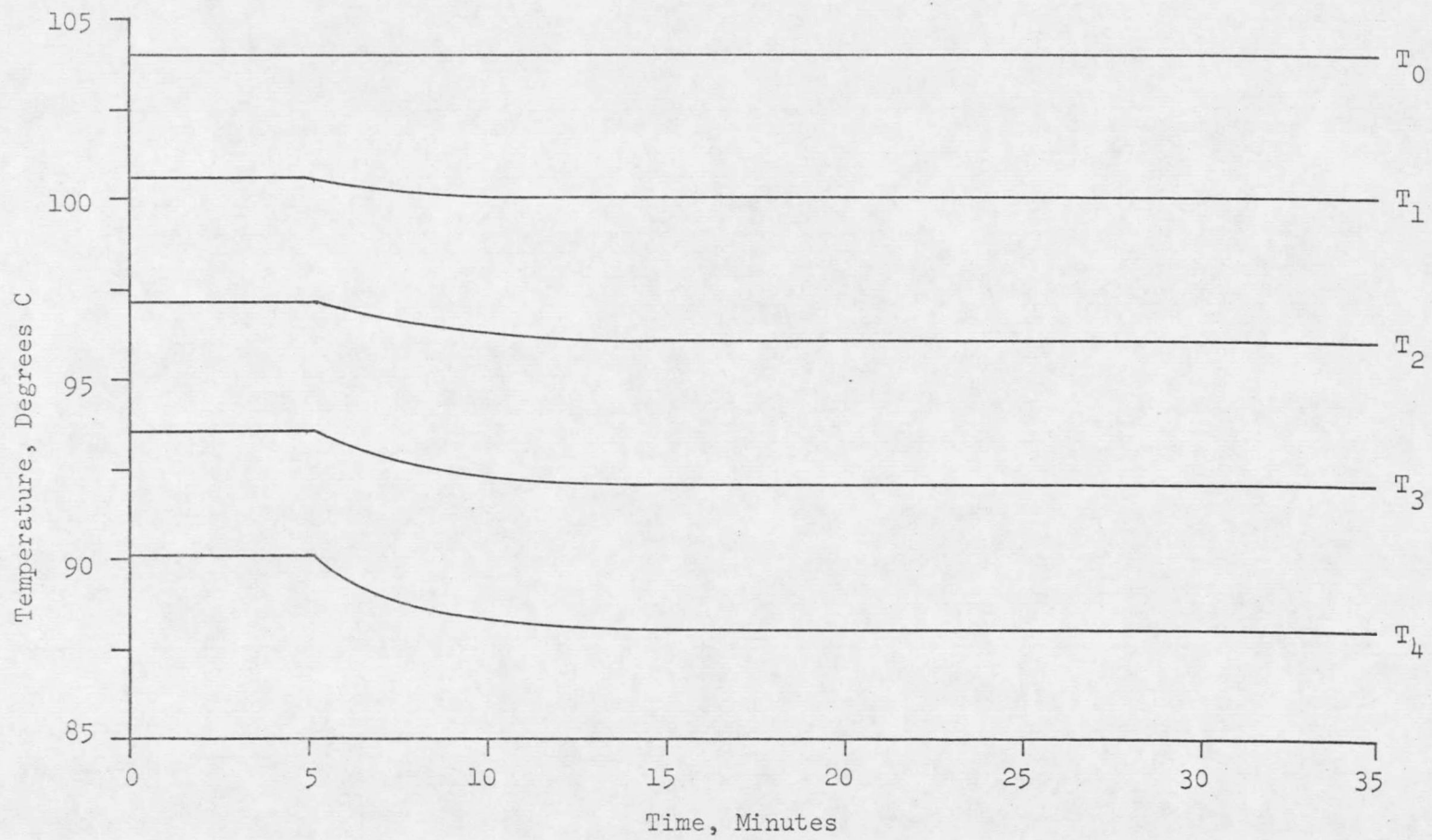
-55-

Figure 26. 4-Tank Simulation, Step Drop in T_0 from 104 - 101 °C, Height Response Curves

was small, a 3 °C change, yet the system nearly went dry in tank 4. A larger upset would have exceeded the limits of stability of the system, and tank 4 would have gone dry. A 3 °C step rise in T_o shows a similar progression of the upset through the tanks, and corresponding changes in heights. H_4 is more stable to a step rise in T_o with these initial heights in each tank, and tends to stabilize as long as the upset is not too large.

In comparison with the 2-tank model, the 4-tank model reacts less to a change in T_o . In the 4-tank model, tanks 2 and 3 are not directly coupled on both ends as tanks 1 and 2 are in the 2-tank model. Upsets decrease in intensity while passing through tanks 2 and 3, while the conditions within the tanks are not greatly affected. By being coupled to tank 2, tank 1 reacts less to the upset. Tank 4 receives a weaker upset and reacts less. The upset in T_o is spread throughout more tanks, upsetting any one tank less.

A step drop in the cooling water or fresh brine temperature T_c from 73 to 68 °C is shown in Figures 27-28. Cooler water in the tube bundle increases the rate of heat transfer from the vapor in each tank to the tube bundle, lowering the temperature in each tank. Because the upset begins with the end tank, tank 4, the effect is strongest there. The drop in the tank temperatures decreases until, in tank 1, there is little change in T_1 . H_4 rises because more heat is removed there by



-57-

Figure 27. 4-Tank Simulation, Step Drop in T_c from 73 - 68 °C, Temperature Response Curves

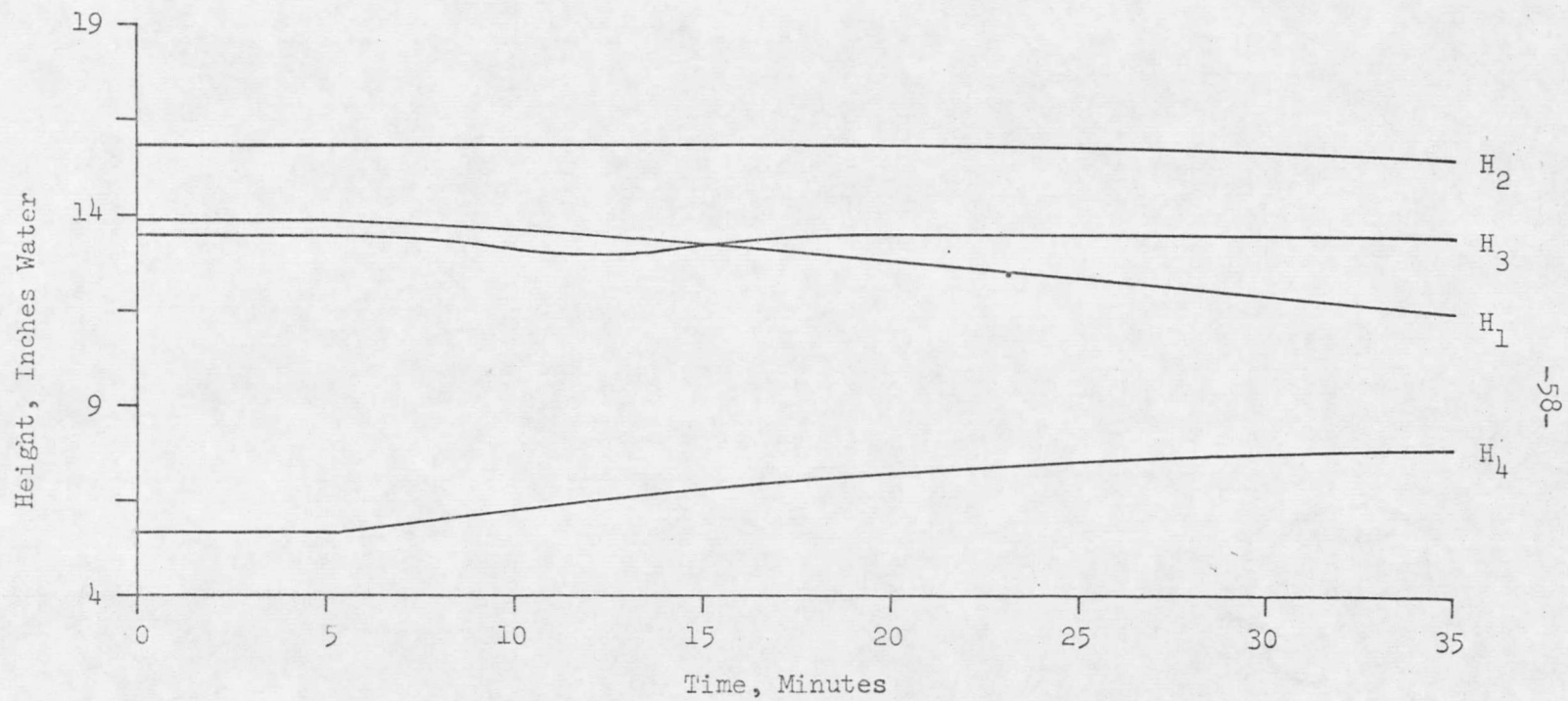


Figure 28. 4-Tank Simulation, Step Drop in T_c from 73 - 68°C, Height Response Curves

the tube bundle, giving a larger ΔT and ΔP between tanks 3 and 4, while the outlet flow is constant. H_1 drops because ΔT and ΔP increase between tanks 1 and 2, causing more water to flow out of tank 1 than enters at the fixed flow rate F_0 . Heights of water in tanks 2 and 3 remain almost constant. For a step rise in T_c from 73 to 78 °C, a corresponding upset is produced. Tanks 1 and 4, the end tanks, are less stable than interior tanks in the system.

Use of the 4-tank simulation not only gave a means to test the stability of a flash evaporator to upsets in feedstream temperatures, but it also gave a way to test changes in equipment design as well. The stability of the 4-tank model as a function of tank size was tested using a step rise in T_0 from 103 to 106 °C. Values of T_1 were observed for evaporators with tank areas of 8 ft², 20 ft², and 50 ft² (Figure 29). The steady-state temperatures in each evaporator were equal, and the equilibrium heights of water in each evaporator were equal. Increased tank area slowed the rate of response to an upset, but it did not alter steady-state conditions. The simulation run with 8 ft² tanks reacted 2 1/2 times faster to a step upset in T_0 than a simulation run with 20 ft² tanks; it reacted about 6 times faster than a simulation run with 50 ft² tanks. The rate of response to a temperature upset is related to the time constant $\tau = (\text{Tank Volume})/(\text{Inlet Flow Rate})$ and is described in a later section. Increased tank size is useful to regulate minor cyclic fluctuations in T_0 , but it will not change the total effect

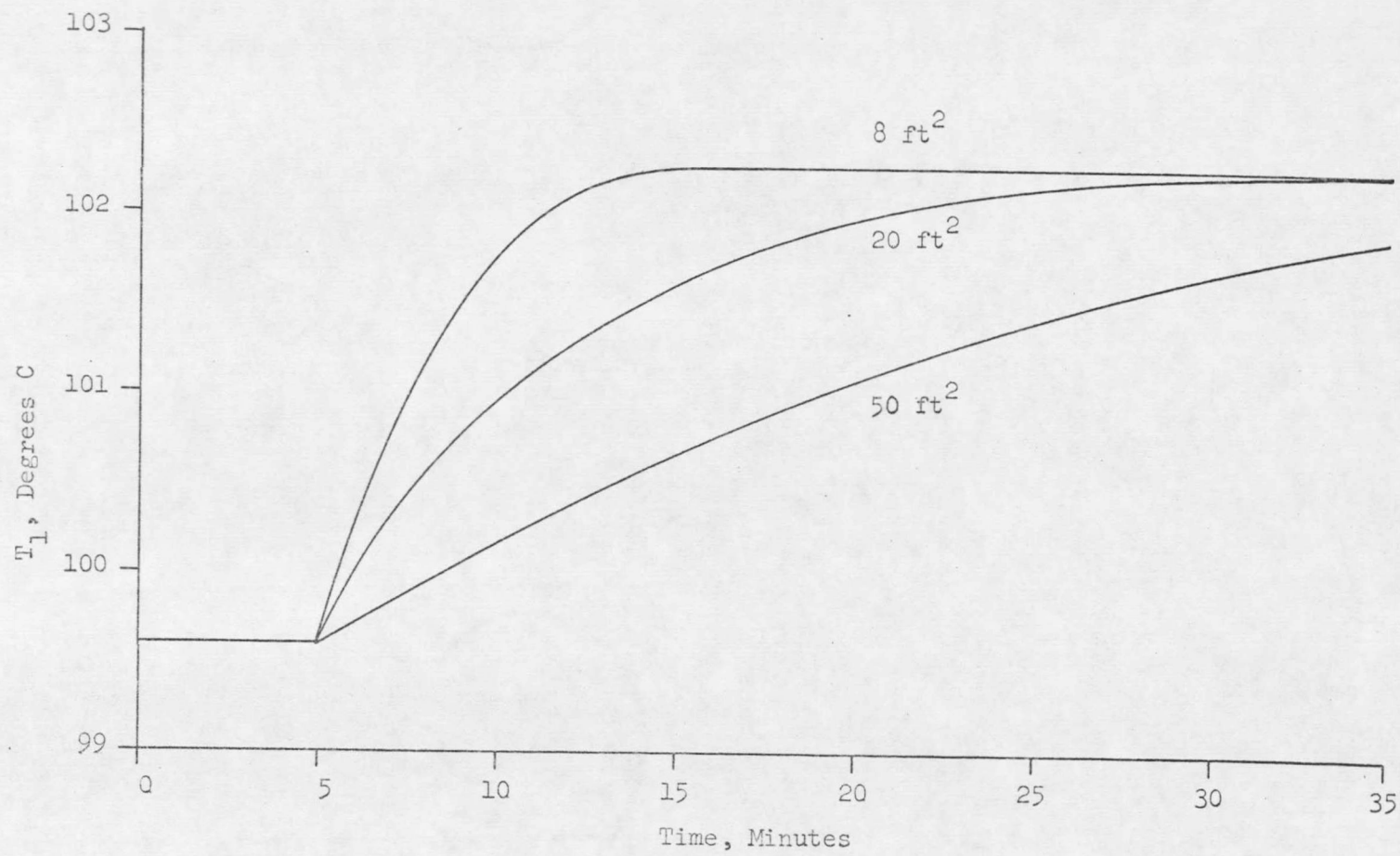


Figure 29. 4-Tank Simulation, Step Rise in T_0 from 103 to 106°C, Response of T_1 for Evaporators with Tank Areas of 8 ft², 20 ft², and 50 ft²

of a step change in T_o .

The effect of tube bundle heat-removal capacity upon evaporator performance was tested using a step rise in T_o from 103 to 106 °C. For heat removal rates 2000 BTU/hr-°F, 4000 BTU/hr-°F, and 8000 BTU/hr-°F, the responses of T_1 to the step rise in T_o are given in Figure 30. Increased heat removal gives different steady-state operating temperatures. A larger heat-removal rate gives a greater ΔT between tanks and a lower equilibrium temperature in each tank. The rate of response of the 4-tank model to an upset in T_o is faster for the runs having a higher heat-removal rate. T_1 reaches its new equilibrium value within 12 minutes after the upset when the heat removal rate is 8000 BTU/hr-°F. When the heat removal rate is 2000 BTU/hr-°F, a new equilibrium value of T_1 is reached in about 15 minutes. No significant differences in the stability of the 4-tank model were observed as functions of the heat removal rate of the tube bundle.

The 4-tank flash evaporator model also enabled steady-state runs to be made at different flow rates. Flow between tanks is a function of both the orifice size and the pressure drop across the orifice. The simplest way to regulate flow rate through the evaporator is to change the size of the orifice between each tank. For an evaporator with fixed orifices, changes in flow must be accomplished by changing the pressure drop across each orifice. This may be done by either

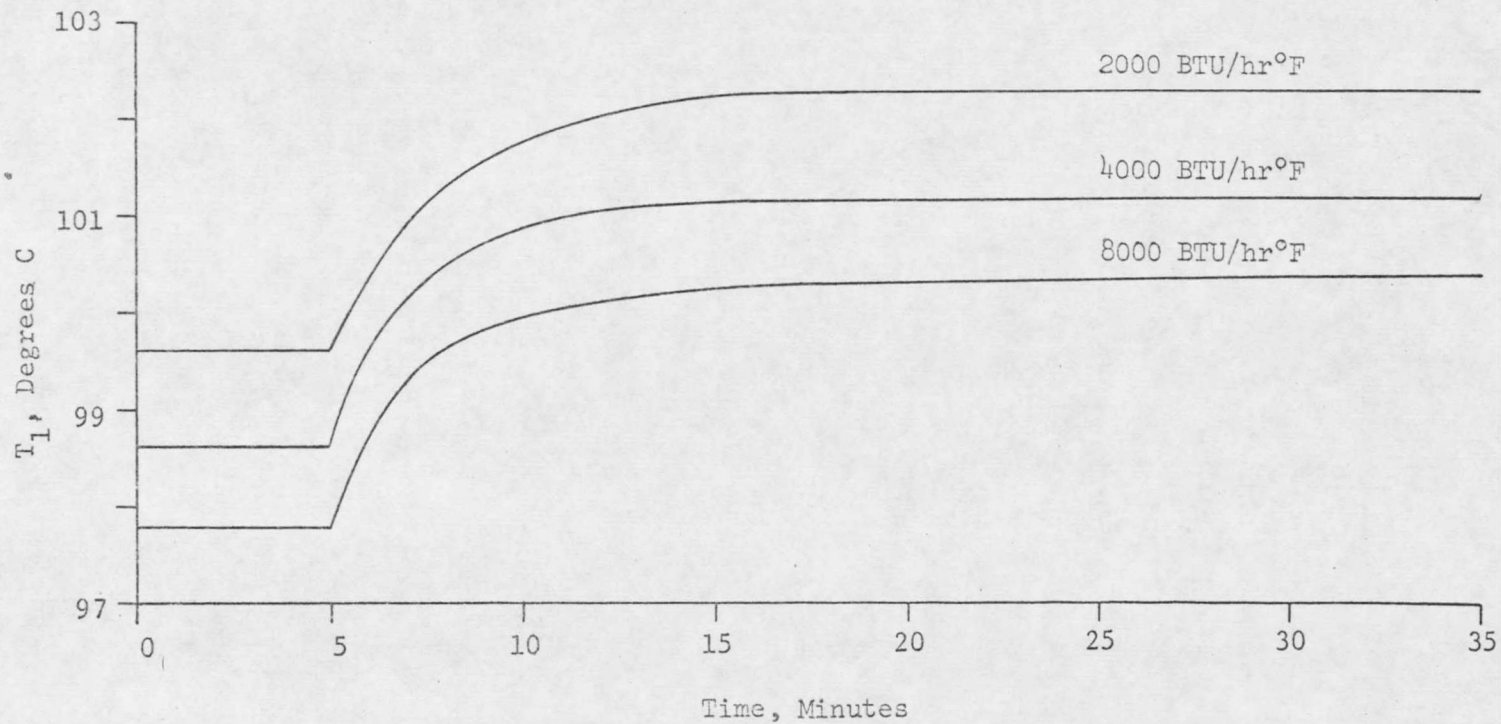


Figure 30. 4-Tank Simulation, Step Rise in T_0 from 103 to 106°C, Response of T_1 for Evaporators with Tube Bundle Heat-Removal Rates of 2000 BTU/hr°F, 4000 BTU/hr°F, and 8000 BTU/hr°F

changing the temperature range over which the evaporator operates or by increasing the heat removal rate in the tube bundle. Increasing the temperature in the evaporator increases the pressure drop from tank to tank because the vapor pressure of water increases with increasing temperature faster than the temperature itself increases. A higher pressure drop between tanks gives more flow. Decreasing the temperature in the evaporator lowers the pressure drop from tank to tank and decreases the flow rate through the evaporator. This effect is small, and only small changes in flow result. For an orifice size between tanks of 0.875 inches and a heat removal rate in each tank of 2000 BTU/hr-°F, a rise in T_o from 103 to 106 °C changes the average flow rate through the evaporator from 152 #/min to 153 #/min. A much more satisfactory way to change the flow rate through the evaporator is to change the tube bundle heat-removal rate in each tank. For a heat-removal rate of 2000 BTU/hr-°F, the average flow through the evaporator is 145 #/min; for 4000 BTU/hr-°F, the average flow is 156 #/min; for 8000 BTU/hr-°F, the average flow is 166 #/min. An increased heat-removal rate may be obtained by decreasing T_c or by increasing the (UA) heat transfer term for each tube bundle. Use of the 4-tank simulation has shown that changes in flow rate through the evaporator cannot be made without changing the temperatures within the system.

Stability of a Flash Evaporator

The temperature upsets discussed for the 2-tank and 4-tank

evaporators were chosen to show how the evaporator would react to a given change. Each upset was small, 3 - 5 °C, so that lineout values for the variables could be obtained. For upsets larger than 3 - 5 °C, the evaporator might or might not have reached equilibrium before a tank either pumped itself dry or filled to capacity. In a mathematical sense, for tanks of infinite size, the flash evaporator is everywhere stable. In actual equipment, finite tank size imposes narrow limits of stability. Increased tank depth increases the stability of a flash evaporator to larger upsets because of the larger head differences between tanks that are possible. Tanks of increased area slow down the rate of response to upsets, but offer no more stability than smaller tanks with equal depths.

Stability depends not only upon the size of the upset but also upon the frequency with which it is applied. A system may contain resonant frequencies, frequencies at which upsets magnify themselves in intensity. A step upset is composed of all frequencies superimposed upon one another. The general stability of the 2- and 4-tank models suggests that there are no resonant frequencies for this system. To confirm that stability existed at all frequencies of forced upsets, a frequency response study of the flash evaporator to upsets in T_0 was run. Teasdale (23) gives a method for finding frequency response data from step response data. Using the response of H_1 to a step change in T_0 on the 4-tank evaporator, a frequency response curve was plotted for

a step rise in T_o and a step drop in T_o . These data were compared to data obtained from actual response of the model to sinusoidal changes in T_o at varying frequencies. (See Figure 31.) A different curve was obtained for a step rise in T_o than for a step drop in T_o due to the slower rate of reaction of the evaporator to a step rise in T_o . The simulation oscillation curve is a combination of the step increase and step decrease functions, and lies between them. The frequency response study shows that the response of the system to a forcing input temperature upset decreases as the frequency increases, and contains no resonant frequencies. The simulation phase lag curve tends to level out at high frequencies, and the amplitude ratio curve slope approaches 2 at high frequencies, indicating that at high frequencies the system order approaches 2.

Rate of Response to Upsets

The rate of response of the flash evaporator to step changes can be estimated using the idea of a time constant. For a first order system undergoing change to a new equilibrium state following a step upset, 63.2% of the change occurs in the time interval equal to 1 time constant, 86% of the change in the time interval equal to 2 time constants, and 95% of the change in the time interval equal to 3 time constants. For the 2-tank evaporator model, the following calculations were made for a step upset in T_o .

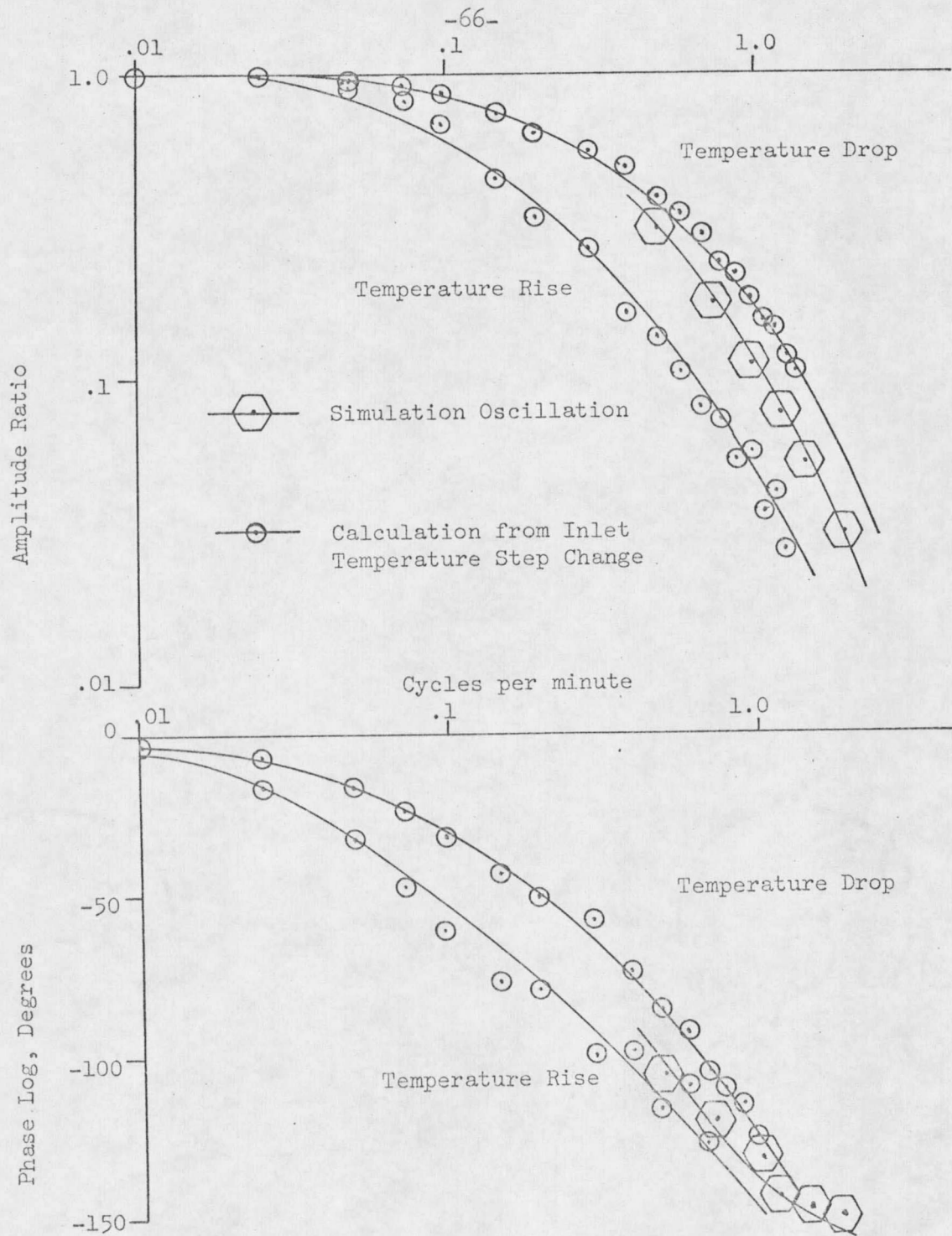


Figure 31. Frequency Response Study

Temperature Rise -

$$\tau = \text{volume/flow} = 4.05 \text{ minutes}$$

2-tank model, response of T_1 .

1 * $\tau = 4.25$ minutes	
2 * $\tau = 8.05$ minutes,	$\tau = 4.03$ minutes
3 * $\tau = 11.85$ minutes,	$\tau = 3.95$ minutes

2-tank model, response of H_1

1 * $\tau = 14.30$ minutes	
2 * $\tau = 26.15$ minutes,	$\tau = 13.07$ minutes
3 * $\tau = 35.65$ minutes,	$\tau = 11.88$ minutes

Temperature Drop -

$$\tau = \text{volume/flow} = 2.48 \text{ minutes}$$

2-tank model, response of T_1

1 * $\tau = 2.05$ minutes	
2 * $\tau = 4.40$ minutes,	$\tau = 2.20$ minutes
3 * $\tau = 7.35$ minutes,	$\tau = 2.45$ minutes

2-tank model, response of H_1

1 * $\tau = 6.50$ minutes	
2 * $\tau = 17.15$ minutes,	$\tau = 8.57$ minutes
3 * $\tau = 29.20$ minutes,	$\tau = 9.73$ minutes

The τ calculated from volume/flow agrees with the τ for the response of T_1 , since the rate of temperature rise in tank 1 follows almost exactly the model of a first-order mixing process. The time constant for the rate of response of H_1 to a step upset in T_0 is about 3 times greater than τ for T_1 . Due to the interaction of the system, the rate of response of H_1 to a step input change is about 3 times slower than the rate of response of T_1 to the change.

For the 4-tank evaporator, the rate of response to temperature upsets is similar to the 2-tank evaporator. Values of $\tau = \text{Vol}/\text{Flow}$ agree generally within 15% of those taken for the temperature in tank 1 at 63.2%, 86%, and 95% of the total temperature change from the upset. The rate of response of the height of water in tank 1 is 2 to 2 1/2 times slower than the rate of response of the temperature. The response rate does not depend upon the rate of heat removal by the tube bundle.

CONTROL OF A FLASH EVAPORATOR

The changes in water heights and temperatures that resulted when load upsets were applied to the 4-tank simulation pointed out the need for stabilizing control action. Because upsets die out as they pass from tank to tank, the stability of the inner tanks of a flash evaporator results from controlling the conditions within the end tanks. Stability of the end tanks follows from control of T_o , F_o , T_c , and the flow rate from the final tank. In a report to the Office of Saline Water (19), Fluor Corporation specifies the necessary control for a flash evaporator as shown in Figure 32. The proper inlet temperature is maintained by control of the steam pressure to the steam heat exchanger. The cooling water temperature is maintained by using a liquid-liquid heat exchanger and by mixing warm waste brine with the cool fresh brine from the ocean. The level in tank 1 is maintained by control of F_o using a pneumatic flow controller. The level in the last tank is maintained by controlling the flow of waste brine from the system. Thermocouples are used to indicate the temperature in each tank, and sight glasses are inserted in each tank to indicate liquid level.

To examine the response of a flash evaporator under corrective controller action, the 4-tank simulation was modified to include proportional-integral (P-I) control. A temperature controller was added to control either T_o or T_c , and a flow controller was added to regulate F_o . The height of water in tank 4 was held constant at

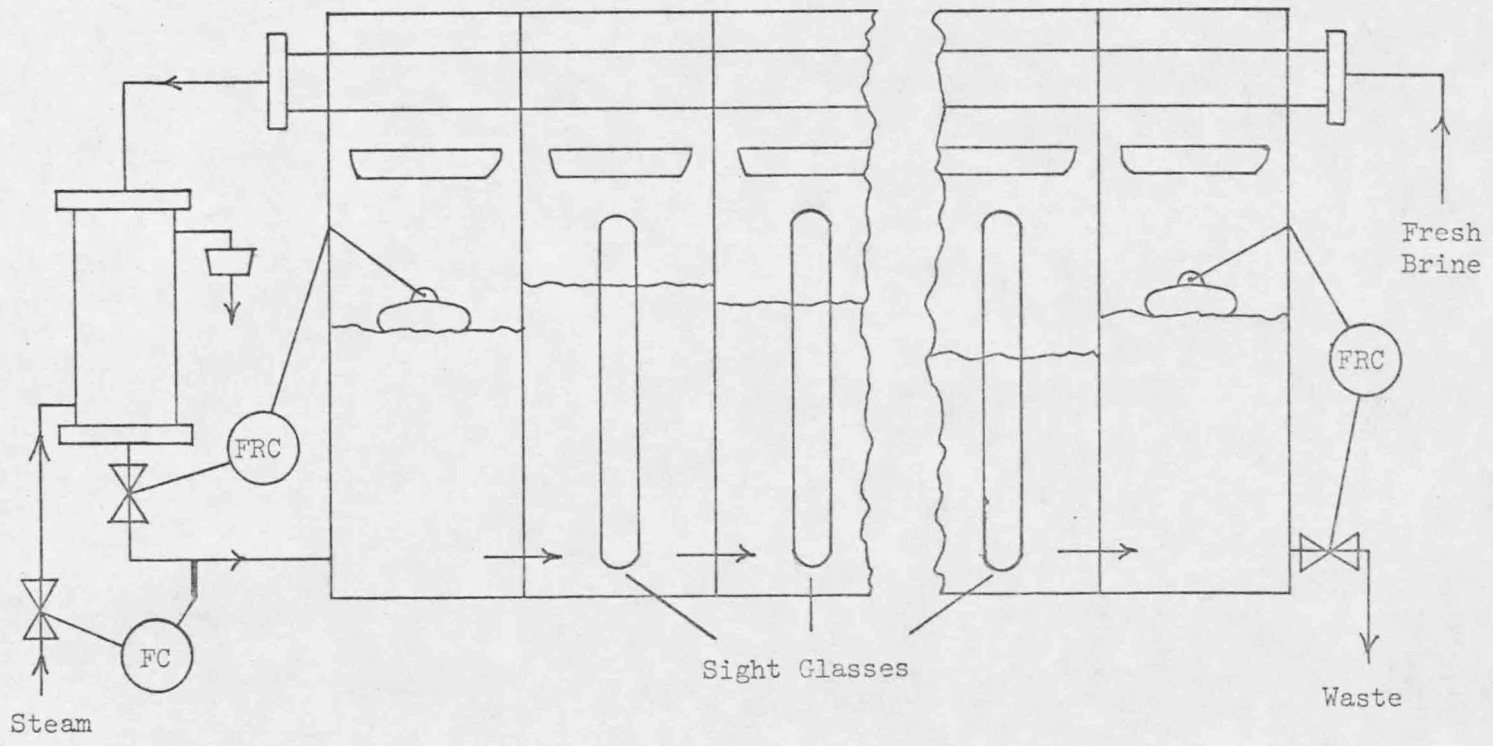


Figure 32. Existing Control

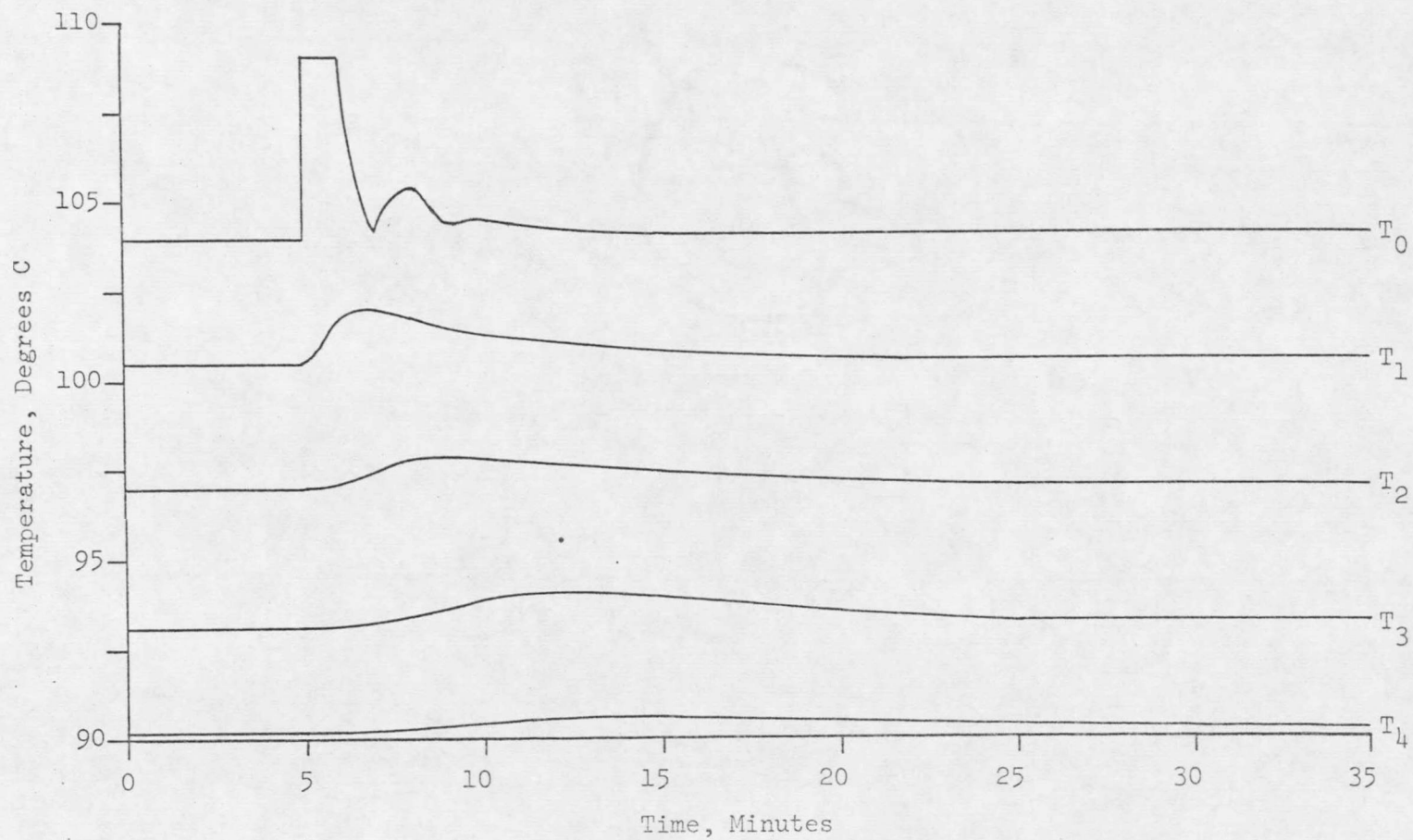
10 inches to approximate the action of an exit flow controller.

Control of T_o or T_c depends upon control of a process heat exchanger subject to variations in flow rate and inlet temperature. Kammen and Koppel (13) report in a dynamic study of a heat exchanger that they experienced a lineout time of approximately 40 seconds for heat exchanger response to a step upset in flow rate. Aikman (1) reported good success in controlling the exit temperature from a steam heat exchanger subject to varying flow rates and inlet temperatures. He gave response times for the heat exchanger of less than one minute.

To approximate the worst response of a heat exchanger to a change in operating conditions, a 1-minute pure lag was added to the temperature controller. Temperature controller constants were chosen using the continuous cycling method as described by Harriott (9). A $K_{max} = 1 \text{ } ^\circ\text{C}/^\circ\text{C}$ and an ultimate period P of 1 minute were obtained for the temperature controller. The suggested controller settings were $K_c = 0.45 * K_{max} = 0.45 \text{ } ^\circ\text{C}/^\circ\text{C}$ and $T_r = P/1.2 = 0.834$ minutes. For the flow controller, control constants were chosen arbitrarily to give a minimum amount of cycling and maintain F_o at a constant value. The proportional band for the flow controller was picked at $K_c = 6 \frac{\text{H}_2\text{O}/\text{min}}{\text{inch H}_2\text{O}}$, and the reset time was picked to be $T_r = 1.5$ min. This combination of control constants gave adequate control of H_1 to upsets in T_o and T_c without excessive cycling of F_o .

Using the 4-tank simulation with T_o and F_o under P-I control, a 5 °C step rise in the inlet temperature to the steam heat exchanger was introduced into the system. (See Figures 33-34.) A large initial upset in tank 1 lined out to +1°C within 10 minutes. In tank 2, the temperature pulsed about 2 °C and then stabilized within 5 minutes. Tank 3 had a small upset of less than 1 °C, and tank 4 recorded a negligible change. All heights remained stable, with H_1 showing the greatest oscillation. There was no tendency for the level in any tank to drift. T_c was held constant at 73 °C.

A step decrease in T_c from 73 to 68 °C with P-I control of T_o and F_o is shown in Figures 35-36. Control settings were left unchanged from the T_o upset run. Because a change in T_c has no effect upon the inlet temperature T_o , the temperature curves of Figure 35 are identical to those shown in Figure 29, which had no inlet temperature control. The H_1 curve oscillates within 1 °C of its set point, and H_4 is steady at its set point. H_2 and H_3 rise to new levels in their respective tanks. Decreasing T_c increases the ΔT and ΔP between tanks and raises the levels of water in tanks 2 and 3. A 5 °C step rise in T_c , with T_c under P-I control, is shown in Figures 37-38. The 1 minute lag was retained with the T_c temperature controller, and control constants of $K_c = 0.45$ °C/°C and $T_r = 0.834$ minutes were used. The flow controller was left unchanged. Upsets in the tank temperatures have magnitudes of less than 1 °C, and die out within 8 minutes. The heights of water are



-73-

Figure 33. 4-Tank Simulation, P-I Control of T_0 and F_0 , 5 °C Step Rise in Inlet Stream to T_0 Heat Exchanger, Temperature Response Curves.

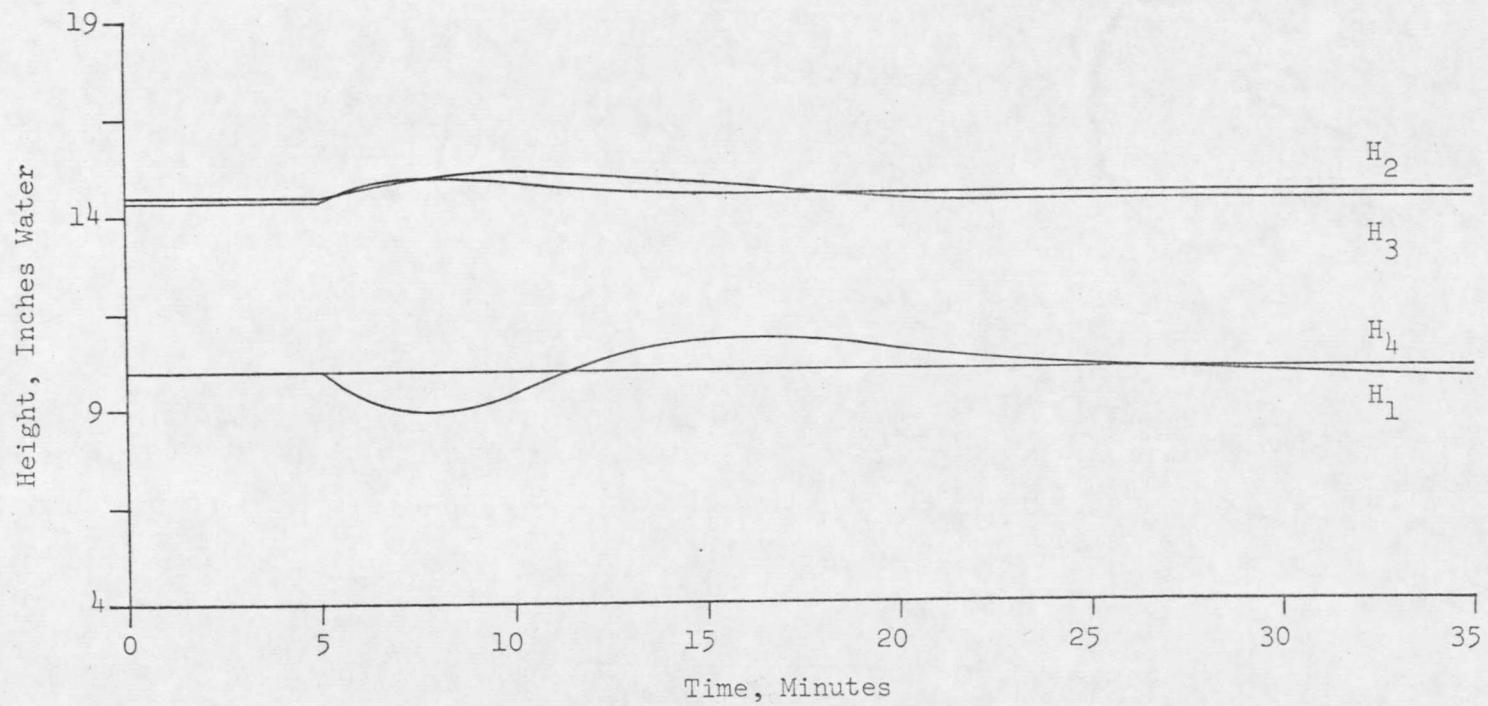


Figure 34. 4-Tank Simulation, P-I Control of T_0 and F_0 , 5 °C Step Rise in Inlet Stream to T_0 Heat Exchanger, Height Response Curves

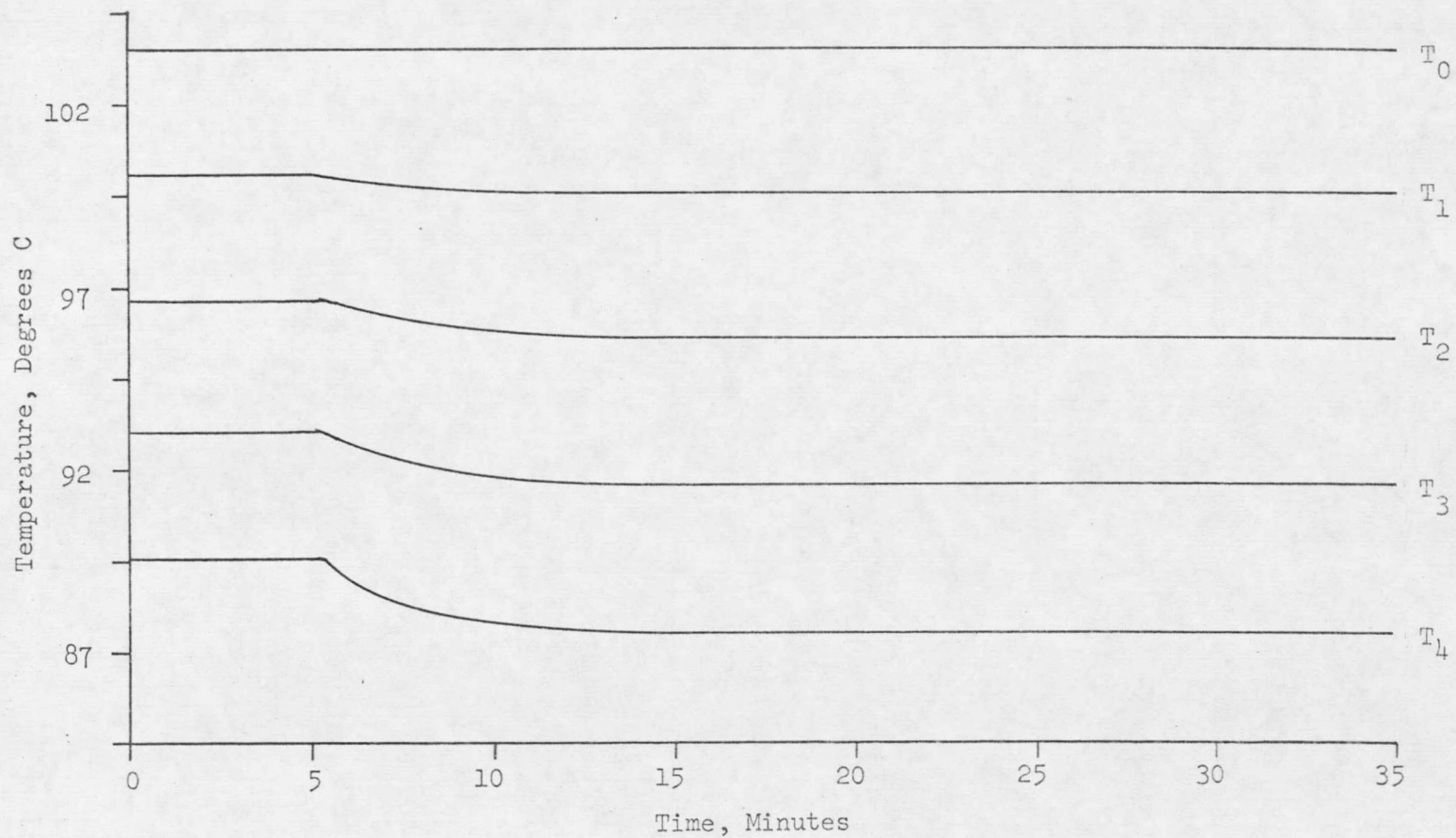


Figure 35. 4-Tank Simulation, P-I Control of T_0 and F_0 , Step Drop in T_c from 73 - 68 °C, Temperature Response Curves

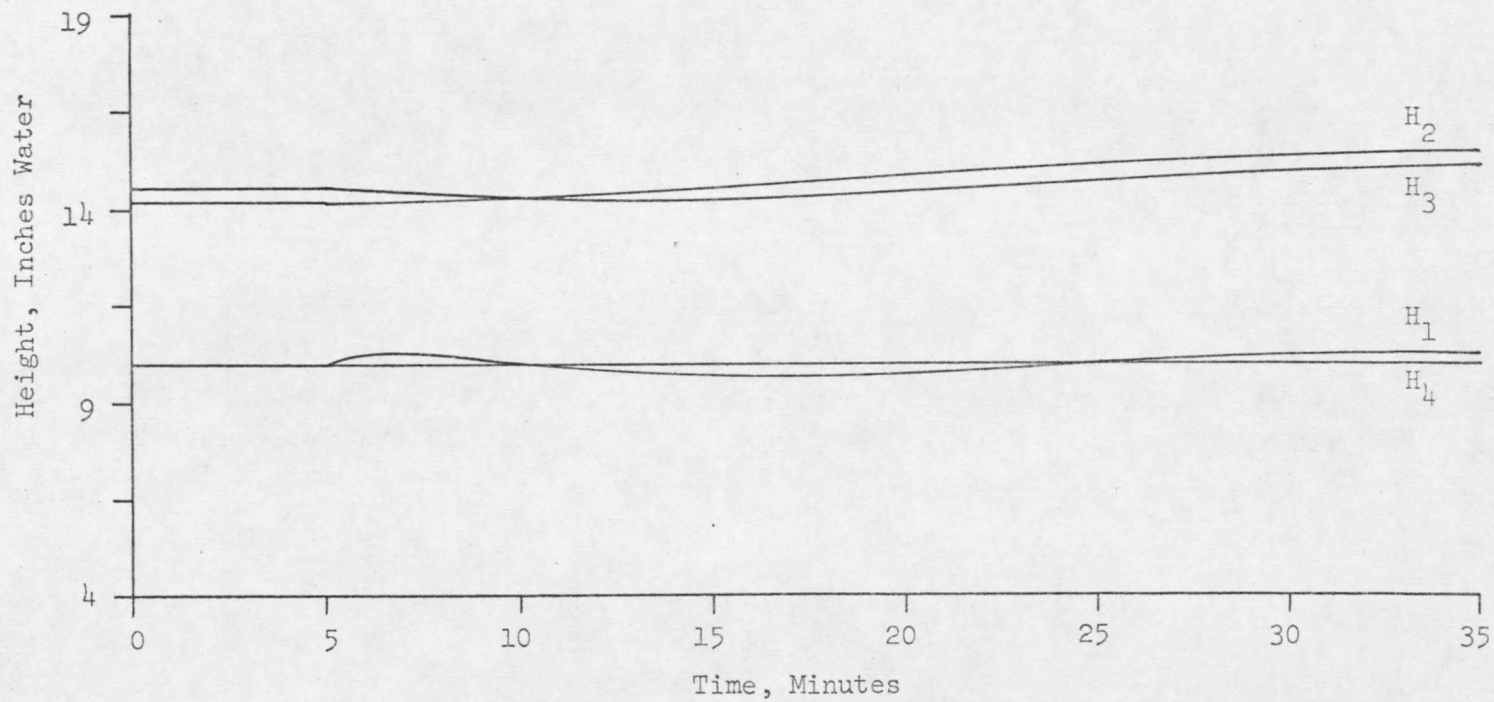


Figure 36. 4-Tank Simulation, P-I Control of T_0 and F_0 , Step Drop in T_c from 73 - 68 °C, Height Response Curves

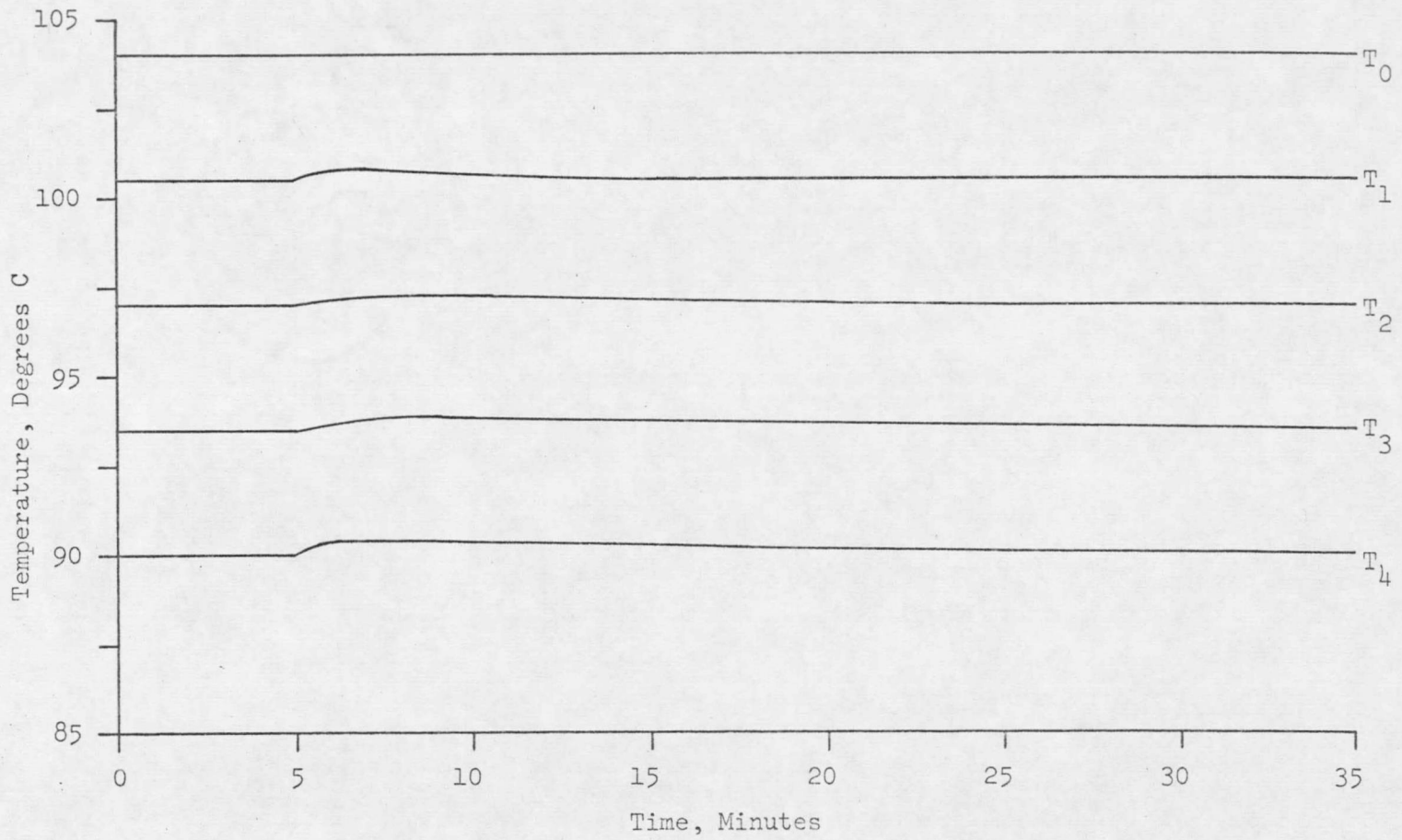


Figure 37. 4-Tank Simulation, P-I Control of T_c and F_0 , 5 °C Step Rise in Inlet Stream to T_c Heat Exchanger, Temperature Response Curves

-11-

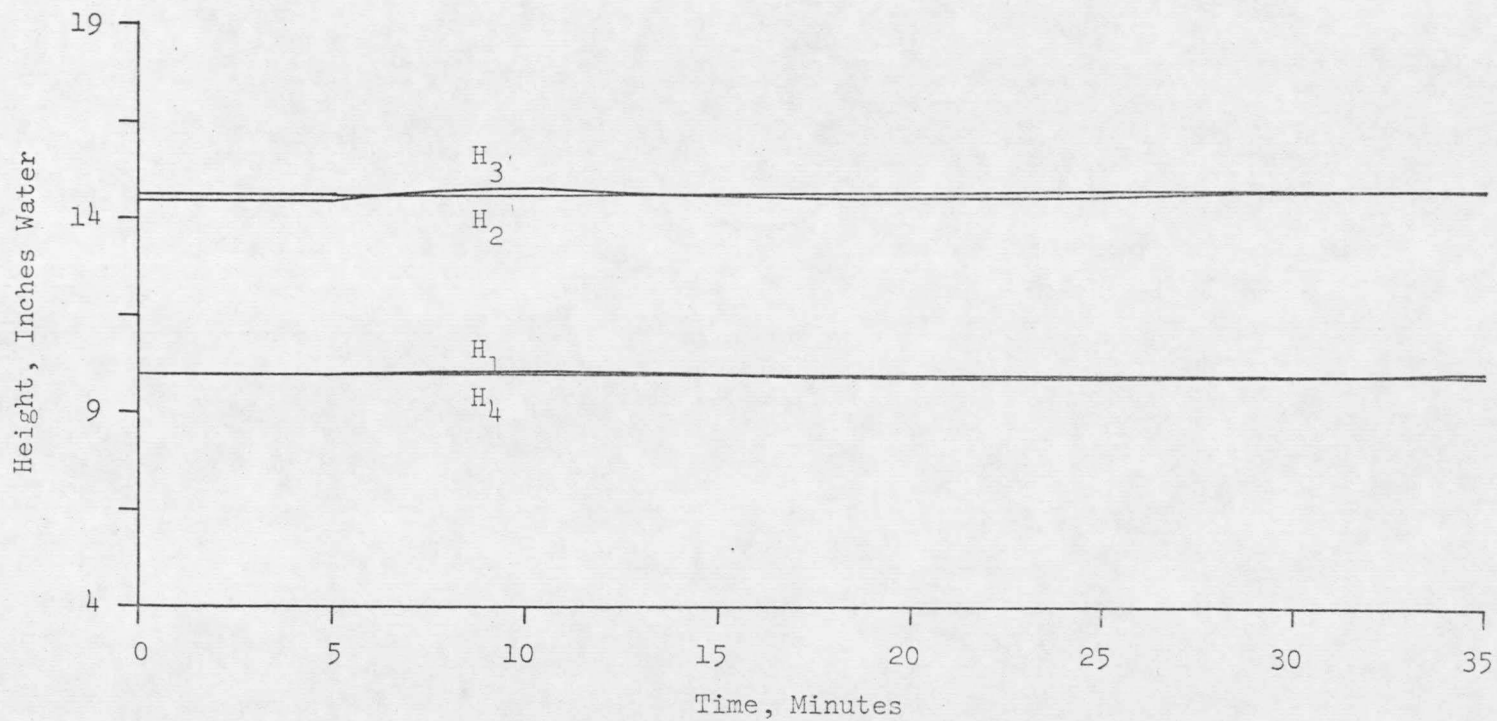


Figure 38. 4-Tank Simulation, P-I Control of T_c and F_0 , 5 °C Step Rise in Inlet Stream to T_c Heat Exchanger, Height Response Curves

very stable, varying less than 1 inch in each tank. There is no tendency for any of the water levels to drift to new levels.

The stability of the flash evaporator under P-I control was also examined by changing the T_o set point from 104 °C to 101 °C. (See Figures 39-40.) A much more severe response of the system was observed than in the previous upsets under controller action, especially for the heights of water in each tank. Lowering the operating temperature 3 °C dropped the ΔT between tanks and lowered H_2 and H_3 from 14.5 inches to 13 inches. H_1 cycled between 11 1/2 inches and 8 1/2 inches before stabilizing back toward the set point value of 10 inches. By increasing K_c and T_r for the flow controller, fluctuation in H_1 is reduced while the variation in F_o is increased. The temperatures in each tank dropped to new steady-state levels. T_1 reached its new value within 10 minutes, and T_4 leveled out in a little more than 20 minutes.

A change in the T_c set point from 73 °C to 76 °C is shown in Figures 41-42. Changes in tank temperatures are small, with T_4 changing about 1 °C and T_1 changing less than 1/ °C. New steady-state values were reached within 15 minutes after the set point change. There was little change in any of the heights of water in any of the tanks.

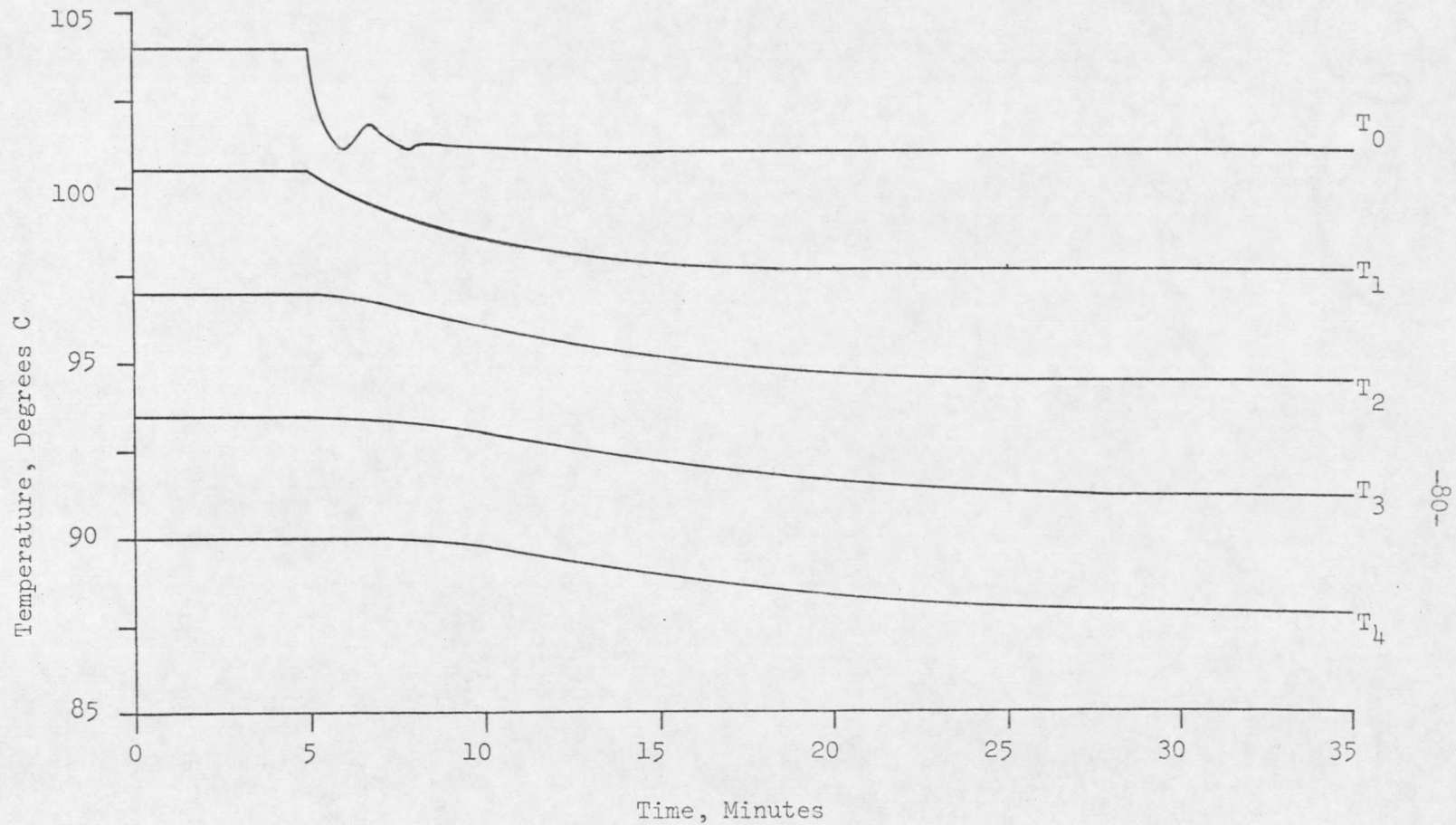


Figure 39. 4-Tank Simulation, P-I Control of T_0 and F_0 , Change of T_0 Set Point from 104 °C to 101 °C, Temperature Response Curves

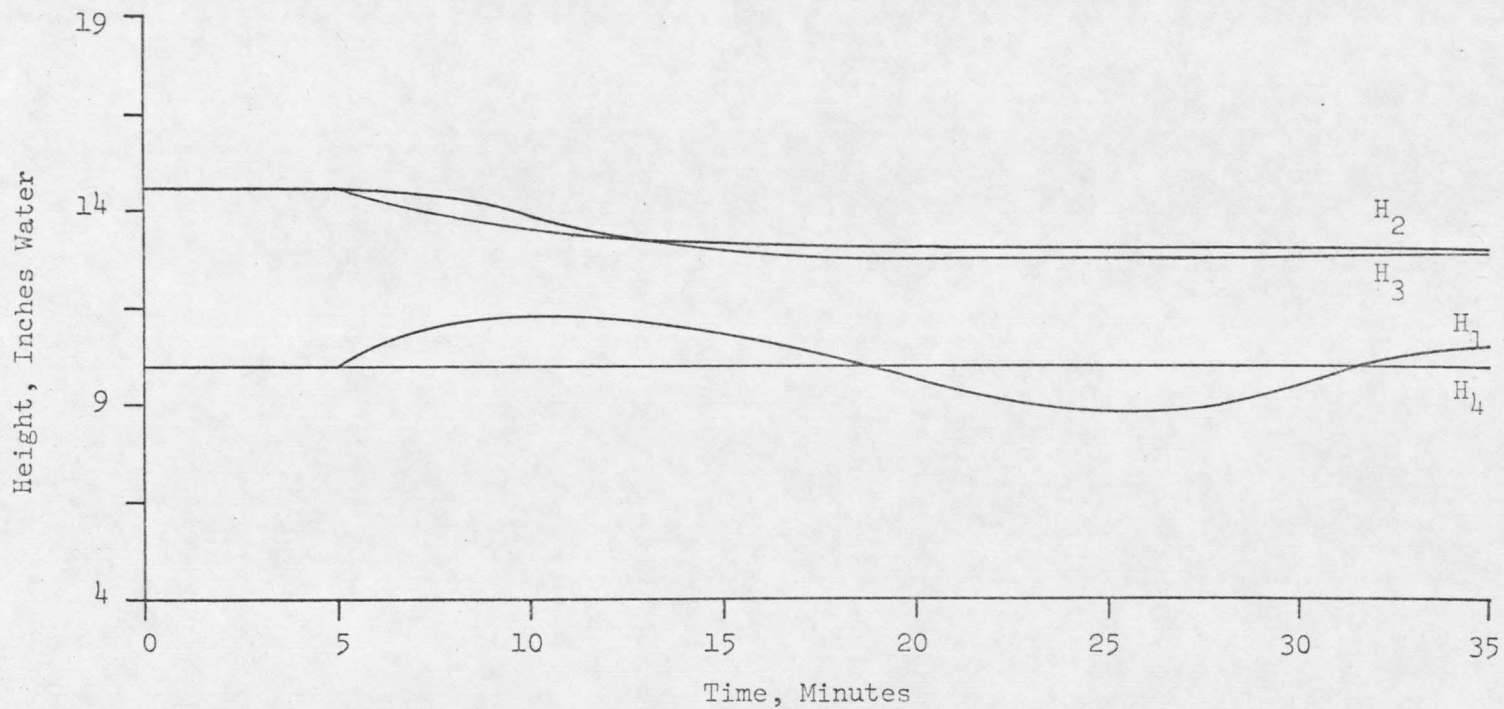
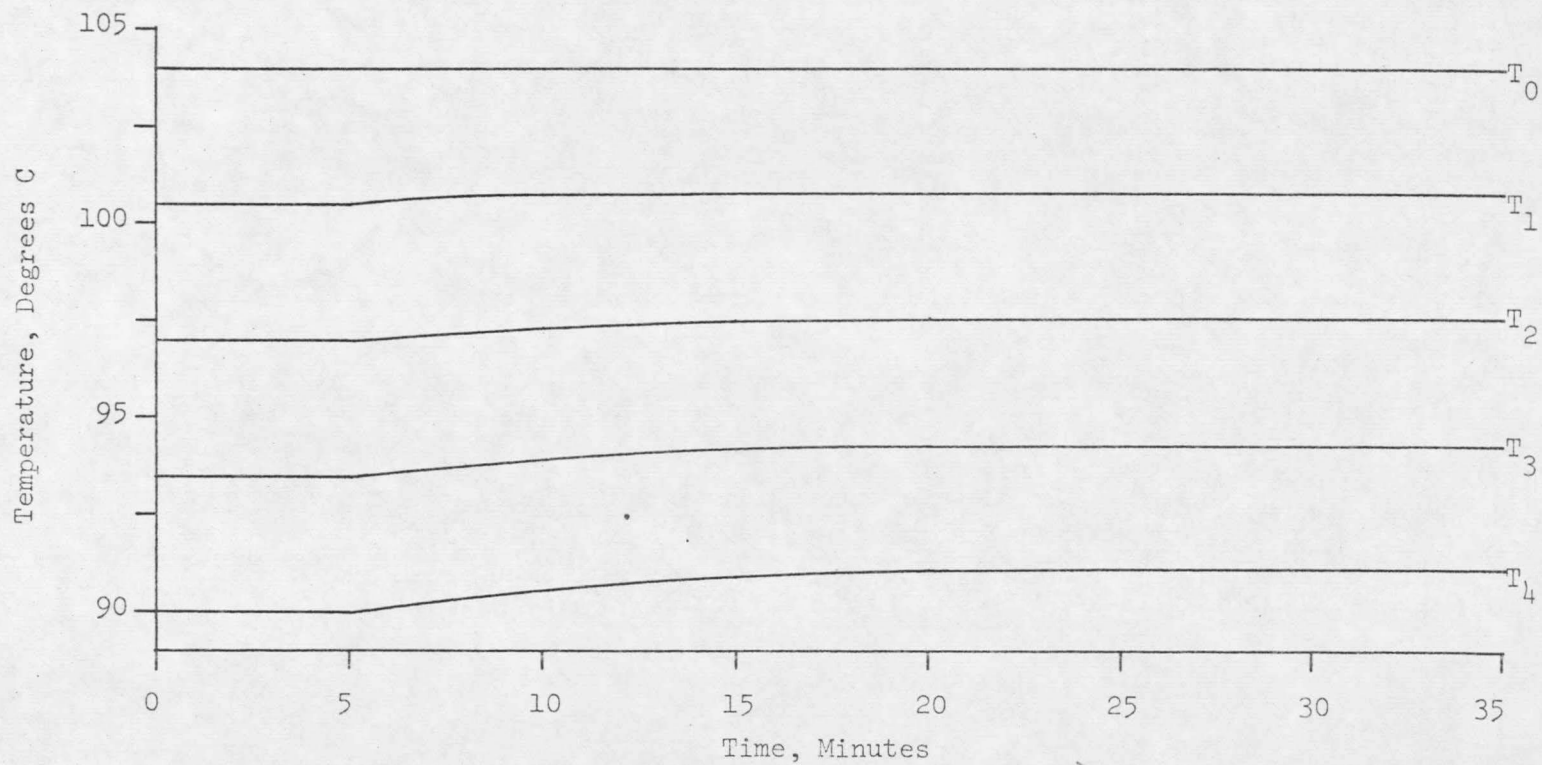


Figure 40. 4-Tank Simulation, P-I Control of T_0 and F_0 , Change of T_0 Set Point from 104 °C to 101 °C, Height Response Curves



-82-

Figure 41. 4-Tank Simulation, P-I Control of T_c and F_0 , Change of T_c Set Point from 73 °C to 76 °C, Temperature Response Curves

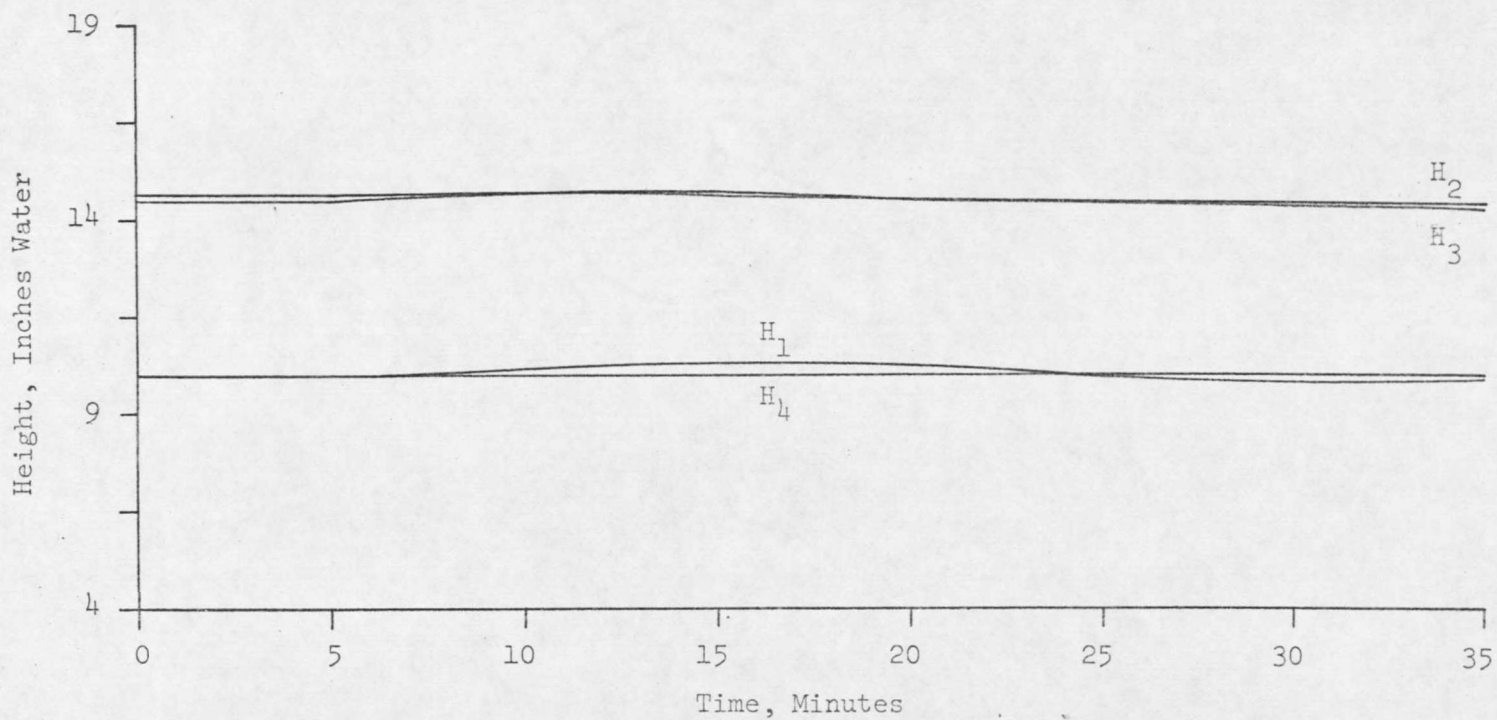


Figure 42. 4-Tank Simulation, P-I Control of T_c and F_0 , Change of T_c Set Point from 73 °C to 76 °C, Height Response Curves

CONCLUSION

The development of a simplified mathematical model for the 2-tank flash evaporator has defined the relationship between the system variables and system stability. The interaction of temperature, pressure, water height, and heat removal rate works to give the unique behavior of the flash evaporator. The extension of the 2-tank model to the 4-tank model has helped clarify the relationship of stability to evaporator design. Use of the 4-tank model showed that P-I control of the inlet temperature, inlet flow rate, cool brine temperature, and exit flow rate was sufficient to control a multi-stage evaporator.

The 4-tank simulation may be used to simulate a 4-tank section of any flash evaporator. Because of the simple design of the model, a minimum of data are needed to adapt to any particular situation. Depending upon the temperature range, correlations for the physical properties of the brine (viscosity, density, enthalpy of vaporization, etc.) must be changed. The orifice equation may be changed to fit orifices of different sizes or may be substituted for by another equation describing another form of restricted flow, such as flow through a weir. Tank size and tube bundle heat-transfer rates are readily adaptable to any particular situation. Various control schemes may be easily added or removed. Simulation runs taking less than 10 minutes of computer time will predict evaporator performance over a

real time period of 70 minutes. It is hoped that the results of this study may be used to aid in the design of future flash evaporators.

SUGGESTIONS FOR FURTHER WORK

1. Rewrite the digital simulation so that it applies to an N-stage evaporator.
2. Add an exit flow controller to the laboratory 2-stage evaporator and test the control scheme proposed in this paper.
3. Modify the 4-tank simulation by including actual heat transfer correlations for the tube bundle.
4. Expand the laboratory evaporator to 3 or 4 tanks and compare its operation with the computer model.
5. Correlate the submerged flow through a variable-area weir.
6. Include the dynamic response of a steam heat exchanger in the 4-tank simulation for the examination of P-I control.
7. Compare the 4-tank model with transient data from the San Diego test module when it becomes available.

APPENDIX

APPENDIX

- A. Definition of Terms.
- B.
 - 1. Computer Listing for 2-Tank Evaporator Model.
 - 2. Computer Listing for 2-Tank Plot Model.
 - 3. Computer Listing for 4-Tank Evaporator Model.
 - 4. Computer Listing for 4-Tank Plot Model.
- C. Sample Experimental Data Listing.

DEFINITION OF TERMS

A_1	Water surface area of tank 1.
A_2	Water surface area of tank 2.
C_p	Heat capacity of water, 1 BTU/#-°F.
ΔT	Temperature drop from tank 1 to tank 2, 2-tank evaporator.
ΔT_{1-2}	Temperature drop from tank 1 to tank 2, 4-tank evaporator.
ΔT_{2-3}	Temperature drop from tank 2 to tank 3, 4-tank evaporator.
ΔT_{3-4}	Temperature drop from tank 3 to tank 4, 4-tank evaporator.
$(-\Delta P)$	Pressure drop across the orifice between 2 adjacent tanks.
ΔP_{1-2}	Pressure drop across the orifice between tank 1 and tank 2, 4-tank evaporator
ΔP_{2-3}	Pressure drop across the orifice between tank 2 and tank 3, 4-tank evaporator.
ΔP_{3-4}	Pressure drop across the orifice between tank 3 and tank 4, 4-tank evaporator.
F_o	Flow rate of water (brine) into tank 1.
F_1	Flow rate of water from tank 1 into tank 2, 2-tank model.
F_1, F_{1-2}	Flow rate of water from tank 1 into tank 2, 4-tank model.
F_2, F_{2-3}	Flow rate of water from tank 2 into tank 3, 4-tank model.
F_3, F_{3-4}	Flow rate of water from tank 3 into tank 4, 4-tank model.
F_4	Flow rate of water out of tank 4, 4-tank model.
ξ_c	Proportionality constant between force and mass.
H	Enthalpy of water vapor.
H_1	Height of water in tank 1.
H_2	Height of water in tank 2.

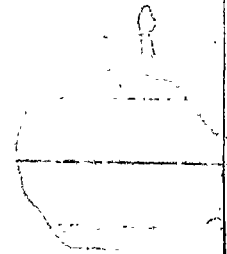
H_3	Height of water in tank 3, 4-tank model.
H_4	Height of water in tank 4, 4-tank model.
λ	Enthalpy of vaporization of water.
P	Vapor pressure of water as a function of temperature.
P_1	Vapor pressure of water in tank 1.
Q	Flow rate of water through an orifice as a function of ΔT , ΔP , and temperature.
ρ_L	Density of water (liquid).
ρ_V	Density of water (vapor).
τ	System time constant.
t_{ref}	Reference temperature, chosen arbitrarily.
t_1	Temperature of cooling water in tube bundle leaving tank 1.
t_2	Temperature of cooling water in tube bundle leaving tank 2.
t_3	Temperature of cooling water in tube bundle leaving tank 3.
T_c	Temperature of cooling water (fresh brine) entering the tube bundle in tank n.
T_o	Temperature of feed water entering tank 1.
T_1	Temperature of water in tank 1.
T_2	Temperature of water in tank 2.
T_3	Temperature of water in tank 3, 4-tank model.
T_4	Temperature of water in tank 4, 4-tank model.
$(UA)_1$	Combined area-heat transfer coefficient term for tube bundle 1.
$(UA)_2$	Combined area-heat transfer coefficient term for tube bundle 2.

V_n Liquid volume in tank n.
 v_n Vapor volume in tank n.
 w Liquid holdup in tube bundle in any tank.
 $\Delta\theta$ Differential increment of time.

Computer listing for 2-tank Evaporator Model

```
|JOB          19069,HOLZBERGER,35
|LIMITS (TIME,9),(PAGES,200)
|ASSIGN F:106,(DEVICE,MTA81)
|MESSAGE MOUNT SCRATCH TAPE ON DRIVE 1 AND LEAVE MOUNTED FOR NEXT JOB.
|FORTRAN
  DIMENSION ARRAY(9;701),T(20)
  DATA A1,A2/8.88,6.57/
  PONE(A) = (29.921/760.)*10.**(7.9668-1668.21/(228+A))
  DPINHG(A,B,C,D)=((C-D)/13.6+PONE(A)-PONE(B))
  RHOL(A)=0.62937173E+02-(0.1754855E-01)*A-(.13551528E-03)*A**2
  QRAD(A) = EPSILN*SIGMA*((1.8*(A+273.))**4-(1.8*298.)**4)/60.
  TDROP2(B)=ALPHA*(B-TCOOL)
  TDROP1(A,B)=BETA*(A-TCOOL-TDROP2(B))
  T1DOT(A,B,C)=(12./(RHOL(A)*A1*C))*(FZERO*(TZERO-A)-FZERO*TDROP1(A,
1B)-SIDEA1*QRAD(A))
  T2DOT(A,B,C,D)=(12./(RHOL(B)*A2*D)*(FLOW(A,B,C,D)*(A-B)-FZERO*TDRO
1P2(B)-SIDEA2*QRAD(B)))
  H1DOT(A,B,C,D)=(12./((RHOL(A)*A1))*(FZERO-FLOW(A,B,C,D))
  H2DOT(A,B,C,D)=(12./((RHOL(B)*A2))*(FLOW(A,B,C,D)-FZERO)
  SIDEA1 = (66*82+44*66+22*41)/144
  SIDEA2 = (4100+2200+41*22)/144
  ALPHA=.23
  BETA=.03
  TCOOL=78.
C
  READ(105,5) T1ZERO,T2ZERO,H1ZERO,H2ZERO
  5 FORMAT(4F10.2)
  READ (105,10) FZERO,DTHETA,TSTEP,EPSILN,TZERO
  10 FORMAT (5F10.1)
```

-92-



```

SIGMA = 1.73D-9
ARRAY(1,1) = TZERO
ARRAY(2,1) = T1ZERO
ARRAY(3,1) = T2ZERO
ARRAY(4,1) = T1ZERO-T2ZERO
ARRAY(5,1) = PONE(T1ZERO)
ARRAY(6,1) = DPINHG(T1ZERO,T2ZERO,H1ZERO,H2ZERO)
ARRAY(7,1) = H1ZERO
ARRAY(8,1) = H2ZERO
ARRAY(9,1) = FLOW(T1ZERO,T2ZERO,H1ZERO,H2ZERO)
21 TIME = 0.0
REWIND 106
WRITE(108,110)
110 FORMAT('1 T-ZERO T-ONE T-TWO DT PONE
1 DP H-ONE H-TWO FLOW TIME FZERO //)
WRITE(108,120) (ARRAY(I,1),I=1,9),TIME,FZERO
DO 150 I=1,700
IF(I.GT.300) TZERO=TSTEP
X1 = T1DOT(T1ZERO,T2ZERO,H1ZERO)*DTHETA
Y1 = T2DOT(T1ZERO,T2ZERO,H1ZERO,H2ZERO)*DTHETA
Z1 = H1DOT(T1ZERO,T2ZERO,H1ZERO,H2ZERO)*DTHETA
W1 = H2DOT(T1ZERO,T2ZERO,H1ZERO,H2ZERO)*DTHETA
TX1 = T1ZERO+X1/2
TY1 = T2ZERO+Y1/2
HZ1 = H1ZERO+Z1/2
HW1 = H2ZERO+W1/2
X2 = T1DOT(TX1,TY1,HZ1)*DTHETA
Y2 = T2DOT(TX1,TY1,HZ1,HW1)*DTHETA
Z2 = H1DOT(TX1,TY1,HZ1,HW1)*DTHETA
W2 = H2DOT(TX1,TY1,HZ1,HW1)*DTHETA
TX2 = T1ZERO+X2/2
TY2 = T2ZERO+Y2/2
HZ2 = H1ZERO + Z2/2
HW2 = H2ZERO + W2/2
X3 = T1DOT(TX2,TY2,HZ2)*DTHETA
Y3 = T2DOT(TX2,TY2,HZ2,HW2)*DTHETA
Z3 = H1DOT(TX2,TY2,HZ2,HW2)*DTHETA

```

```

W3 = H2DOT(TX2, TY2, HZ2, HW2)*DTHETA
TX3 = T1ZERO + X3
TY3 = T2ZERO + Y3
HZ3 = H1ZERO + Z3
HW3 = H2ZERO + W3
X4 = T1DOT(TX3, TY3, HZ3, HW3)*DTHETA
Y4 = T2DOT(TX3, TY3, HZ3, HW3)*DTHETA
Z4 = H1DOT(TX3, TY3, HZ3, HW3)*DTHETA
W4 = H2DOT(TX3, TY3, HZ3, HW3)*DTHETA
DELTAX = (X1+2*X2+2*X3+X4)/6.
T1 = T1ZERO+DELTAX
DELTAY = (Y1+2*Y2+2*Y3+Y4)/6.
T2 = T2ZERO+DELTAY
DELTAH = (Z1+2*Z2+2*Z3+Z4)/6.
H1 = H1ZERO+DELTAH
DELH2 = (W1+2*W2+2*W3+W4)/6.
H2 = H2ZERO+DELH2
J = I + 1
ARRAY(1,J) = TZERO
ARRAY(2,J) = T1
ARRAY(3,J) = T2
ARRAY(4,J) = T1-T2
ARRAY(5,J) = PONE(T1)
ARRAY(6,J) = DPINHG(T1, T2, H1, H2)
ARRAY(7,J) = H1
ARRAY(8,J) = H2
ARRAY(9,J) = FLOW(T1, T2, H1, H2)
T1ZERO = T1
T2ZERO = T2
H1ZERO = H1
H2ZERO = H2
TIME = DTHETA*I
DT1=TDROP1(T1, T2)
DT2=TDROP2(T2)
WRITE(108, 120) (ARRAY(K, J), K=1, 9), TIME, FZERO
120 FORMAT (3(F8.2, 3X), F9.3, 3X, F9.3, 2X, F9.3, 3X, F8.2, 3X, F8.2, 4X, F7.1, 4X
1, F6.2, 4X, F7.1)

```

```

      IF(H1.GT.20..OR.H1.LT.(.01)) GO TO 190
250 CONTINUE
290 WRITE(108,200) DTHETA, EPSILN, ALPHA, BETA, TCOOL
200 FORMAT(//' DTHETA=',F5.2,5X,' EPSILON=',F4.1,5X,' ALPHA=',F4.2,5X,' B
ETA=',F4.2,5X,' TCOOL=',F4.0)
      DO 204 J=210,690,4
      WRITE (106,202) (ARRAY(I,J), I=1,9)
202 FORMAT (9(F8.3))
204 CONTINUE
      ENDFILE 106
      REWIND 106
205 CONTINUE
210 CALL EXIT
      END
      FUNCTION FLOW(A,B,C,D)
      DATA A1,A2,CONST/8.88,6.57,0.192069215E+2/
      PONE(A) = (29.921/760.)*10.**(7.9668-1668.21/(228+A))
      RHOL(A)= 0.62937173D+02-(0.1754855D-01)*A-(.13551528D-03)*A**2
      ENTHAL(A)=(.1074063D+4-(.9336113D0)*A-(.10453132D-02)*A**2)*778.
      DPCMHG(A,B,C,D)=((C-D)/13.6+PONE(A)-PONE(B))*2.54
      DP=DPCMHG(A,B,C,D)
      IF (DP.GT.(0.0)) GO TO 10
      FLOW = 25.
      GO TO 20
10 FLOW=CONST*(VIS(A)**.174)*(RHOL(A)**.2566)*((DPCMHG(A,B,C,D)*27.84
15)**.5694)/(ENTHAL(A)**.1564)
20 RETURN
      END
      FUNCTION VIS(A)
      VIS=(0.93535666-(0.10130378E-01)*A+(0.3616155)*A**2)
      IF (VIS.LT.(0.24)) GO TO 15
      GO TO 20
15 VIS = 0.24
      GO TO 30
20 IF (VIS.GT.(0.4)) GO TO 25
      GO TO 30
25 VIS = 0.40

```

30 VIS = VIS*2.42

RETURN

END

LOAD

RUN

DATA

96.5

93.0

12.0

12.0

148.

.05

95.0

0.1

97.

EOD

FIN

Computer Listing for 2-tank Plot Program.

```
JOB          19069,HOLZBERGER,34
LIMITS (TIME,12),(PAGES,150)
ASSIGN F:106,(DEVICE,MTA81)
FORTRAN
C   THIS PROGRAM REQUIRES TWO HEADING CARDS.
    DIMENSION ARRAY(9,150),LINE(120),LABEL(10),TIME(21),NAME1(18),NAME
    12(12)
    INTEGER BLANK/'  '/
    INTEGER STAR/'*  '/
    DATA LABEL/'T-IN', 'TONE', 'TTWO', 'DT  ', 'PONE', 'DP  ', 'HONE', 'HTWO'
    1, 'FLOW', '  ' /
    REWIND 106
    READ(105,1) NAME1
    1 FORMAT(18A4)
    READ (105,2) NAME2
    2 FORMAT(12A4)
    READ(105,4) NSKIP,DTHETA
    4 FORMAT(I2,F10.3)
    DO 15 I=1,13
    15 TIME(I)=(I-1)*DTHETA*NSKIP*10.
    3 DO 5 J=1,150
    READ(106,10,END=11,ERR=11) (ARRAY(I,J),I=1,9)
    10 FORMAT (9(F8.3))
    NCOUNT = J
    IF(NCOUNT .GT. 120) NCOUNT=120
    5 CONTINUE
    11 CONTINUE
    12 DO 200 I=1,9
    XMAX=1.E-10
    XMIN=1.E+10
    DO 20 J=1,NCOUNT
```

```

    IF (ARRAY(I,J) .GT. XMAX) XMAX=ARRAY(I,J)
20  IF (ARRAY(I,J) .LT. XMIN) XMIN=ARRAY(I,J)
    GO TO (31,31,31,50,56,60,70,70,80),I
31  NXMAX = XMAX + 1
    NXMIN = XMIN
    IF ((NXMAX-NXMIN).GT.6.) GO TO 34
    NXMIN = NXMAX - 6
    DO 33 J=1,NCOUNT
    ARRAY(I,J) = (ARRAY(I,J)-NXMIN)*6.
33  CONTINUE
    XMAX = NXMAX
    DELTA = 1
    NAXIX = 6
    GO TO 90
34  IF((NXMAX-NXMIN).GT.9) GO TO 200
    NXMIN = NXMAX - 9
    DO 35 J = 1,NCOUNT
35  ARRAY(I,J) = (ARRAY(I,J)-NXMIN)*36./9.
    CONTINUE
    XMAX = NXMAX
    DELTA = 1
    NAXIX = 4
    GO TO 90.
50  INT = XMAX*5.+1.
    XMAX = INT*.2
    INT = XMIN*5.
    XMIN = INT*(.2)
    IF((XMAX-XMIN).GT.1.2) GO TO 53
    DIFF = 1.2-(XMAX-XMIN)
    XMAX = XMAX + DIFF/2.
    XMIN = XMAX-1.2
    DO 52 J=1,NCOUNT
    ARRAY(I,J) = (ARRAY(I,J)-XMIN)*30.
52  CONTINUE
    DELTA = 0.2
    NAXIX = 6
    GO TO 90

```

```
53 IF((XMAX-XMIN).GT.1.8) GO TO 200
    XMIN=XMAX-1.8
    DO 54 J=1,NCOUNT
54 ARRAY(I,J) = (ARRAY(I,J)-XMIN)*36./1.8
    DELTA=0.2
    NAXIX = 4
    GO TO 90
56 IF (XMAX.GT.31) GO TO 200
    IF (XMIN.LT.24) GO TO 200
    XMAX = 31
    XMIN = 24
    DO 58 J=1,NCOUNT
    ARRAY(I,J) = (ARRAY(I,J)-XMIN)*36./7.
58 CONTINUE
    DELTA = 1
    NAXIX = 5
    GO TO 90
60 INT = XMAX*10.+1.
    XMAX=INT*(.1)
    INT=XMIN*5.
    XMIN=INT*(.2)
    DIFF = 1.2-(XMAX-XMIN)
    IF (DIFF.LT.(0.0)) GO TO 65
    XMIN = XMAX-1.2
    DO 63 J=1,NCOUNT
    ARRAY(I,J) = (ARRAY(I,J)-XMIN)*30.
63 CONTINUE
    DELTA = 0.2
    NAXIX = 6
    GO TO 90
65 DIFF = 1.8 - (XMAX-XMIN)
    IF (DIFF.LT.0.0) GO TO 200
    XMIN = XMAX - 1.8
    DO 67 J=1,NCOUNT
    ARRAY(I,J) = (ARRAY(I,J)-XMIN)*36./1.8
67 CONTINUE
    DELTA = 0.2
```

```

NAXIX = 4
GO TO 90
70 XMAX=15
XMIN=9
DO 75 J=1,NCOUNT
ARRAY(I,J)=(ARRAY(I,J)-9.)*6.
75 CONTINUE
DELTA=1
NAXIX=6
GO TO 90
80 INTMAX=XMAX*.1+1
XMAX=INTMAX*10.
IF((XMAX-XMIN).GT.60.) GO TO 200
XMIN=XMAX-60.
DO 85 J=1,NCOUNT
85 ARRAY(I,J) = (ARRAY(I,J)-XMIN)*(.6)
DELTA = 10.
NAXIX = 6
90 SMALL = 36.
NREPT = -1
DO 150 KKK=1,35
NREPT = NREPT + 1
BIG = SMALL
SMALL = BIG - 1
DO 92 J=1,120
LINE(J) = BLANK
92 CONTINUE
DO 95 J=1,NCOUNT
IF (BIG.GE.ARRAY(I,J).AND.(SMALL.LT.ARRAY(I,J))) LINE(J)=STAR
95 CONTINUE
KNT = KKK
IF (KNT.GT.1) GO TO 100
WRITE (108,96) XMAX,(LINE(J), J=1,120)
96 FORMAT ('1',4X,F6.2,'=',120A1)
GO TO 150
100 IF(KNT.NE.18) GO TO 110
JJ = I

```

```

      GO TO 112
110  JJ = 10
112  IF (NREPT .NE.NAXIX) GO TO 120
      NREPT = 0
      XMAX = XMAX-DELTA
      WRITE (108,115) LABEL(JJ),XMAX,(LINE(J), J=1,120)
115  FORMAT (A4,1X,F6.2,'≠',120A1)
      GO TO 150
120  WRITE (108,125) LABEL(JJ),(LINE(J), J=1,120)
125  FORMAT (A4,7X,'≠',120A1)
150  CONTINUE
      WRITE(108,170) NAME1,NAME2
170  FORMAT(11X,'≠',18A4,12A4)
      WRITE (108,153)
153  FORMAT (11X,'#####
1#####
2≠')
      WRITE(108,180) (TIME(KI), KI=1,13)
180  FORMAT(2X,13(6X,F4.0))
200  CONTINUE
      REWIND 106
      CALL EXIT
      END

```

-TOT-

```

|LOAD
|RUN
|DATA

```

```

6/1/69  RUN 1, TWO-TANK EVAPORATOR.      STEP DROP IN TZERO FROM 97 TO 9
5 DEGREES CENTIGRADE.

```

```

  4  0.05
|EOD
|FIN

```

Computer Listing for 4-tank Evaporator Model.

```

JOB          12370,HOLZBERGER,50
MESSAGE     MOUNT SCRATCH TAPE ON DRIVE 1 AND LEAVE ON FOR NEXT JOB.
ASSIGN F:106,(DEVICE,MTA81)
LIMITS (TIME,10),(PAGES,125)
FORTRAN

C
C      THIS PROGRAM SIMULATES A FOUR-TANK EVAPORATOR.
C      TIN IS THE FEED TEMPERATURE TO THE HEAT EXCHANGER.
C      TZERO IS THE FEED TEMPERATURE INTO TANK 1.
C
C
      DIMENSION ARRAY(20,701),T(20)
      DATA A1,A2,A3,A4/8.,8.,8.,8./
      PONE(A) = (29.921/760.)*10.**((7.9668-1668.21/(228+A)))
      DPINHG(A,B,C,D)=((C-D)/13.6+PONE(A)-PONE(B))
      RHOL(A)=0.62937173E+02-(0.1754855E-01)*A-(.13551528E-03)*A**2
      TDROP4(D)=(2.*BDLH1*BDLA1/(2.*FZERO*60.+BDLH1*BDLA1))*(D-TCOOL)
      TDROP3(C,D)=(2.*BDLH2*BDLA2/(2.*FZERO*60.+BDLH2*BDLA2))*(C-TCOOL-T
1DRO4(D))
      TDROP2(B,C,D)=(2.*BDLH3*BDLA3/(2.*FZERO*60.+BDLH3*BDLA3))*(B-TCOOL
1-TDRO4(D)-TDRO3(C,D))
      TDROP1(A,B,C,D)=(2.*BDLH4*BDLA4/(2.*FZERO*60.+BDLH4*BDLA4))*(A-TCO
10L-TDRO4(D)-TDRO3(C,D)-TDRO2(B,C,D))
      T1DOT(A,B,C,D,E)=(12./((RHOL(A)*A1*E)))*(FZERO*(TZERO-A)-FZERO*TDROP
11(A,B,C,D))
      T2DOT(A,B,C,D,E,F)=(12./((RHOL(B)*A2*F)))*(FLOW(A,B,E,F)*(A-B)-FZERO
1*TDROP2(B,C,D))
      T3DOT(B,C,D,F,G)=(12./((RHOL(C)*A3*G)))*(FLOW(B,C,F,G)*(B-C)-FZERO*T
1DRO3(C,D))
      T4DOT(C,D,G,H)=(12./((RHOL(D)*A4*H)))*(FLOW(C,D,G,H)*(C-D)-FZERO*TDRO
1OP4(D))
      H1DOT(A,B,E,F)=(12./((RHOL(A)*A1)))*(FZERO-FLOW(A,B,E,F))
      H2DOT(A,B,C,E,F,G)=12./((RHOL(B)*A2))*(FLOW(A,B,E,F)-FLOW(B,C,F,G))
      H3DOT(B,C,D,F,G,H)=12./((RHOL(C)*A3))*(FLOW(B,C,F,G)-FLOW(C,D,G,H))

```

-102-

```

H4DOT(C,D,G,H)=12./(RHOL(D)*A4)*(FLOW(C,D,G,H)-FZERO)
REWIND 106
TCOOL=73.
READ (105,10) TZERO,T1ZERO,T2ZERO,T3ZERO,T4ZERO
10 FORMAT(5F10.1)
READ(105,12) H1ZERO,H2ZERO,H3ZERO,H4ZERO
12 FORMAT(4F10.2)
READ (105,12) FZERO,DTHETA,TSTEP,TIN
READ(105,14) BDLA1,BDLA2,BDLA3,BDLA4
14 FORMAT(4F10.1)
READ(105,14) BDLH1,BDLH2,BDLH3,BDLH4
READ(105,18) PROPT,PROPH,SETT,SETH,RESETT,RESETH
18 FORMAT(6F10.2)
TIME = 0.0
SUMERT=(TCOOL-TIN)*RESETT/(PROPT*DTHETA)
SUMERH=(FZERO-145.)*RESETH/(PROPH*DTHETA)
DO 30 I=1,20
30 T(I)=TCOOL
DO 210 LAPS=1,2
WRITE(108,110)
110 FORMAT('1 T-ZERO T-ONE T-TWO T-THREE T-FOUR
1DT1 DT2 DT3 DT4 H-ONE H-TWO T
2IME'//)
112 FORMAT(5(F8.2,3X),4(F6.2,5X),1X,F5.2,6X,F5.2,3X,F8.2)
DO 150 I=1,700
ERRORH=SETH-H1ZERO
SUMERH=SUMERH+ERRORH
FZERO=145.+PROPH*(ERRORH+SUMERH*DTHETA/RESETH)
IF(FZERO.LT.120.) FZERO=120.
IF(FZERO.GT.180.) FZERO=180.
ERRORT=SETT-T(1)
SUMERT=SUMERT+ERRORT
TCOOL=TIN+PROPT*(ERRORT+SUMERT*DTHETA/RESETT)
DO 114 IJ=1,19
114 T(IJ)=T(IJ+1)
T(20)=TCOOL
IF(LAPS.EQ.1) GO TO 120

```

-103-

```

N=I+700
GO TO 125
120 N=I
125 IF(N.GT.250) TIN =TSTEP
S1=T1DOT(T1ZERO,T2ZERO,T3ZERO,T4ZERO,H1ZERO)*DTHETA
T1=T2DOT(T1ZERO,T2ZERO,T3ZERO,T4ZERO,H1ZERO,H2ZERO)*DTHETA
U1=T3DOT(T2ZERO,T3ZERO,T4ZERO,H2ZERO,H3ZERO)*DTHETA
V1=T4DOT(T3ZERO,T4ZERO,H3ZERO,H4ZERO)*DTHETA
W1=H1DOT(T1ZERO,T2ZERO,H1ZERO,H2ZERO)*DTHETA
X1=H2DOT(T1ZERO,T2ZERO,T3ZERO,H1ZERO,H2ZERO,H3ZERO)*DTHETA
Y1=H3DOT(T2ZERO,T3ZERO,T4ZERO,H2ZERO,H3ZERO,H4ZERO)*DTHETA
Z1=H4DOT(T3ZERO,T4ZERO,H3ZERO,H4ZERO)*DTHETA
TS1=T1ZERO+S1/2
TT1=T2ZERO+T1/2
TU1=T3ZERO+U1/2
TV1=T4ZERO+V1/2
HW1=H1ZERO+W1/2
HX1=H2ZERO+X1/2
HY1=H3ZERO+Y1/2
HZ1=H4ZERO+Z1/2
S2=T1DOT(TS1,TT1,TU1,TV1,HW1)*DTHETA
T2=T2DOT(TS1,TT1,TU1,TV1,HW1,HX1)*DTHETA
U2=T3DOT(TT1,TU1,TV1,HX1,HY1)*DTHETA
V2=T4DOT(TU1,TV1,HY1,HZ1)*DTHETA
W2=H1DOT(TS1,TT1,HW1,HX1)*DTHETA
X2=H2DOT(TS1,TT1,TU1,HW1,HX1,HY1)*DTHETA
Y2=H3DOT(TT1,TU1,TV1,HX1,HY1,HZ1)*DTHETA
Z2=H4DOT(TU1,TV1,HY1,HZ1)*DTHETA
TS2=T1ZERO+S2/2
TT2=T2ZERO+T2/2
TU2=T3ZERO+U2/2
TV2=T4ZERO+V2/2
HW2=H1ZERO+W2/2
HX2=H2ZERO+X2/2
HY2=H3ZERO+Y2/2
HZ2=H4ZERO+Z2/2
S3=T1DOT(TS2,TT2,TU2,TV2,HW2)*DTHETA

```

$T3 = T2DOT(TS2, TT2, TU2, TV2, HW2, HX2) * DTHETA$
 $U3 = T3DOT(TT2, TU2, TV2, HX2, HY2) * DTHETA$
 $V3 = T4DOT(TU2, TV2, HY2, HZ2) * DTHETA$
 $W3 = H1DOT(TS2, TT2, HW2, HX2) * DTHETA$
 $X3 = H2DOT(TS2, TT2, TU2, HW2, HX2, HY2) * DTHETA$
 $Y3 = H3DOT(TT2, TU2, TV2, HX2, HY2, HZ2) * DTHETA$
 $Z3 = H4DOT(TU2, TV2, HY2, HZ2) * DTHETA$
 $TS3 = T1ZERO + S3$
 $TT3 = T2ZERO + T3$
 $TU3 = T3ZERO + U3$
 $TV3 = T4ZERO + V3$
 $HW3 = H1ZERO + W3$
 $HX3 = H2ZERO + X3$
 $HY3 = H3ZERO + Y3$
 $HZ3 = H4ZERO + Z3$
 $S4 = T1DOT(TS3, TT3, TU3, TV3, HW3) * DTHETA$
 $T4 = T2DOT(TS3, TT3, TU3, TV3, HW3, HX3) * DTHETA$
 $U4 = T3DOT(TT3, TU3, TV3, HX3, HY3) * DTHETA$
 $V4 = T4DOT(TU3, TV3, HY3, HZ3) * DTHETA$
 $W4 = H1DOT(TS3, TT3, HW3, HX3) * DTHETA$
 $X4 = H2DOT(TS3, TT3, TU3, HW3, HX3, HY3) * DTHETA$
 $Y4 = H3DOT(TT3, TU3, TV3, HX3, HY3, HZ3) * DTHETA$
 $Z4 = H4DOT(TU3, TV3, HY3, HZ3) * DTHETA$
 $DELTAS = (S1 + 2 * S2 + 2 * S3 + S4) / 6.$
 $DELTAT = (T1 + 2 * T2 + 2 * T3 + T4) / 6.$
 $DELTAU = (U1 + 2 * U2 + 2 * U3 + U4) / 6.$
 $DELTAV = (V1 + 2 * V2 + 2 * V3 + V4) / 6.$
 $DELTAW = (W1 + 2 * W2 + 2 * W3 + W4) / 6.$
 $DELTAX = (X1 + 2 * X2 + 2 * X3 + X4) / 6.$
 $DELTAY = (Y1 + 2 * Y2 + 2 * Y3 + Y4) / 6.$
 $DELTAZ = (Z1 + 2 * Z2 + 2 * Z3 + Z4) / 6.$
 $TONE = T1ZERO + DELTAS$
 $TTWO = T2ZERO + DELTAT$
 $TTHREE = T3ZERO + DELTAU$
 $TFOUR = T4ZERO + DELTAV$
 $H1 = H1ZERO + DELTAW$
 $H2 = H2ZERO + DELTAX$

```

H3=H3ZERO+DELTAY
H4=H4ZERO+DELTAZ
J=I
ARRAY(1,J)=TZERO
ARRAY(2,J)=TONE
ARRAY(3,J)=TTWO
ARRAY(4,J)=TTHREE
ARRAY(5,J)=TFOUR
ARRAY(6,J)=H1
ARRAY(7,J)=H2
ARRAY(8,J)=H3
ARRAY(9,J)=H4
ARRAY(10,J)=FLOW(TONE,TTWO,H1,H2)
ARRAY(11,J)=FLOW(TTWO,TTHREE,H2,H3)
ARRAY(12,J)=FLOW(TTHREE,TFOUR,H3,H4)
ARRAY(13,J)=DPINHG(TONE,TTWO,H1,H2)
ARRAY(14,J)=DPINHG(TTWO,TTHREE,H2,H3)
ARRAY(15,J)=DPINHG(TTHREE,TFOUR,H3,H4)
ARRAY(16,J)=ARRAY(2,J)-ARRAY(3,J)
ARRAY(17,J)=ARRAY(3,J)-ARRAY(4,J)
ARRAY(18,J)=ARRAY(4,J)-ARRAY(5,J)
ARRAY(19,J)=FZERO
ARRAY(20,J)=TIN
T1ZERO=TONE
T2ZERO=TTWO
T3ZERO=TTHREE
T4ZERO=TFOUR
H1ZERO=H1
H2ZERO=H2
H3ZERO=H3
H4ZERO=H4
TIME=DTHETA*(N-1)
DT1=TDROP1(TONE,TTWO,TTHREE,TFOUR)
DT2=TDROP2(TTWO,TTHREE,TFOUR)
DT3=TDROP3(TTHREE,TFOUR)
DT4=TDROP4(TFOUR)
INDEX=J

```

```

WRITE(108,112)(ARRAY(K,J),K=1,5),DT1,DT2,DT3,DT4,(ARRAY(K,J),K=6,7
1),TIME
IF(H1.GT.20.OR.H1.LT.(.01)) GO TO 160
150 CONTINUE
160 WRITE(108,162)
162 FORMAT('1H-THREE   H-FOUR   FLOW1-2   FLOW2-3   FLOW3-4   DP1-2
1      DP2-3      DP3-4      DT1-2      DT2-3      DT3-4      TIME      FZE
2RO'//)
DO 170 J=1,INDEX
N=J
IF(LAPS.EQ.2) N=J+700
TIME=(N-1)*DTHETA
WRITE(108,164)(ARRAY(I,J),I=8,18),TIME,ARRAY(19,J)
164 FORMAT(5(F7.2,3X),6(F8.3,2X),F8.2,2X,F7.2)
170 CONTINUE
WRITE(108,180) PROPT,PROPH,SETT,SETH,RESETT,RESETH
180 FORMAT(/' PROP-T=',F5.2,5X,' PROP-H=',F5.2,5X,' SET-T=',F5.1,5X,' SET
1-H=',F5.1,5X,' RESET-T=',F5.1,5X,' RESET-H=',F5.1,/)
IF(LAPS.EQ.2) GO TO 205
DO 195 J=220,INDEX,4
WRITE(106,190) (ARRAY(I,J),I=1,9)
190 FORMAT(9F8.3)
195 CONTINUE
ENDFILE 106
DO 198 J=220,INDEX,4
WRITE(106,190)(ARRAY(I,J),I=10,18)
198 CONTINUE
ENDFILE 106
DO 204 J=220,INDEX,4
WRITE(106,200) (ARRAY(I,J),I=19,20)
200 FORMAT(2F8.3)
204 CONTINUE
ENDFILE 106
GO TO 210
205 IF(INDEX.GT.484) INDEX=484
DO 206 J=4,INDEX,4
WRITE(106,190) (ARRAY(I,J),I=1,9)

```

```

0 206 CONTINUE
      ENDFILE 106
      DO 207 J=4,INDEX,4
      WRITE(106,190)(ARRAY(I,J),I=10,18)
207 CONTINUE
      ENDFILE 106
      DO 209 J=4,INDEX,4
      WRITE(106,200)(ARRAY(I,J),I=19,20)
209 CONTINUE
      ENDFILE 106
210 CONTINUE
      REWIND 106
250 CALL EXIT
      END
      FUNCTION FLOW(A,B,C,D)
      PONE(A) = (29.921/760.)*10.**(7.9668-1668.21/(228+A))
      RHOL(A) = 0.62937173D+02-(0.1754855D-01)*A-(.13551528D-03)*A**2
      ENTHAL(A) = (.1074063D+4-(.9336113D0)*A-(.10453132D-02)*A**2)*778
      DPCMHG(A,B,C,D) = ((C-D)/13.6+PONE(A)-PONE(B))*2.54
      CONST = 0.192069215E+2
      DP = DPCMHG(A,B,C,D)
      IF (DP.GT.(0.0)) GO TO 10
      FLOW = 25.
      GO TO 20
10 FLOW = CONST*(VIS(A)**.174)*(RHOL(A)**.2566)*((DPCMHG(A,B,C,D)*27.84
15)**.5694)/(ENTHAL(A)**.1564)
20 RETURN
      END
      FUNCTION VIS(A)
      VIS = (0.93535666-(0.10130378E-01)*A+(0.3616155)*A**2)
      IF (VIS.LT.(0.24)) GO TO 15
      GO TO 20
15 VIS = 0.24
      GO TO 30
20 IF (VIS.GT.(0.4)) GO TO 25
      GO TO 30
25 VIS = 0.40

```

Computer Listing for 4-tank Plot Program.

```
|JOB          12370,HOLZBERGER,55
|ASSIGN F:106,(DEVICE,MTA81)
|LIMITS (TIME,9),(PAGES,200)
|FORTRAN
C   THIS PROGRAM REQUIRES TWO HEADING CARDS.
    DIMENSION ARRAY(20,130),LINE(120),LABEL(21),TIME(28),NAME1(18),NAM
1E2(12)
    INTEGER BLANK/'  '/
    INTEGER STAR/'*  '/
    DATA LABEL/'T-0 ','TONE','TTWO','T-3 ','T-4 ','H-1 ','H-2 ','H-3 '
1,'H-4 ','F1-2','F2-3','F3-4','DP12','DP23','DP34','DT12','DT23','D
2T34','F-IN','T-IN','  '/
    REWIND 106
    READ(105,1) NAME1
1  FORMAT(18A4)
    READ (105,2) NAME2
2  FORMAT(12A4)
    READ(105,4) NSKIP,DTHETA
4  FORMAT(I2,F10.3)
    DO 15 I=1,28
15  TIME(I)=(I-1)*DTHETA*NSKIP*10.
    DO 200 LAPS=1,2
    3  DO 5 J=1,130
    READ(106,10,END=11,ERR=11) (ARRAY(I,J),I=1,9)
10  FORMAT (9F8.3)
    NCOUNT = J
    IF(NCOUNT .GT. 120) NCOUNT=120
    5  CONTINUE
11  DO 12 J=1,130
    READ(106,10,END=13,ERR=13)(ARRAY(I,J),I=10,18)
12  CONTINUE
```

```

13 DO 14 J=1,130
    READ(106,6,END=16,ERR=16) ARRAY(19,J),ARRAY(20,J)
    6 FORMAT(2F8.3)
14 CONTINUE
16 DO 200 I=1,20
    XMAX=1.E-10
    XMIN=1.E+10
    DO 20 J=1,NCOUNT
    IF(ARRAY(I,J) .GT. XMAX) XMAX=ARRAY(I,J)
20 IF(ARRAY(I,J) .LT. XMIN) XMIN=ARRAY(I,J)
    GO TO(31,31,31,31,31,70,70,70,70,80,80,80,60,60,60,50,50,50,80,31)
    1,I
31 NXMAX = XMAX + 1
    NXMIN=XMIN
    IF ((NXMAX-NXMIN).GT.6.) GO TO 34
    NXMIN = NXMAX - 6
    DO 33 J=1,NCOUNT
    ARRAY(I,J) = (ARRAY(I,J)-NXMIN)*6
33 CONTINUE
    XMAX = NXMAX
    DELTA = 1
    NAXIX = 6
    GO TO 90
34 IF((NXMAX-NXMIN).GT.12) GO TO 200
    NXMIN = NXMAX - 12
    DO 35 J = 1,NCOUNT
    ARRAY(I,J) = (ARRAY(I,J)-NXMIN)*3
35 CONTINUE
    XMAX = NXMAX
    DELTA = 2
    NAXIX = 6
    GO TO 90
50 INT = XMAX*5.+1
    XMAX = INT*.2
    INT = XMIN*5.
    XMIN = INT*(.2)
    IF((XMAX-XMIN).GT.1.2) GO TO 53

```

```

DIFF = 1.2-(XMAX-XMIN)
XMAX = XMAX + DIFF/2.
XMIN = XMAX-1.2
DO 52 J=1,NCOUNT
ARRAY(I,J) = (ARRAY(I,J)-XMIN)*30.
52 CONTINUE
DELTA = 0.2
NAXIX = 6
GO TO 90
53 IF((XMAX-XMIN).GT.1.8) GO TO 200
XMIN=XMAX-1.8
DO 54 J=1,NCOUNT
54 ARRAY(I,J) = (ARRAY(I,J)-XMIN)*36./1.8
DELTA=0.2
NAXIX = 4
GO TO 90
60 INT = XMAX*10.+1.
XMAX=INT*(.1)
INT=XMIN*5.
XMIN=INT*(.2)
DIFF = 1.2-(XMAX-XMIN)
IF (DIFF.LT.(0.0)) GO TO 65
XMIN = XMAX-1.2
DO 63 J=1,NCOUNT
ARRAY(I,J) = (ARRAY(I,J)-XMIN)*30.
63 CONTINUE
DELTA = 0.2
NAXIX = 6
GO TO 90
65 DIFF = 1.8 - (XMAX-XMIN)
IF (DIFF.LT.0.0) GO TO 200
XMIN = XMAX - 1.8
DO 67 J=1,NCOUNT
ARRAY(I,J) = (ARRAY(I,J)-XMIN)*36./1.8
67 CONTINUE
DELTA = 0.2
NAXIX = 4

```

```

      GO TO 90
70  NXMAX=XMAX+2
      XMAX=NXMAX
      NXMIN=XMAX-6
      IF(XMIN.LT.NXMIN) GO TO 74
      DO 72 J=1,NCOUNT
72  ARRAY(I,J)=(ARRAY(I,J)-NXMIN)*6.
      DELTA=1.
      NAXIX=6
      GO TO 90
74  XMAX=19
      XMIN = 1
      DO 75 J=1,NCOUNT
      ARRAY(I,J) = (ARRAY(I,J)-1)*2
75  CONTINUE
      DELTA = 1
      NAXIX = 2
      GO TO 90
80  INTMAX=XMAX*.1+1
      XMAX=INTMAX*10.
      IF((XMAX-XMIN).GT.60.) GO TO 86
      XMIN=XMAX-60.
      DO 85 J=1,NCOUNT
85  ARRAY(I,J) = (ARRAY(I,J)-XMIN)*(.6)
      DELTA = 10.
      NAXIX = 6
      GO TO 90
86  XMIN =XMAX-120.
      DO 87 J=1,NCOUNT
87  ARRAY(I,J)=(ARRAY(I,J)-XMIN)*(0.3)
      DELTA=20.
      NAXIX=6
90  SMALL = 36.
      NREPT = -1
      DO 150 KKK=1,35
      NREPT = NREPT + 1
      BIG = SMALL

```

```

SMALL = BIG - 1
DO 92 J=1,120
LINE (J) = BLANK
92 CONTINUE
DO 95 J=1,NCOUNT
IF (BIG.GE.ARRAY(I,J).AND.(SMALL.LT.ARRAY(I,J))) LINE(J)=STAR
95 CONTINUE
KNT = KKK
IF (KNT.GT.1) GO TO 100
WRITE (108,96) XMAX,(LINE(J), J=1,120)
96 FORMAT ('1',4X,F6.2,'=',120A1)
GO TO 150
100 IF(KNT.NE.18) GO TO 110
JJ = I
GO TO 112
110 JJ = 21
112 IF (NREPT .NE.NAXIX) GO TO 120
NREPT = 0
XMAX = XMAX-DELTA
WRITE (108,115) LABEL(JJ),XMAX,(LINE(J), J=1,120)
115 FORMAT (A4,1X,F6.2,'=',120A1)
GO TO 150
120 WRITE (108,125) LABEL(JJ),(LINE(J), J=1,120)
125 FORMAT (A4,7X,'=',120A1)
150 CONTINUE
WRITE(108,170) NAME1,NAME2
170 FORMAT(11X,'=',18A4,12A4)
WRITE (108,153)
153 FORMAT (11X,'*****
1*****
2=')
IF(LAPS.EQ.2) GO TO 165
160 WRITE(108,180) (TIME(KI), KI=1,13)
GO TO 200
165 WRITE(108,180) (TIME(KI),KI=13,25)
180 FORMAT(2X,13(6X,F4.0))
200 CONTINUE

```

REWIND 106
CALL EXIT
END

|LOAD

|RUN

|DATA

7/21/69 RUN 3, FOUR-TANK EVAPORATOR. P-I CONTROL ON TZERO, TCOOL.
STEP DROP IN TCOOL FROM 60 TO 55 DEGREES C.

4 0.05

|EOD

|FIN

SAMPLE EXPERIMENTAL DATA LISTING

DELTA-P CALIBRATION

A(2) = 0.54758377E+02
A(1) = 0.29872143E+00
A(0) = 0.15684624E+01

X	Y	YCAL	ABS. ERR
39.1700	4.8750	4.8679	0.0071
39.6400	4.8125	4.8054	0.0071
40.1400	4.7500	4.7364	0.0136
40.4400	4.6875	4.6936	0.0061
40.9200	4.6250	4.6231	0.0019
41.3000	4.5625	4.5656	0.0031
41.7200	4.5000	4.5001	0.0001
41.9800	4.4375	4.4586	0.0211
42.3200	4.3750	4.4032	0.0282
42.8200	4.3125	4.3195	0.0070
43.2100	4.2500	4.2523	0.0023
43.5700	4.1875	4.1887	0.0012
43.9700	4.1250	4.1165	0.0085
44.4600	4.0625	4.0256	0.0369
44.7600	4.0000	3.9686	0.0314
45.0500	3.8750	3.9126	0.0376

P=ONE CALIBRATION

BETA = 0.3893 ALPHA = 27.6401
CORRELATION COEFFICIENT = 0.998307

TZERØ	TØNE	DT	PØNE	DP	HØNE	HTWØ	TIME
96.80	95.73	3.11	26.10	3.93	16.51	6.64	0.00
96.80	95.73	3.15	26.09	3.93	16.51	6.60	0.33
97.00	95.73	3.11	26.08	3.91	16.51	6.61	0.67
96.80	95.73	3.11	26.08	3.93	16.50	6.60	1.00
96.80	95.73	3.15	26.07	3.91	16.50	6.62	1.33
96.80	95.73	3.11	26.07	3.92	16.50	6.59	1.67
96.80	95.73	3.07	26.06	3.91	16.50	6.58	2.00
97.00	95.73	3.11	26.05	3.91	16.50	6.56	2.33
97.00	95.92	3.07	26.04	3.91	16.50	6.54	2.67
97.00	95.73	3.11	26.03	3.90	16.52	6.54	3.00
97.00	95.73	3.11	26.03	4.15	16.60	6.59	3.33
97.38	96.30	3.11	26.68	4.70	16.88	6.91	3.67
97.96	96.69	3.22	27.13	4.93	16.90	6.90	4.00
98.34	97.07	3.37	27.28	4.87	16.73	7.13	4.33
98.53	97.45	3.48	27.48	4.87	16.70	7.24	4.67
98.72	97.84	3.63	27.66	4.90	16.64	7.46	5.00
98.92	97.84	3.67	27.78	4.87	16.57	7.65	5.33
99.11	98.22	3.74	27.90	4.81	16.40	7.85	5.67
99.11	98.22	3.78	27.90	4.76	16.25	8.01	6.00
99.30	98.22	3.78	28.05	4.77	16.12	8.12	6.33
99.30	98.60	3.78	28.17	4.80	16.00	8.32	6.67
99.49	98.80	3.78	28.21	4.77	15.87	8.46	7.00
99.68	98.60	3.85	28.22	4.75	15.71	8.64	7.33
99.68	98.99	3.89	28.37	4.74	15.55	8.79	7.67
99.68	98.99	3.81	28.37	4.73	15.47	8.95	8.00
99.88	98.99	3.85	28.47	4.76	15.30	9.11	8.33
99.88	98.99	3.81	28.55	4.71	15.17	9.28	8.67
99.88	98.99	3.81	28.55	4.70	15.06	9.46	9.00
100.07	99.18	3.85	28.69	4.69	14.95	9.60	9.33
100.07	99.18	3.89	28.73	4.68	14.84	9.76	9.67
100.07	99.37	3.85	28.73	4.64	14.72	9.89	10.00
100.26	99.56	3.85	28.73	4.63	14.54	10.04	10.33
100.26	99.37	3.85	28.73	4.57	14.35	10.20	10.67
100.26	99.56	3.85	28.70	4.57	14.18	10.32	11.00
100.26	99.37	3.81	28.97	4.59	14.02	10.45	11.33
100.26	99.37	3.85	28.98	4.58	13.87	10.59	11.67
100.26	99.37	3.85	28.98	4.57	13.74	10.74	12.00
100.45	99.76	3.85	29.04	4.59	13.67	10.86	12.33
100.45	99.76	3.85	29.04	4.55	13.57	11.02	12.67
100.45	99.76	3.85	29.04	4.50	13.46	11.15	13.00
100.45	99.75	3.85	29.03	4.48	13.30	11.25	13.33
100.45	99.76	3.85	29.08	4.46	13.23	11.34	13.67
100.45	99.56	3.85	29.10	4.47	13.15	11.44	14.00
100.45	99.76	3.81	29.10	4.46	13.08	11.56	14.33
100.45	99.95	3.85	29.10	4.41	13.01	11.67	14.67

100.45	99.76	3.85	29.09	4.40	12.93	11.76	15.00
100.45	99.95	3.85	29.09	4.37	12.82	11.86	15.33
100.45	99.95	3.85	29.09	4.36	12.68	11.95	15.67
100.45	99.95	3.81	29.08	4.37	12.60	12.04	16.00
100.45	99.95	3.81	29.17	4.37	12.52	12.15	16.33
100.45	99.95	3.81	29.18	4.37	12.48	12.21	16.67
100.45	99.95	3.81	29.18	4.36	12.37	12.29	17.00
100.64	100.14	3.81	29.18	4.32	12.30	12.41	17.33
100.64	99.95	3.85	29.18	4.28	12.21	12.47	17.67
100.45	99.95	3.78	29.17	4.32	12.07	12.55	18.00
100.64	100.14	3.81	29.18	4.32	12.10	12.65	18.33
100.64	99.95	3.85	29.17	4.32	12.00	12.73	18.67
100.64	100.14	3.81	29.17	4.32	11.96	12.84	19.00
100.64	99.95	3.81	29.17	4.27	12.05	12.91	19.33
100.64	100.14	3.85	29.17	4.25	11.93	12.98	19.67
100.64	100.14	3.81	29.17	4.22	11.92	13.04	20.00
100.64	100.14	3.81	29.17	4.25	11.92	13.12	20.33
100.64	100.33	3.85	29.16	4.21	11.84	13.19	20.67
100.64	100.14	3.78	29.15	4.25	11.85	13.27	21.00
100.64	100.33	3.81	29.16	4.25	11.80	13.36	21.33
100.64	100.14	3.81	29.15	4.22	11.80	13.44	21.67
100.64	100.14	3.81	29.15	4.26	11.76	13.49	22.00
100.64	100.14	3.85	29.16	4.23	11.67	13.57	22.33
100.64	100.14	3.85	29.14	4.19	11.68	13.63	22.67
100.64	100.14	3.85	29.15	4.19	11.57	13.72	23.00
100.64	100.33	3.81	29.15	4.16	11.53	13.76	23.33
100.64	100.14	3.81	29.14	4.16	11.49	13.78	23.67
100.64	100.14	3.81	29.14	4.16	11.32	13.84	24.00
100.64	100.14	3.78	29.13	4.12	11.33	13.88	24.33
100.64	100.14	3.78	29.14	4.12	11.23	13.97	24.67
100.64	100.14	3.81	29.13	4.12	11.16	14.00	25.00
100.64	100.33	3.81	29.13	4.13	11.12	14.04	25.33
100.64	100.14	3.81	29.14	4.14	11.04	14.10	25.67
100.64	100.33	3.81	29.13	4.15	11.00	14.15	26.00
100.64	100.14	3.78	29.13	4.14	10.83	14.20	26.33
100.64	100.14	3.81	29.12	4.13	10.86	14.25	26.67
100.64	100.14	3.81	29.13	4.14	10.80	14.32	27.00
100.64	100.33	3.81	29.13	4.11	10.78	14.36	27.33
100.64	100.33	3.81	29.12	4.10	10.75	14.40	27.67
100.45	100.33	3.85	29.12	4.09	10.64	14.44	28.00
100.64	100.14	3.81	29.12	4.07	10.61	14.47	28.33
100.64	100.33	3.81	29.12	4.07	10.50	14.52	28.67
100.64	100.33	3.85	29.12	4.00	10.49	14.53	29.00
100.64	100.14	3.81	29.11	4.07	10.42	14.60	29.33
100.64	100.14	3.81	29.11	4.10	10.42	14.62	29.67
100.64	100.33	3.81	29.11	4.06	10.42	14.68	30.00
100.64	100.33	3.85	29.11	4.06	10.48	14.71	30.33
100.64	100.33	3.81	29.11	4.03	10.51	14.76	30.67
100.64	100.33	3.81	29.11	4.04	10.52	14.80	31.00
100.64	100.33	3.85	29.11	4.04	10.49	14.84	31.33

100.64	100.52	3.85	29.11	4.07	10.52	14.88	31.67
100.64	100.33	3.85	29.11	4.09	10.54	14.96	32.00
100.64	100.52	3.85	29.10	4.08	10.53	14.96	32.33
100.64	100.14	3.85	29.11	4.06	10.52	15.03	32.67
100.64	100.33	3.89	29.11	4.10	10.52	15.05	33.00
100.64	100.52	3.85	29.11	4.09	10.52	15.11	33.33
100.64	100.52	3.85	29.10	4.05	10.49	15.17	33.67
100.64	100.52	3.85	29.10	4.06	10.46	15.20	34.00
100.84	100.52	3.89	29.09	4.03	10.51	15.22	34.33
100.45	100.14	3.81	29.09	4.03	10.44	15.27	34.67
100.64	100.14	3.85	29.08	4.03	10.41	15.31	35.00
100.45	100.33	3.85	29.08	3.99	10.39	15.36	35.33
100.45	100.14	3.85	29.08	4.02	10.29	15.40	35.67
100.64	100.14	3.81	29.09	3.99	10.25	15.41	36.00
100.45	100.14	3.85	29.08	3.95	10.18	15.45	36.33
100.45	100.14	3.85	29.08	3.93	10.08	15.46	36.67
100.45	100.14	3.81	29.08	3.97	10.03	15.46	37.00
100.45	100.14	3.85	29.06	3.96	9.94	15.49	37.33
100.26	100.14	3.81	29.05	4.00	9.85	15.52	37.67
100.45	100.14	3.81	29.06	4.00	9.84	15.56	38.00
100.45	100.14	3.81	29.05	3.96	9.79	15.59	38.33
100.45	100.14	3.81	29.05	3.92	9.84	15.63	38.67
100.45	100.14	3.85	29.05	3.87	9.80	15.64	39.00
100.45	99.95	3.85	29.06	3.88	9.74	15.65	39.33
100.26	100.14	3.81	29.06	3.87	9.72	15.67	39.67
100.26	100.14	3.81	29.06	3.91	9.69	15.67	40.00

LITERATURE CITED

1. Aikman, A. R., "Frequency-Response Analysis and Controllability of a Chemical Plant"; Trans. A.S.M.E., Vol 76, Nov 1954, p. 1313-20.
2. Andersen, J. A., L. W. A. Glasson, and F. P. Lees, "The Control of a Single-Effect Concentrating Evaporator", Trans. Society of Instrument Technology, March 1961, p. 21-36.
3. Andre, H., and R. A. Ritter, "Dynamic Response of a Double Effect Evaporator", The Canadian Journal of Chemical Engineering, Vol 46, August, 1968.
4. Arad, Nathan, "An Evaluation of the System Effectiveness and Cost Effectiveness of Large Multistage Flash Seawater Desalting Plants", Ph.D. Thesis, George Washington University (1969).
5. Doninger, J. E., and W. F. Stevens, "The Dynamic Behavior of a Packed Liquid Extraction Column", A.I.Ch.E. Journal, Vol 14, No 4, p. 591-98.
6. Evans, R. H., "Guantanamo's Power-Desalination is One of the World's Largest", Power Engineering, April 1965, p. 45-6.
7. Fahidy, T. Z., and C. A. Luke, "Digital Simulation of Chemical Reactor Dynamics", Instruments and Control Schemes, Vol 41, March 1968, p. 113-17.
8. Finley, I. C., "Determining the Dynamic Response of Heat Exchangers", Chemical and Process Engineering-Heat Transfer Survey, 1966, p. 142-50.
9. Harriott, Peter, "Process Control", McGraw-Hill, New York, 1964, p. 178-79.
10. Huntsinger, R. C., "Flow Correlations For Brine Flashing Through Round & Square Submerged Orifices", Ph.D. Thesis, Montana State University (1966).
11. Itahara, Seiji, "Optimal Design of Evaporator Systems by Dynamic Programming", Ph.D. Thesis, Syracuse University (1967).
12. Jabens, R. H., and D. I. Dykstra, "Advances in Sea Water Distillation", Chemical Engineering Progress, Vol 6, No 8, August 1965, p. 68-73.

13. Kamman, D. T., and L. B. Koppel, "Dynamics of a Forced Flow Heat Exchanger", I. & E.C. Fundamentals, Vol 5, No 2, May 1966, p. 208-11.
14. Kogan, A., "Heat and Mass Transfer in Flash Distillation Without Metallic Interfaces", Israel Institute of Technology, Dept of Aeronautical Engineering, Report 47, 1965.
15. Koppel, L. B., "Dynamics and Control of a Batch Reactor", I. & E.C. Progress Design and Development, Vol 17, No 3, July 1968, p. 416-21.
16. Kreyszig, E., "Advanced Engineering Mathematics", John Wiley & Sons, New York, 1962.
17. Narsimhan, G., "On the Transient Behaviour of Multiple-Effect Evaporators", Indian Institute of Chemical Engineering, Vol 14, 1961-62, p. 98-100.
18. Office of Saline Water, U. S. Department of Interior, Research and Development Progress Report No. 214, "The Oak Ridge National Laboratory Conceptual Design of a 250-MGD Desalination Plant", U. W. Government Printing Office, Washington D. C., September 1966.
19. Office of Saline Water, U. S. Department of Interior, Research and Development Progress Report No. 233, "Conceptual Design Study of a 50 Million Gallon Per Day MSF Desalination Plant and Test Module", U. S. Government Printing Office, Washington D. C., November 1966.
20. Office of Saline Water, U. S. Department of Interior, Research and Development Progress Report No. 277, "Summary Evaluation of Conceptual Design for 50 MGD Desalination Plant", U. S. Government Printing Office, Washington, D. C., August 1967.
21. Office of Saline Water, U. S. Department of Interior, Research and Development Report Under Contract No. 14-01-0001-1142 by Electronics Associates, Inc., "Computer Simulation of a 150-Million Gallon Per Day Desalting Plant", October 1967.
22. Seider, E. N., "The Office of Saline Water Module Program", Chemical Engineering Progress, Vol 63, No 1, January 1967, p. 59-63.
23. Teasdale, A. K., "Get Frequency Response From Transient Data by Adding Vectors", Control Engineering, October 1955, p. 56-59.

24. Tetlow, N. J., D. M. Graves, and C. D. Holland, "A Generalized Model for the Dynamic Behavior of a Distillation Column"; A.I.Ch.E. Journal, Vol 13, No 3, May 1967, p. 476-85.

